

1. Report No. FHWA/TX-12/5-6362-01-1	2. Government Accession No.	3. Recipient's Catalog No.	
5. Title and Subtitle IMPLEMENTATION OF TECHNOLOGY FOR RAPID FIELD DETECTION OF SULFATE AND ORGANIC CONTENT IN SOILS: TECHNICAL REPORT		5. Report Date March 2012 Published: June 2012	
		6. Performing Organization Code	
7. Author(s) Chang-Seon Shon, Stephen Sebesta, and Tom Scullion		8. Performing Organization Report No. Report 5-6362-01-1	
9. Performing Organization Name and Address Texas Transportation Institute The Texas A&M University System College Station, Texas 77843-3135		10. Work Unit No. (TRAIS)	
		11. Contract or Grant No. Project 5-6362-01	
12. Sponsoring Agency Name and Address Texas Department of Transportation Research and Technology Implementation Office P. O. Box 5080 Austin, Texas 78763-5080		13. Type of Report and Period Covered Technical Report: February 2011–December 2011	
		14. Sponsoring Agency Code	
15. Supplementary Notes Project performed in cooperation with the Texas Department of Transportation and the Federal Highway Administration. Project Title: Implementation of Technology for Rapid Field Detection of Sulfate and Organic Content in Soils URL: http://tti.tamu.edu/documents/5-6362-01-1.pdf			
16. Abstract <p>The protocol using the Veris 3150 for determination of sulfate-rich soils has been implemented to two full-scale projects in Dallas and Paris Districts. The determination of organic-rich soil was not implemented in this project due to the unavailability of proper equipment. Researchers collected electrical conductivity (EC) data from two Veris 3150 units equipped at both TxDOT and TTI, simultaneously. Soil samples were collected on the basis of the constructed EC color map. The data collected from these projects were analyzed to identify potential relationships between Veris EC measurements and sulfate contents for different types of soil.</p> <p>Statistical modeling results indicate that Veris EC is a linear function of the natural log of the sulfate content, directly if other soil parameters such as moisture content, organic matter content, and clay content remain constant. Higher EC of soil responds to higher sulfate content of soil. It is imperative that soil samples be collected based on the EC map generated from the Veris 3150 data. Therefore, it is recommended that the Veris EC be used as a viable screening tool to identify areas where high sulfate-bearing soils may exist.</p> <p>A color-coded map indicates that the area that has the greater EC shows the higher sulfate content. The comparison study of TxDOT and TTI Veris units shows that the units produce comparable sets of data although the actual EC values may not be exactly matched.</p>			
17. Key Words Veris 3150 Unit, Electrical Conductivity, Sulfate-Rich Soil, Color-Coded Map		18. Distribution Statement No restrictions. This document is available to the public through NTIS: National Technical Information Service Alexandria, Virginia 22312 http://www.ntis.gov	
19. Security Classif. (of this report) Unclassified	20. Security Classif. (of this page) Unclassified	21. No. of Pages 94	22. Price

**IMPLEMENTATION OF TECHNOLOGY FOR RAPID FIELD
DETECTION OF SULFATE AND ORGANIC CONTENT IN SOILS:
TECHNICAL REPORT**

by

Chang-Seon Shon
Assistant Research Scientist
Texas Transportation Institute

Stephen Sebesta
Associate Research Scientist
Texas Transportation Institute

and

Tom Scullion, P.E.
Senior Research Engineer
Texas Transportation Institute

Report 5-6362-01-1
Project 5-6362-01

Performed in cooperation with the
Texas Department of Transportation
and the
Federal Highway Administration

March 2012
Published: June 2012

Project Title: Implementation of Technology for Rapid Field Detection of Sulfate and Organic
Content in Soils

TEXAS TRANSPORTATION INSTITUTE
The Texas A&M University System
College Station, Texas 77843-3135

DISCLAIMER

This research was performed in cooperation with the Texas Department of Transportation (TxDOT) and the Federal Highway Administration (FHWA). The contents of this report reflect the views of the authors, who are responsible for the facts and the accuracy of the data presented herein. The report does not necessarily reflect the official view or policies of the FHWA or TxDOT. This report neither constitutes a standard, specification, or regulation, nor is it intended for construction, bidding, or permits purposes.

The United States Government and the State of Texas do not endorse products or manufacturers. Trade or manufacturers' names appear herein solely because they are considered essential to the object of this report. The engineer in charge of the project was Chang-Seon Shon.

ACKNOWLEDGMENTS

The authors express their appreciation to the Texas Department of Transportation personnel for their support throughout this project, as well as the Federal Highway Administration. We thank a program coordinator, Dr. German Claros, P.E., and a project director, Dr. Jimmy Si, P.E. Ms. Caroline Herrera, P.E., Mr. Wade Blackmon, P.E., Mr. Miles Garrison, P.E., and Mr. Abbas Mehdibeigi, P.E., from TxDOT, have also been active in assisting the researchers with their valuable technical comments during this project.

TABLE OF CONTENTS

	Page
Chapter 1: Introduction.....	3
Chapter 2: Implementation Program.....	5
Research Objectives and Implementation Scope.....	5
Protocol for Rapid Field Detection of Sulfate and Organic Content in Soils.....	5
Selection of Implementation Site.....	7
Chapter 3: Evaluation of US67.....	9
Soil Sampling and Engineering Properties of Soil	9
Electrical Conductivity Analysis	12
Chapter 4: Evaluation of US82.....	19
Soil Sampling and Characterization of Soil Properties.....	19
Electrical Conductivity Analysis	22
Chapter 5: Development of Soil Sulfate Map.....	27
Overview of Veris Data Analysis for Soil Sulfate Mapping	27
Geospatial Data Grouping Analysis.....	27
Development of Soil Sulfate Map.....	31
Chapter 6: Discussion	35
Sensitivity of Soil Properties on Electrical Conductivity of Soil	35
Effect of Lime Treatment on Soil Properties and Electrical Conductivity.....	36
Comparison of TXDOT VERIS 3150 to TTI VERIS 3150 Units	40
Chapter 7: Conclusions and Recommendations	43
References.....	45
Appendix A: Creating Electrical Conductivity Map with ARCGIS-ARCMAP 10 Using Field Data Obtained from VERIS 3150 Device	47

Appendix B: Determination of Organic Carbon Content Using Stellarnet UV-VIS Spectrometer	59
Appendix C: VERIS Electrical Conductivity, Sulfate Content, Organic Content, Water Content, and Plasticity Index for Combined US67 and US82 Data	73

LIST OF FIGURES

	Page
Figure 2-1. Protocol for Rapid Field Detection of Sulfate and Organic Content in Soils. .	6
Figure 2-2. Principle of Operation for Veris EC Sensor.....	7
Figure 2-3. Selection of Implementation Sites.	8
Figure 3-1. Electrical Conductivity Data for Miller East (Scale 1:1500 and 0–2 Ft).....	9
Figure 3-2. Electrical Conductivity Data for Miller West (Scale 1:1500 and 0–2 Ft).....	10
Figure 3-3. Auger Used to Collect Soil Samples (Every 1 Ft to a Depth of 4 Ft).....	10
Figure 3-4. Relationship between EC and Sulfate Content through Average Values.	12
Figure 3-5. Natural Log of Sulfate Content versus Soil EC.	13
Figure 3-6. Relationship between Measured SC and Predicted SC.....	16
Figure 3-7. Relationship between EC and Sulfate Content (0–4 Ft).	17
Figure 4-1. Sampling Location on US82.	19
Figure 4-2. Electrical Conductivity Map on US82 (Sec. 0, Scale 1:5500 and 0–2 Ft).....	19
Figure 4-3. Electrical Conductivity Map on US82 (Sec. 1, Scale 1:5500 and 0–2 Ft).....	20
Figure 4-4. Electrical Conductivity Map on US82 (Sec. 2, Scale 1:5500 and 0–2 Ft).....	20
Figure 4-5. Electrical Conductivity Map on US82 (Sec. 3, Scale 1:5500 and 0–2 Ft).....	20
Figure 4-6. Natural Log of Sulfate Content versus Veris 3150 EC.	22
Figure 4-7. Relationship between Measured SC and Predicted SC.....	24
Figure 4-8. Relationship between Measured SC and Predicted SC Using All Soil Parameters.....	24
Figure 4-9. Relationship between EC and Sulfate Content (0–4 Ft).	25
Figure 5-1. Natural Log of Sulfate Content versus Veris 3150 EC.	28
Figure 5-2. Geospatially Grouped Transformed Sulfate Content and EC Data.	30
Figure 5-3. Relationship between Grouped EC and SC Data.	31
Figure 5-4. Electrical Conductivity and Sulfate Content Prediction Map (US67 East). ..	31
Figure 5-5. Electrical Conductivity and Sulfate Content Prediction Map (US67 West)..	32
Figure 5-6. Electrical Conductivity and Sulfate Content Prediction Map (US82).	32
Figure 6-1. Plasticity Index Changes before and after Lime Treatment on US82.....	37
Figure 6-2. Sulfate Content before and after Lime Treatment on US82.	38
Figure 6-3. Moisture Content before and after Lime Treatment on US82.	38

Figure 6-4. Organic Matter Content before and after Lime Treatment on US82.	39
Figure 6-5. Electrical Conductivity before and after Lime Treatment on US82 (Station 334 to 358).....	39
Figure 6-6. Electrical Conductivity Map (IH30–Spur 594 NE; 1:500 Scales).	40
Figure 6-7. Electrical Conductivity Map (US67 East; 1:1500 Scales).	41
Figure 6-8. Electrical Conductivity Map (US82 Station 258 to 291; 1:5500 Scales).....	41
Figure A-1. Insert SD Card into SD Drive on the Computer.....	49
Figure A-2. Open Data File with Excel.	49
Figure A-3. Combining Two Date Files into a Single Excel Sheet.....	50
Figure A-4. Label Columns.	50
Figure A-5. Removal of Anomalous Data.	51
Figure A-6. Saving the Edited File as an MS Excel Workbook.....	51
Figure A-7. Opening ArcMap.....	52
Figure A-8. Installation of Geostatistical Analyst.	52
Figure A-9. Adding Data to ArcMap.....	53
Figure A-10. Selection of X and Y Field.....	54
Figure A-11. Selection of Geographic Coordinate System.	54
Figure A-12. Utilization of Geostatistical Wizard for EC Mapping.....	55
Figure A-13. Creating Inversion Distance Weight Prediction Map	55
Figure A-14. Reclassification of EC Categories.....	56
Figure A-15. Producing EC Map Containing Field Collected Data.	57
Figure A-16. Addition of Legend, Scale Bar, Etc.....	57
Figure B-1. Materials for Preparing Reagents.	61
Figure B-2. Standard Materials and Their Organic Carbon Contents.	62
Figure B-3. Preparation of Soil Samples.	63
Figure B-4. Chemical Treatment to Extract Organic Matter.	64
Figure B-5. Stellarnet UV-VIS Spectrometer Device.....	65
Figure B-6. Connection of the BP2 Battery to the Power Regulator.....	66
Figure B-7. Connection of UV-VIS Tungsten Halogen Light Source to the Power Regulator.....	66

Figure B-8. Connection of Fiber Optic Cable to Green Wave Spectrometer and UV-VIS Tungsten Halogen Light Source.	67
Figure B-9. Connection of the Green Wave Spectrometer to Laptop Computer.....	67
Figure B-10. Spectrawiz Excel Spreadsheet for Measuring Soil Organic Carbon.	68
Figure B-11. Analysis Setup Procedure.....	69
Figure B-12. Collection of Dark Spectrum.....	69
Figure B-13. Collection of Reference Spectrum.....	70
Figure B-14. Measurement of Soil Organic Carbon Content.	71

LIST OF TABLES

	Page
Table 3-1. Engineering Properties of Soil Samples from US67 (0–2 Ft and 0–4 Ft).	11
Table 3-2. Data for Predicting EC Using Natural Log of Sulfate Content, Organic Content, Moisture Content, and Plasticity Index.....	13
Table 3-3. Multivariate Regression Output Using the Natural Log.....	14
Table 3-4. Robust Regression Output Using the Natural Log.	14
Table 3-5. Multivariate Regression Output Using the Natural Log (0–4 Ft).....	17
Table 3-6. Robust Regression Output Using the Natural Log (0–4 Ft).	18
Table 4-1. Engineering Properties of Soil Samples from US82 (0–2 Ft).	21
Table 4-2. Engineering Properties of Soil Samples from US82 (0–4 Ft).	21
Table 4-3. Multivariate Regression Output for Predicting Veris EC.....	23
Table 4-4. Robust Regression Output Using the Natural Log.	23
Table 4-5. Multivariate Regression Output Using the Natural Log (0–4 Ft).....	25
Table 4-6. Robust Regression Output Using the Natural Log (0–4 Ft).	26
Table 5-1. Veris Electrical Conductivity, Sulfate Content, Organic Content, Water Content, and Plasticity Index for Shallow Measurement (0–2 Ft).	28
Table 5-2. Multivariate Regression Output for Predicting Veris EC.....	29
Table 5-3. Robust Regression Output Using the Natural Log.	29
Table 5-4. Multiple Ordered Logit Regression Output.....	33
Table 6-1. Summary of All Regression Analyses Results.....	36
Table C-1. Data for All-Range Shallow EC and Average OC, MC, PI, and ln(SC).	74
Table C-2. Data for All-Range Shallow EC and All-Range OC, MC, PI, and ln(SC).	75
Table C-3. Data for Shallow EC _{>100} and Average OC, MC, PI, and ln(SC).	76
Table C-4. Data for Shallow EC _{>100} and All-Range OC, MC, PI, and ln(SC).	77
Table C-5. Data for All-Range Deep EC and Average OC, MC, PI, and ln(SC).....	78
Table C-6. Data for All-Range Deep EC and All-Range OC, MC, PI, and ln(SC).....	79
Table C-7. Data for Deep EC _{>100} and Average OC, MC, PI, and ln(SC).	80
Table C-8. Data for Deep EC _{>100} and All-Range OC, MC, PI, and ln(SC).....	81

EXECUTIVE SUMMARY

The protocol using the Veris 3150 for determining sulfate-rich soils has been implemented to two full-scale projects in Dallas and Paris Districts. The determination of organic-rich soils was not implemented in this project due to the unavailability of proper equipment. Researchers collected electrical conductivity (EC) data using two Veris 3150 units equipped at both TxDOT and TTI. Soil samples were collected based on EC color-coded map generated from the EC data. The data collected from these projects were analyzed to identify potential relationships between Veris EC measurements and sulfate contents for different types of soil.

Statistical modeling results indicate that Veris electrical conductivity is a linear function of the natural log of the sulfate content, directly if other soil parameters such as moisture content, organic matter content, and clay content remain constant. Higher EC of soil responds to higher sulfate content of soil. It is imperative that soil samples be collected based on the EC map generated from the Veris 3150 data for verification purpose. Therefore, researchers recommended that the Veris EC be used as a viable screening tool to detect sulfate content of soils.

A color-coded map indicates that the area with the greater EC shows the higher sulfate content. The comparison study of TxDOT and TTI Veris units shows that the two units produce comparable sets of data although the actual EC values may not be exactly matched.

CHAPTER 1: INTRODUCTION

In roadway construction, there are many different methods to stabilize a subgrade. These include thermal, electrical, mechanical, and chemical stabilization. Among these, mechanical and chemical stabilization are the most commonly used because they are fast, efficient, and reliable (Puppala et al., 2003). Mechanical stabilization is simply achieved by physical soil modification processes using compaction or fiber reinforcement of subgrade, while chemical stabilization is achieved by mixing the subgrade with calcium-based cementitious materials such as portland cement, lime, and fly ash. It has also been well established that chemical stabilization utilizing these additives can enhance many engineering properties of the subgrade, such as compressive strength, resilient modulus, shear strength, plasticity, and long-term durability.

When a calcium-based stabilizing material is combined with the subgrade, it also provides an excellent source of fine materials to the mixture. Simultaneously, the calcium hydroxide content of cementitious materials promotes a pozzolanic reaction with the silica and alumina of the system. Due to the existence of cementing products, such as calcium silicate hydrate (C-S-H) or calcium aluminate hydrate (C-A-H), this reaction leads to a progressive increase in strength (Saylak et al., 2005).

A number of cases have been reported where a cement- or lime-stabilized subgrade had experienced a significant amount of heave leading to pavement failure. This problem was due to the formation of ettringite, which is a highly expansive crystalline mineral resulting from the chemical reaction between soluble sulfate minerals in the soil and the lime or cement added for stabilization (Harris et al., 2004).

Additionally, pavement subgrade stabilized by cement or lime in some regions of the state with organic-rich soil also underwent rapid deterioration. This was due to the loss of subgrade stabilizer effectiveness through the following mechanisms:

- Alteration of the composition and structure of C-S-H gel.
- A delayed strengthening reaction.

- Limiting the water available for hydration due to water absorption.
- Limited availability of Ca^{2+} ions for the pozzolanic reaction due to their consumption by organic matter (Tastan et al., 2011).

The potential for sulfate attack on soils stabilized using calcium-based stabilizing materials and the effect of organic matter on the stabilization of soil are widely recognized and documented. Laboratory test methods to determine both sulfate and organic contents are also well established. However, only limited research work has been carried out for determining both sulfate and organic content in the field. Using multivariate statistical analyses, the research team identified that soil conductivity is related to the sulfates, moisture content, and plasticity of the clay, but has poor correlation to organic content of soil in research project 0-6362 (Report 6362-1 Rapid Field Detection of Sulfate and Organic Content in Soils).

In this implementation project, the protocol developed in Project 0-6362 using a device called Veris 3150 system was applied to determine sulfate and organic-rich soils in full-scale projects in selected districts. Electrical conductivity (EC) data collected using two Veris 3150 devices at both Texas Transportation Institute (TTI) and Texas Department of Transportation (TxDOT) were analyzed to identify potential relationships between EC measurements and sulfate contents for different types of soils. An EC color-coded map was constructed based on the data collected using Arc GIS software to help identify sampling locations where high sulfate soil may exist. Furthermore, EC data collected before and after lime treatment were compared in Paris District.

CHAPTER 2: IMPLEMENTATION PROGRAM

RESEARCH OBJECTIVES AND IMPLEMENTATION SCOPE

An objective of this research is to implement the Veris 3150 system for identifying sulfate- and organic-rich soils and to help districts select the best remediation techniques in the problematic areas. The organic-rich soil identification was not implemented due to the unavailability of equipment. The potential savings with the implementation of this system are substantial since this device can be applied for developing rehabilitation options for existing roads that have sulfate-bearing soils. This goal was accomplished by a two-phase comprehensive program: (1) implementing the testing protocol using the Veris 3150 to full-scale projects in selected districts, and (2) training and demonstrating TxDOT personnel how to analyze the conductivity data.

The protocol developed as a part of the Research Project 0-6362 using the Veris 3150 for determination of sulfate-rich soils has been implemented to two full scale projects in Dallas and Paris Districts. Researchers at both Texas Transportation Institute and Texas Department of Transportation collected electrical conductivity data with their Veris 3150 units simultaneously. Soil samples for plasticity index, moisture content, sulfate content, and organic content tests were collected on the basis of the EC color-coded map. The TTI researchers analyzed the data collected from these projects to identify potential relationships between conductivity measurements and sulfate contents for different types of soil.

PROTOCOL FOR RAPID FIELD DETECTION OF SULFATE CONTENT IN SOILS

Figure 2-1 illustrates an overview of the steps recommended to conduct the protocol for rapid field detection of sulfate content in soils. The first step is to collect electrical conductivity data by scanning roadways with the Veris 3150 instrument. The Veris 3150 unit uses coulter electrodes to make contact with the soil and to measure the EC. Figure 2-2 shows that three pairs of coulter electrodes are mounted on a toolbar. Selected coulter electrodes act as transmitting electrodes, which provide electrical current into the soil, while

other coulters act as receiving electrodes that measure the voltage drop between them. Soil EC information is recorded in a data logger along with location information by a global positioning system (GPS). Because the Veris 3150 unit uses contact sensor measurements, coulters need to penetrate 1-2 inches into the soil.

The second step is to create the EC color-coded map using the Geostatistical Analyst of the ArcGIS® 10.1 software package. A well-known spatial interpolation technique, Inverse Distance Weighting (IDW) is applied for generating the EC color-coded map. Appendix A describes a more detailed procedure to create this map.

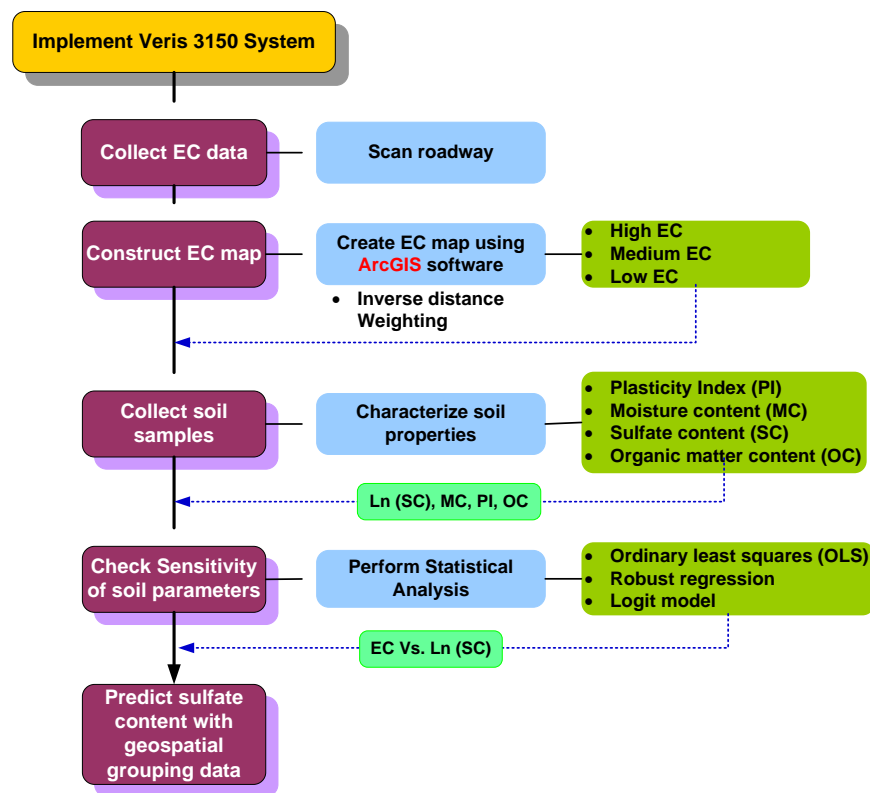


Figure 2-1. Protocol for Rapid Field Detection of Sulfate Content in Soils.

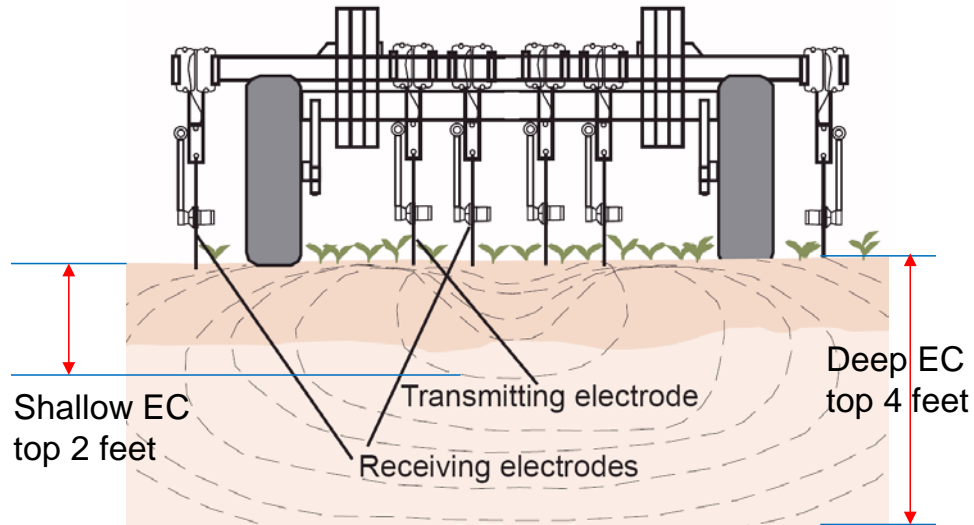


Figure 2-2. Principle of Operation for Veris EC Sensor.

The third step is to collect soil samples and analyze soil properties such as plasticity index, moisture content, organic content, and sulfate content. Soil sampling location is selected on the basis of EC changes on the EC map and the soil samples are obtained in 1-ft increments up to a depth of 4 ft. The multiple lab soil measurements collected for each depth are conducted in accordance with TxDOT standard testing procedures.

The next step is to check the sensitivity of soil parameters affecting a field soil's EC. Exploratory analysis including descriptive statistics such as multivariate regression, robust regression, and a logit model is implemented.

The final step is to develop the prediction maps of sulfate content for an individual project using interpolation procedures with geospatial grouping data. The geospatial grouping approach will usually result in a model with lower standard error and better fit.

SELECTION OF IMPLEMENTATION SITE

Figure 2-3 shows that three different test sites located in the Dallas, Paris, and Atlanta Districts were selected for this implementation study. These geographic regions of Texas had well-documented data that their soils contained considerable concentrations

of soluble sulfate and had reported cases of problems caused by the stabilization of the subgrade using calcium-based additives.

The protocol for rapid field detection of sulfate content in soils, developed as a part of Research Project 0-6362 using the Veris 3150 for determining sulfate-rich soils, has been implemented on two full-scale projects in Dallas and Paris Districts. For the test site at the intersection of IH30 and Spur594, the protocol could not be applied because the soil samples could not be obtained.

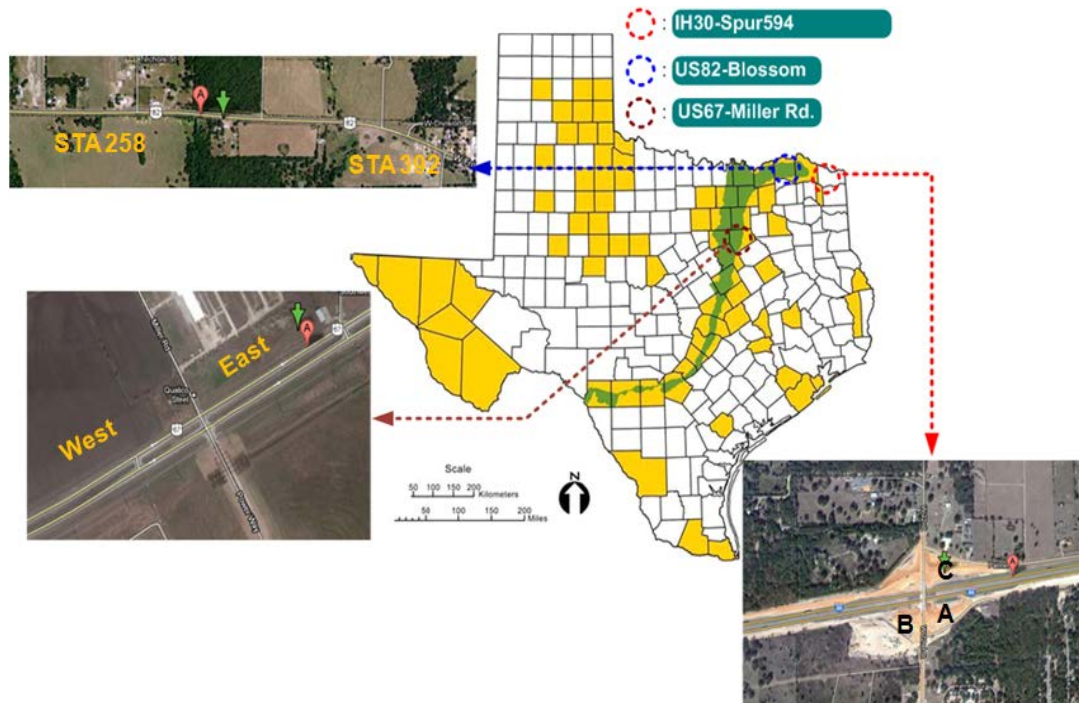


Figure 2-3. Selection of Implementation Sites.

CHAPTER 3: EVALUATION OF US67

SOIL SAMPLING AND ENGINEERING PROPERTIES OF SOIL

As described earlier, the research team had an opportunity to evaluate the Veris 3150 protocol on a project in Dallas District. The project was at the intersection of US67 and Miller Road. Electrical conductivity data at both shallow (up to 2 ft) and deep (up to 4 ft) readings were collected using Veris 3150 machine for both west and east sides of Miller Road.

Figures 3-1 and 3-2 show the EC data from the Veris 3150 plotted with ArcGIS software using the Inverse Distance Weighting interpolation method. The data were grouped into six classifications. The diamond spot on the figures represent the GPS coordinates as well as the trace of the readings that Veris 3150 had collected.

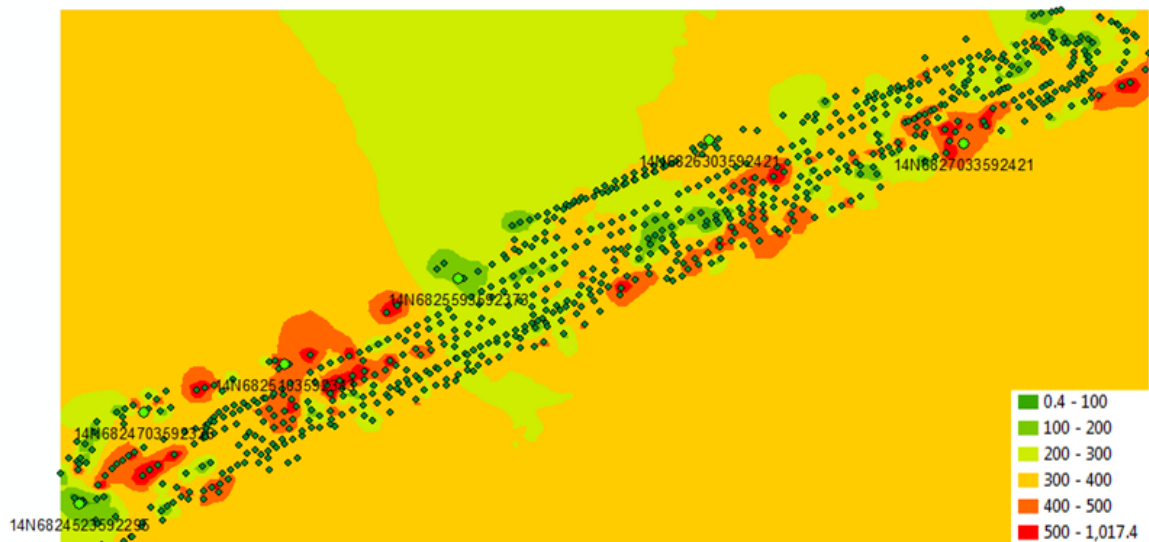


Figure 3-1. Electrical Conductivity Data for Miller East (Scale 1:1500 and 0–2 Ft).



Figure 3-2. Electrical Conductivity Data for Miller West (Scale 1:1500 and 0–2 Ft).

Based on EC changes, two high-, two medium-, and two low-conductivity areas were selected for collection of soil samples. The soil samples were obtained in 1-ft increments to a depth of 4 ft in six areas that represented large variations in EC. Figure 3-3 shows the soil samples were taken using an auger attached to a Bobcat.



Figure 3-3. Auger Used to Collect Soil Samples (Every 1 Ft to a Depth of 4 Ft).

Soil texture, cation exchange capacity (CEC), moisture conditions, organic matter, salinity, and subsoil characteristics all affect soil EC. Harris et al. (2011) reported that high EC in soil is caused by increased clay content, increased moisture content, and dissolved ions in solution. Therefore, four soil parameters including moisture content, plasticity index, organic content, and sulfate content were measured to determine the relationship between EC and sulfate content.

Table 3-1 shows engineering properties of the soils along with EC data obtained from the east and west sides of US67 Miller Road. The plasticity index of these soils ranged from 32 to 38 regardless of depth and was determined to be relatively high. The moisture content of the soils also ranged from 20 to 30 percent and did not vary significantly with the depth. The organic matter contents do not necessarily show a decreasing trend with depth. However, the sulfate content of the top 0–2 feet of the soil is lower than that of 0–4 feet soil. In general, sulfate salt can be easily dissolved with water and penetrate into the ground. Therefore, 0–4 feet soil seems to contain more sulfate than topsoil.

Table 3-1. Engineering Properties of Soil Samples from US67 (0–2 Ft and 0–4 Ft).

Sample ID	EC Shallow (0-2 ft)	SC-avg.	OC_avg.	MC_avg.	PI_avg.
US67 (MW)-H1-1	392.975	635	2.931574	27.94649	34.95441
US67 (MW)-H2-1	339.738	905	2.702655	27.20052	29.39879
US67 (MW)-M2-1	142.415	105	2.311651	27.58761	34.12721
US67 (ME)-H1-1	444.808	1555	3.166768	29.73874	38.45446
US67 (ME)-M1-1	336.807	200	2.859623	30.40501	37.44797
US67 (ME)-M2-1	288.077	140	2.133216	29.31561	36.12919
US67 (ME)-L1-1	51.1545	240	3.255291	25.68263	32.12448
US67 (ME)-L2-1	110.733	125	3.539853	20.54208	37.17692
Sample ID	EC Deep (0-4 ft)	SC-avg.	OC_avg.	MC_avg.	PI_avg.
US67 (MW)-H1-4	135.422	1032.5	2.896531	30.00686	36.05086
US67 (MW)-H2-4	139.492	1222.5	2.520075	29.9823	32.48766
US67 (MW)-M2-4	97.9775	288.75	2.304114	29.05221	33.33691
US67 (ME)-H1-4	397.482	8587.5	2.365159	29.60519	38.22562
US67 (ME)-M1-4	231.107	8997.5	2.120001	29.24655	34.80691
US67 (ME)-M2-4	317.735	561.25	1.721706	30.90202	38.41846
US67 (ME)-L1-4	36.7984	4182.5	2.896626	31.65751	35.11701
US67 (ME)-L2-4	145.233	8103.75	2.426793	24.65767	37.21192

ELECTRICAL CONDUCTIVITY ANALYSIS

The main objective of this project was to evaluate how the Veris EC device can be used to detect geospatial zones of high sulfate content (SC). To accomplish this goal, researchers analyzed Veris EC data to find the relationship between Veris EC and soil sulfate content by using several statistical models as described in Chapter 2.

EC Shallow (0–2 ft) Data Analysis

To begin the data review, a simple correlation between soil SC and soil EC was determined (see Figure 3-4). The correlation coefficient (R^2 value) of the best-fit curve through all points is 0.50, indicating a relationship between EC and SC. However, multiple factors such as moisture content, plasticity index, organic content, and sulfate content all affect electrical conductivity data. Therefore, the research team employed a cross-section multivariate analysis.

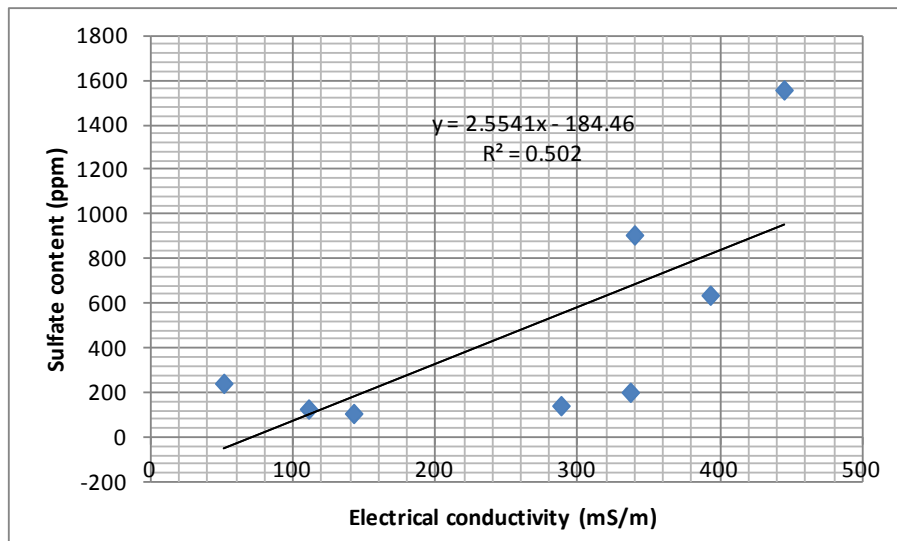


Figure 3-4. Relationship between EC and Sulfate Content through Average Values.

Before performing the regression analysis, the research team took the natural log of the measured sulfate contents, $\ln(SC)$, to make this relationship between sulfate content (expressed as a natural log of the measured value) and measured EC appear linear (see Figure 3-5).

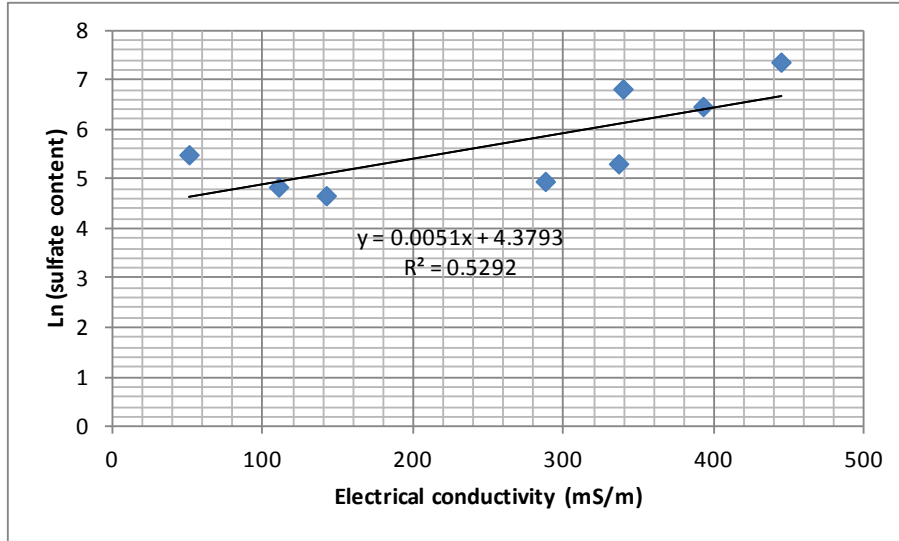


Figure 3-5. Natural Log of Sulfate Content versus Soil EC.

Using the transformed data in Table 3-2, where the sulfate contents are expressed as the natural log of the measured concentration, researchers developed the multivariate regression to predict the Veris EC from sulfate content.

Table 3-2. Data for Predicting EC Using Natural Log of Sulfate Content, Organic Content, Moisture Content, and Plasticity Index.

Sample ID	EC Shallow (0-2 ft)	Ln (SC-avg.)	OC_avg.	MC_avg.	PI_avg.
US67 (MW)-H1-1	392.975	6.454	2.932	27.946	34.954
US67 (MW)-H2-1	339.738	6.808	2.703	27.201	29.399
US67 (MW)-M2-1	142.415	4.654	2.312	27.588	34.127
US67 (ME)-H1-1	444.808	7.349	3.167	29.739	38.454
US67 (ME)-H2-1	486.439	5.298	2.742	26.230	34.193
US67 (ME)-M1-1	336.807	4.942	2.860	30.405	37.448
US67 (ME)-M2-1	288.077	5.481	2.133	29.316	36.129
US67 (ME)-L1-1	51.155	4.828	3.255	25.683	32.124
Sample ID	EC Deep (0-4 ft)	Ln (SC-avg.)	OC_avg.	MC_avg.	PI_avg.
US67 (MW)-H1-4	135.422	6.940	30.007	36.051	36.051
US67 (MW)-H2-4	139.492	7.109	29.982	32.488	32.488
US67 (MW)-M2-4	97.978	5.666	29.052	33.337	33.337
US67 (ME)-H1-4	397.482	9.058	29.605	38.226	38.226
US67 (ME)-M1-4	231.107	9.105	29.247	34.807	34.807
US67 (ME)-M2-4	317.735	6.330	30.902	38.418	38.418
US67 (ME)-L1-4	36.798	8.339	31.658	35.117	35.117
US67 (ME)-L2-4	145.233	9.000	24.658	37.212	37.212

The results in Table 3-3 show that only the regression coefficient for ln(SC) is significant at the 90 percent confidence level. Thus, the multivariate analysis with these data shows EC as a function of sulfate content and intercept. This means that, given constant plasticity, percent moisture content, and percent organic content, the Veris EC can be described as correlating directly with the sulfate content.

To verify this relationship, the research team performed a robust regression analysis. In fact, robust regression is used as an alternative to least squares regression when data are contaminated with outliers or influential observations; it can also be used to detect influential observations. The results in Table 3-4 using the robust model are similar to the results in Table 3-3. These test results support the previous finding that the Veris EC has correlated directly with the sulfate content (Harris et al., 2011).

Table 3-3. Multivariate Regression Output Using the Natural Log.

```
. regress shallow oc_avg mc_avg pi_avg lnscavg
```

Source	SS	df	MS	Number of obs = 8		
Model	126345.326	4	31586.3316	F(4, 3) =	5.21	
Residual	18170.964	3	6056.98798	Prob > F	= 0.1031	
Total	144516.29	7	20645.1843	R-squared	= 0.8743	
				Adj R-squared	= 0.7066	
				Root MSE	= 77.827	

shallow	Coef.	Std. Err.	t	P> t	[95% Conf. Interval]	
oc_avg	-136.1903	113.1394	-1.20	0.315	-496.2503	223.8696
mc_avg	2.785829	17.48539	0.16	0.884	-52.8605	58.43216
pi_avg	21.20578	11.93914	1.78	0.174	-16.78991	59.20146
lnscavg	124.4167	44.00407	2.83	0.066	-15.62392	264.4573
_cons	-877.0712	525.2738	-1.67	0.194	-2548.727	794.5845

Table 3-4. Robust Regression Output Using the Natural Log.

```
Robust regression
```

				Number of obs = 8		
				F(4, 4) =	4.17	
				Prob > F	= 0.0977	

shallow	Coef.	Std. Err.	t	P> t	[95% Conf. Interval]	
oc_avg	-133.417	121.7117	-1.10	0.335	-471.3428	204.5088
mc_avg	2.980208	19.42904	0.15	0.886	-50.96346	56.92388
pi_avg	21.6421	13.73378	1.58	0.190	-16.48898	59.77319
lnscavg	126.1562	48.69625	2.59	0.061	-9.046255	261.3587
_cons	-914.8845	586.2921	-1.56	0.194	-2542.692	712.9233

The results thus far show that the Veris EC is a linear function of the natural log of the sulfate content with electrical conductivity if other soil parameters remain constant. The regression equation (Eq. 3-1) was achieved as follows:

$$\ln(\text{SC}) = 0.0051 (\text{EC}) + 4.38 \quad (\text{Eq. 3-1})$$

where SC = sulfate content and EC = electrical conductivity.

Figure 3-6 shows the comparison of measured SC to predicted SC. The correlation coefficient measures the SC of the relationship between the measured and calculated SC data. The standard error of the estimate is the square root of the average of the squared prediction residuals over the prediction period. The R^2 value of 0.69 was achieved.

Although both models in Tables 3-3 and 3-4 reduced the number of predictor variables down to one instead of four, the real desire is to consider all parameters. Therefore, an investigation was initiated to define, by multivariate regression, a simple prediction formula that defines sulfate content as a function of those four parameters:

$$\text{SC} = \text{A}(\text{EC}) + \text{B}(\text{MC}) + \text{C}(\text{OC}) + \text{D}(\text{PI}) + \text{E} \quad (\text{Eq. 3-2})$$

where SC = sulfate content, EC = electrical conductivity, MC = moisture content; OC = organic content; PI = plasticity index; and A, B, C, D, E = regression coefficient.

Figure 3-6 shows a scatter plot of experimentally measured SC versus calculated SC. The R^2 was computed to be 0.76. Apparently, the prediction model on the basis of best-fit analysis provides an accurate prediction of the measured SC, but a measure of the quality of fit needs to be on the basis of lab-derived parameters to field-derived SC.

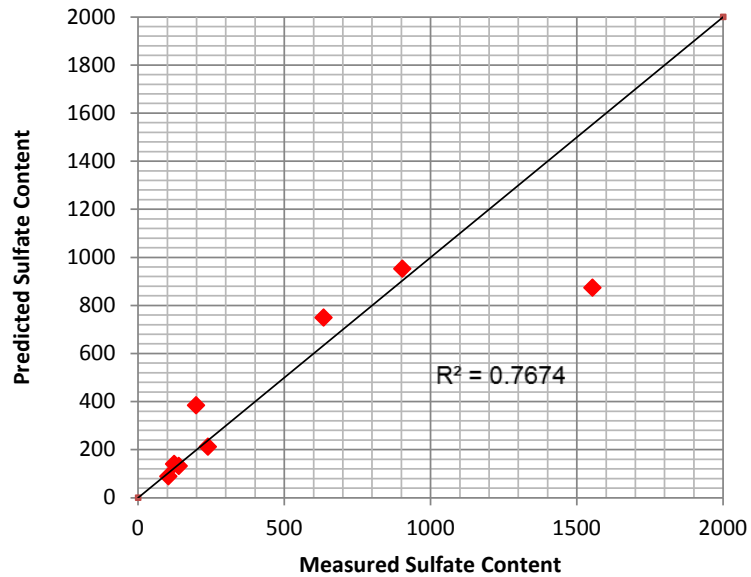


Figure 3-6. Relationship between Measured SC and Predicted SC.

EC Deep (0–4 ft) Data Analysis

The same EC data analysis procedure for deep EC data (0–4 ft) was applied to check the sensitivity of soil parameters listed in Table 3-2 and Figure 3-7. At 0–4 ft, sulfate content does not appear to vary linearly with the EC. Using the transformed data expressed as the natural log of the measured concentration, both the multivariate regression and robust regression were conducted to predict the Veris EC from sulfate content. The intercept and coefficient for all soil properties are not significant at the 90 percent confidence level (see Tables 3-5 and 3-6).

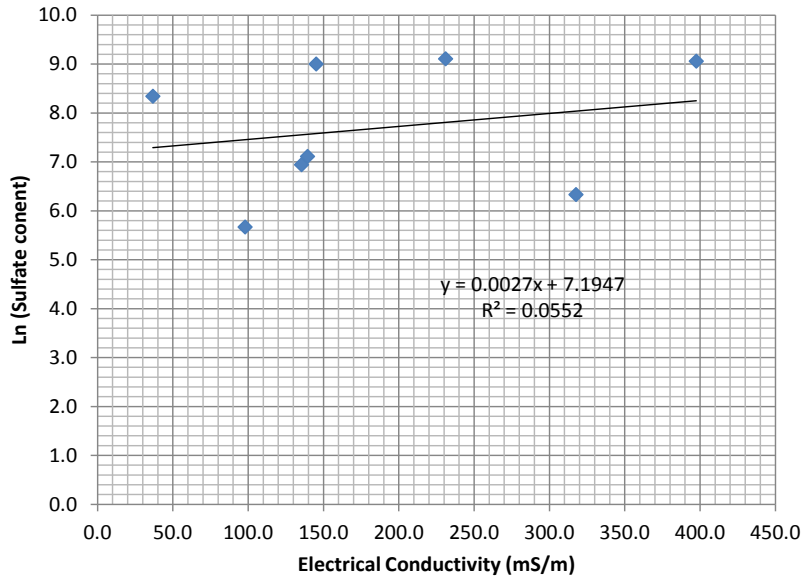


Figure 3-7. Relationship between EC and Sulfate Content (0–4 Ft).

Table 3-5. Multivariate Regression Output Using the Natural Log (0–4 Ft).

```
. regress deep oc_avg mc_avg pi_avg lnscavg
```

Source	SS	df	MS	Number of obs = 8		
Model	70345.2806	4	17586.3201	F(4, 3) =	1.75	
Residual	30135.9843	3	10045.3281	Prob > F =	0.3367	
Total	100481.265	7	14354.4664	R-squared =	0.7001	
				Adj R-squared =	0.3002	
				Root MSE =	100.23	

deep	Coef.	Std. Err.	t	P> t	[95% Conf. Interval]	
oc_avg	-162.2187	105.6008	-1.54	0.222	-498.2875	173.85
mc_avg	13.87336	19.68583	0.70	0.532	-48.77573	76.52244
pi_avg	25.04436	19.74035	1.27	0.294	-37.77823	87.86695
lnscavg	24.03362	32.73112	0.73	0.516	-80.13142	128.1987
_cons	-909.7438	981.0578	-0.93	0.422	-4031.908	2212.42

Table 3-6. Robust Regression Output Using the Natural Log (0–4 Ft).

```
. rreg deep oc_avg mc_avg pi_avg lnsavg
      Huber iteration 1: maximum difference in weights = .43662405
      Huber iteration 2: maximum difference in weights = .10229936
      Huber iteration 3: maximum difference in weights = .11912587
      Huber iteration 4: maximum difference in weights = .0813094
      Huber iteration 5: maximum difference in weights = .06409254
      Huber iteration 6: maximum difference in weights = .04858848
Biweight iteration 7: maximum difference in weights = .15776742
Biweight iteration 8: maximum difference in weights = .24696016
Biweight iteration 9: maximum difference in weights = .15894516
Biweight iteration 10: maximum difference in weights = .3943475
all weights went to zero;
no observations
```

CHAPTER 4: EVALUATION OF US82

SOIL SAMPLING AND CHARACTERIZATION OF SOIL PROPERTIES

To further investigate the relationship between electrical conductivity and sulfate content, another project was conducted on Blossom-US82 in Paris District as described in Chapter 2. Electrical conductivity data at both shallow (up to 2 ft) and deep (up to 4 ft) readings using the Veris 3150 machine were collected between stations 258+00 and 384+00. Figure 4-1 illustrates the soil sampling locations.



Figure 4-1. Sampling Location on US82.

As shown in Figures 4-2 through 4-5, the EC data from the Veris 3150 were plotted with ArcGIS software using the Inverse Distance Weighting interpolation method. The data were grouped into six classifications and plotted. Based on EC changes, two high-, two medium-, and two low-conductivity areas at each section were selected from which to collect soil samples. The green color spots on the EC maps represent soil sampling locations. The soil samples were obtained in 1-ft increments to a depth of 4 ft in six areas that represented large variations in EC.

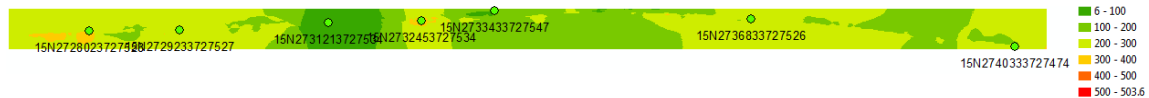


Figure 4-2. Electrical Conductivity Map on US82 (Sec. 0, Scale 1:5500 and 0–2 Ft).



Figure 4-3. Electrical Conductivity Map on US82 (Sec. 1, Scale 1:5500 and 0–2 Ft).

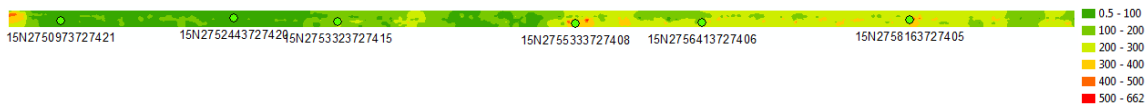


Figure 4-4. Electrical Conductivity Map on US82 (Sec. 2, Scale 1:5500 and 0–2 Ft).

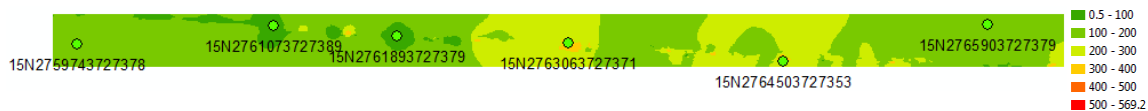


Figure 4-5. Electrical Conductivity Map on US82 (Sec. 3, Scale 1:5500 and 0–2 Ft).

As described in Chapter 3, four soil parameters including moisture content (MC), plasticity index (PI), organic content (OC), and sulfate content (SC) were measured to determine the relationship between EC and SC. Table 4-1 shows engineering properties of the soils along with EC data (0–2 ft) obtained on US82. The PI of these soils varies from 22 to 50 and is determined to be high. The MC of soils also ranged from 13 to 30 and the OC shows large variation from 0.3 to 3.0. The highest SC on this top soil (0–2 ft) was 1220 ppm and this soil was determined to contain low sulfate.

Table 4-2 gives the soil properties at 0–4 ft depth on US82. All obtained soil properties are varied and each soil parameter is relatively lower than that at the 0–2 ft depth.

Table 4-1. Engineering Properties of Soil Samples from US82 (0–2 Ft).

Station No.	Sample ID	EC Shallow (0-2 ft)	SC-avg.	OC_avg.	MC_avg.	PI_avg.	Ln (Sc-avg)
258+65	US82-H1-1	296.133	487.5	0.573064	24.7754	46.44893	6.19
273+18	US82-H2-1	328.752	1220	0.443506	23.09838	44.53815	7.11
287+46	US82-M1-1	239.931	955	0.62914	21.64843	50.14149	6.86
262+35	US82-M2-1	236.155	700	0.467743	24.07009	41.30566	6.55
269+10	US82-L1-1	49.0989	122.5	0.527754	17.24768	22.24233	4.81
276+46	US82-L2-1	114.866	110	0.510002	18.04266	33.18525	4.70
327+75	US82-S1-H1-1	462.74	480	0.906862	22.60516	39.65889	6.17
332+83	US82-S1-H2-1	355.077	680	2.547969	22.35231	48.5001	6.52
312+80	US82-S1-M1-1	163.669	240	0.546594	27.50182	39.68782	5.48
314+18	US82-S1-M2-1	271.47	520	0.506704	21.00602	41.50627	6.25
310+75	US82-S1-L1-1	80.7868	290	0.769787	12.9653	41.65131	5.67
322+32	US82-S1-L2-1	78.9403	352.5	3.040613	17.03376	39.13322	5.87
348+50	US82-S2-H1-1	390.088	475	1.665025	20.39022	42.90251	6.16
357+75	US82-S2-H2-1	336.003	295	0.325055	24.98475	40.27898	5.69
341+82	US82-S2-M1-1	252.729	220	0.313674	30.21631	44.4971	5.39
352+00	US82-S2-M2-1	278.993	495	1.253118	26.40745	40.46836	6.20
334+16	US82-S2-L1-1	55.1563	140	0.47251	26.74831	25.13383	4.94
338+79	US82-S2-L2-1	61.5419	100	0.579956	26.81619	26.63872	4.61
373+81	US82-S3-H1-1	301.879	202.5	0.63971	21.04139	34.42811	5.31
378+65	US82-S3-H2-1	326.329	450	0.932022	22.77265	29.16052	6.11
363+00	US82-S3-M1-1	132.846	220	0.698308	22.70902	34.06075	5.39
383+20	US82-S3-M2-1	143.52	280	0.576256	17.08272	35.80724	5.63
367+20	US82-S3-L1-1	69.1454	100	0.663894	13.83161	26.76813	4.61
370+34	US82-S3-L2-1	29.0198	215	1.410642	25.24618	26.36132	5.37

Table 4-2. Engineering Properties of Soil Samples from US82 (0–4 Ft).

Station No.	Sample ID	EC Deep (0-4 ft)	SC-avg.	OC_avg.	MC_avg.	PI_avg.	Ln (Sc-avg)
258+65	US82-H1-1	117.263	306.25	0.510575	25.05419	39.52047	5.72
273+18	US82-H2-1	137.163	673.75	0.427126	22.93428	33.77005	6.51
287+46	US82-M1-1	148.74	598.75	0.574817	24.77818	42.90493	6.39
262+35	US82-M2-1	131.059	520	0.479733	25.33754	34.56261	6.25
269+10	US82-L1-1	51.4695	111.25	0.489599	18.51666	24.79983	4.71
276+46	US82-L2-1	96.222	105	0.423996	15.03454	20.72428	4.65
327+75	US82-S1-H1-1	205.252	318.75	0.692292	21.72821	30.564	5.76
332+83	US82-S1-H2-1	187.22	402.5	2.937814	22.75956	33.68441	6.00
312+80	US82-S1-M1-1	98.203	233.75	0.555459	22.71222	36.08735	5.45
314+18	US82-S1-M2-1	153.841	343.75	0.4009	23.3145	37.38848	5.84
310+75	US82-S1-L1-1	60.9678	262.5	0.669154	14.19963	36.54768	5.57
322+32	US82-S1-L2-1	63.7959	330	1.770131	23.36977	42.65334	5.80
348+50	US82-S2-H1-1	240.734	296.25	1.403928	23.34588	33.27494	5.69
357+75	US82-S2-H2-1	178.774	406.25	0.431138	24.216	36.05685	6.01
341+82	US82-S2-M1-1	134.638	413.75	0.238781	28.32155	46.7503	6.03
352+00	US82-S2-M2-1	151.467	312.5	0.959648	26.14872	39.91029	5.74
334+16	US82-S2-L1-1	35.5878	131.25	0.286817	25.73084	26.06212	4.88
338+79	US82-S2-L2-1	47.9819	426.25	0.766524	27.84687	39.3683	6.06
373+81	US82-S3-H1-1	165.984	186.25	0.68935	22.77524	33.92672	5.23
378+65	US82-S3-H2-1	59.7041	468.75	0.764409	22.04117	27.3185	6.15
363+00	US82-S3-M1-1	89.4058	160	0.640508	23.88109	31.67153	5.08
383+20	US82-S3-M2-1	93.0676	325	1.084481	21.1691	39.63802	5.78
367+20	US82-S3-L1-1	73.4058	100	0.630497	15.52158	18.32111	4.61
370+34	US82-S3-L2-1	40.0967	157.5	0.961703	23.13485	23.83136	5.06

ELECTRICAL CONDUCTIVITY ANALYSIS

EC Shallow (0–2 ft) Data Analysis

As shown in Figure 4-6, the linear relationship between the natural log of the measured sulfate content, $\ln(\text{SC})$, and EC was first identified.

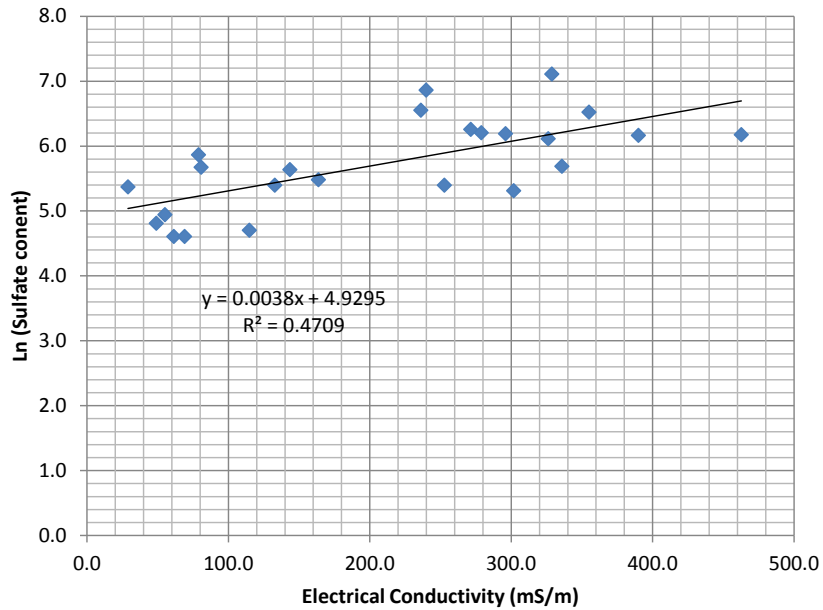


Figure 4-6. Natural Log of Sulfate Content versus Veris 3150 EC.

Next, the multivariate regression presented in Table 4-3 was developed to predict the Veris EC from SC using MC, OC, PI, and $\ln(\text{SC})$ listed in Table 4-1. Similar to the top 0–2 ft soil data analysis for US67, only the regression coefficient for $\ln(\text{SC})$ is significant at the 90 percent confidence level. Thus, the multivariate analysis with these data shows EC as a function of sulfate content and intercept. This means the Veris EC has a direct correlation with the sulfate content.

Robust regression analysis was performed to verify this relationship. The same test results were obtained from the robust model (see Table 4-4). The results thus far show that the Veris EC is a linear function of $\ln(\text{SC})$ if other soil parameters remain constant.

Table 4-3. Multivariate Regression Output for Predicting Veris EC.

```
. regress ecshallow02ft oc_avg mc_avg pi_avg lnscavg
```

Source	SS	df	MS			
Model	194595.013	4	48648.7532	Number of obs =	24	
Residual	174009.954	19	9158.41865	F(4, 19) =	5.31	
Total	368604.967	23	16026.3029	Prob > F =	0.0048	
				R-squared =	0.5279	
				Adj R-squared =	0.4285	
				Root MSE =	95.7	

ecshallow0~t	Coef.	Std. Err.	t	P> t	[95% Conf. Interval]	
oc_avg	-13.60613	31.03515	-0.44	0.666	-78.56345	51.3512
mc_avg	4.493511	4.763789	0.94	0.357	-5.477214	14.46423
pi_avg	3.82164	4.093347	0.93	0.362	-4.745835	12.38911
lnscavg	89.29133	46.30129	1.93	0.069	-7.618382	186.201
_cons	-531.1543	191.3933	-2.78	0.012	-931.745	-130.5635

Table 4-4. Robust Regression Output Using the Natural Log.

```
Robust regression
```

ecshallow0~t	Coef.	Std. Err.	t	P> t	[95% Conf. Interval]	
oc_avg	-12.96047	34.00109	-0.38	0.707	-84.12557	58.20464
mc_avg	4.361353	5.21905	0.84	0.414	-6.562244	15.28495
pi_avg	4.240714	4.484537	0.95	0.356	-5.145529	13.62696
lnscavg	82.43697	50.72617	1.63	0.091	-23.73412	188.6081
_cons	-511.0265	209.6842	-2.44	0.025	-949.9006	-72.15245

The comparison chart of measured SC to predicted SC was obtained using the following regression equation (Eq. 4-1) and was given in Figure 4-7. The correlation coefficient was 0.23 between the measured and calculated SC data.

$$\ln(\text{SC}) = 0.0041 (\text{EC}) + 5.10 \quad (\text{Eq. 4-1})$$

where SC = sulfate content and EC = electrical conductivity.

Although the relationship that Veris EC is a linear function of $\ln(\text{SC})$ was obtained from Tables 4-3 and 4-4, the prediction model considering all soil parameters such as SC, OC, EC, and PI was developed again as described in Chapter 3. Figure 4-8 gives a scatter plot of experimentally measured versus calculated sulfate contents. The R^2 was computed to be 0.44.

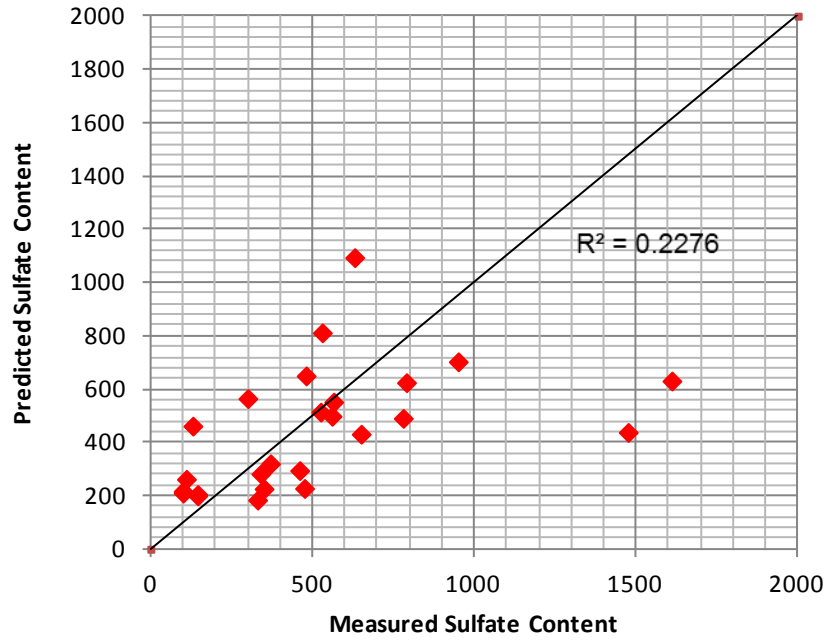


Figure 4-7. Relationship between Measured SC and Predicted SC.

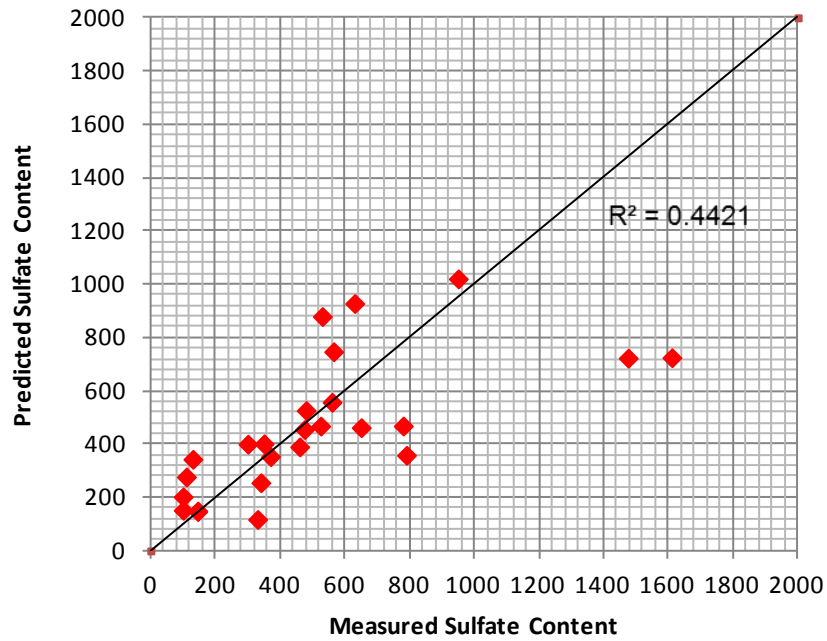


Figure 4-8. Relationship between Measured SC and Predicted SC Using All Soil Parameters.

EC Deep (0–4 ft) Data Analysis

The same EC data analysis procedure for deep EC data (0–4 ft) was applied to check the sensitivity of soil parameter listed in Table 4-2 and Figure 4-9. Using the transformed data expressed as the natural log of the measured concentration, both the multivariate regression and robust regression were conducted to predict the Veris EC from sulfate content. Similar to US67, sulfate content for 0–4 ft soil does not appear to be a linear relationship with the EC as shown in Tables 4-5 and 4-6. The intercept and coefficient for all soil properties are not significant at the 90 percent confidence level.

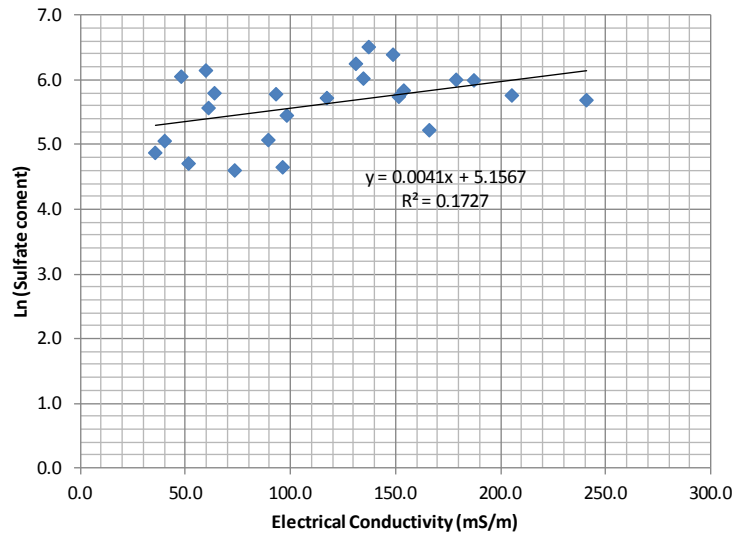


Figure 4-9. Relationship between EC and Sulfate Content (0–4 Ft).

Table 4-5. Multivariate Regression Output Using the Natural Log (0–4 Ft).

```
. regress ecdeep04ft oc_avg mc_avg pi_avg lnscavg
```

Source	SS	df	MS			
Model	14817.8918	4	3704.47295	Number of obs =	24	
Residual	58679.5803	19	3088.39896	F(4, 19) =	1.20	
Total	73497.4721	23	3195.54227	Prob > F =	0.3433	
				R-squared =	0.2016	
				Adj R-squared =	0.0335	
				Root MSE =	55.573	

ecdeep04ft	Coef.	Std. Err.	t	P> t	[95% Conf. Interval]	
oc_avg	17.13766	20.44916	0.84	0.412	-25.66293	59.93825
mc_avg	.2182806	4.065826	0.05	0.958	-8.291591	8.728152
pi_avg	.0741495	2.445959	0.03	0.976	-5.045302	5.193601
lnscavg	38.25578	30.67781	1.25	0.228	-25.95361	102.4652
_cons	-120.9198	129.1278	-0.94	0.361	-391.1874	149.3478

Table 4-6. Robust Regression Output Using the Natural Log (0–4 Ft).

Robust regression

Number of obs = 24
 F(3, 20) = 0.98
 Prob > F = 0.4239

ecdeep04ft	Coef.	Std. Err.	t	P> t	[95% Conf. Interval]	
oc_avg	19.90154	22.4936	0.88	0.387	-27.01928	66.82236
mc_avg	1.214694	4.419498	0.27	0.786	-8.004217	10.43361
pi_avg	2.053208	2.235891	0.92	0.369	-2.610779	6.717195
_cons	1.266633	83.94912	0.02	0.988	-173.8482	176.3814

CHAPTER 5: DEVELOPMENT OF SOIL SULFATE MAP

OVERVIEW OF VERIS DATA ANALYSIS FOR SOIL SULFATE MAPPING

Veris data analysis results in Chapters 3 and 4 shows that the Veris electrical conductivity (EC) is related to soil sulfate content, although the EC of soil varies depending on the amount of moisture held by soil particles, plasticity index, and organic content. A cross-section multivariate analysis using the natural log of the measured sulfate content and other raw engineered soil data showed that the Veris EC could be successfully predicted with a linear multivariate regression. This chapter presents the development of a soil sulfate map. The combined data from both US67 and US82 projects were used to develop the model by performing a geospatial grouping. The geospatial grouping approach sorts data obtained from the point sample locations in the field into geospatial zones and averages data from within each geospatial population zone. The average group data are used as input values for the model development. This geospatial grouping approach improves the model with lower standard error and better fit.

GEOSPATIAL DATA GROUPING ANALYSIS

As the first step to develop soil sulfate map, raw data including electrical conductivity, moisture content, plasticity index, organic content, and sulfate content from all test sites (US67 and US82) were combined as listed in Table 5-1. Figure 4-6 shows the linear relationship between the natural log of the measured SC and measured EC was identified.

Using the transformed data in Table 5-1, where the sulfate contents are expressed as the natural log of the measured SC, the multivariate regression analysis and robust regression shown in Tables 5-2 and 5-3 were conducted to identify the most sensitive soil parameters to influence on the Veris EC. Both regression analyses showed that only significant coefficients (90 percent confidence level) with this data set were for the relationship between log SC and MC. Estimated coefficients for OC and PI were not significantly different from zero.

Table 5-1. Veris Electrical Conductivity, Sulfate Content, Organic Content, Water Content, and Plasticity Index for Shallow Measurement (0–2 Ft).

Roadway	Sample ID	EC Shallow (0-2 ft)	SC_avg.	OC_avg.	MC_avg.	PL_avg.	Ln (Sc_avg)
	US67 (MW)-H1-1	393.0	635.0	2.9	27.9	35.0	6.5
	US67 (MW)-H2-1	339.7	905.0	2.7	27.2	29.4	6.8
	US67 (MW)-M2-1	142.4	105.0	2.3	27.6	34.1	4.7
US67	US67 (ME)-H1-1	444.8	1555.0	3.2	29.7	38.5	7.3
	US67 (ME)-M1-1	336.8	200.0	2.9	30.4	37.4	5.3
	US67 (ME)-M2-1	288.1	140.0	2.1	29.3	36.1	4.9
	US67 (ME)-L1-1	51.2	240.0	3.3	25.7	32.1	5.5
	US67 (ME)-L2-1	110.7	125.0	3.5	20.5	37.2	4.8
	US82-H1-1	296.1	487.5	0.6	24.8	46.4	6.2
	US82-H2-1	328.8	1220.0	0.4	23.1	44.5	7.1
	US82-M1-1	239.9	955.0	0.6	21.6	50.1	6.9
	US82-M2-1	236.2	700.0	0.5	24.1	41.3	6.6
	US82-L1-1	49.1	122.5	0.5	17.2	22.2	4.8
	US82-L2-1	114.9	110.0	0.5	18.0	33.2	4.7
	US82-S1-H1-1	462.7	480.0	0.9	22.6	39.7	6.2
	US82-S1-H2-1	355.1	680.0	2.5	22.4	48.5	6.5
	US82-S1-M1-1	163.7	240.0	0.5	27.5	39.7	5.5
US82	US82-S1-M2-1	271.5	520.0	0.5	21.0	41.5	6.3
	US82-S1-L1-1	80.8	290.0	0.8	13.0	41.7	5.7
	US82-S1-L2-1	78.9	352.5	3.0	17.0	39.1	5.9
	US82-S2-H1-1	390.1	475.0	1.7	20.4	42.9	6.2
	US82-S2-H2-1	336.0	295.0	0.3	25.0	40.3	5.7
	US82-S2-M1-1	252.7	220.0	0.3	30.2	44.5	5.4
	US82-S2-M2-1	279.0	495.0	1.3	26.4	40.5	6.2
	US82-S2-L1-1	55.2	140.0	0.5	26.7	25.1	4.9
	US82-S2-L2-1	61.5	100.0	0.6	26.8	26.6	4.6
	US82-S3-H1-1	301.9	202.5	0.6	21.0	34.4	5.3
	US82-S3-H2-1	326.3	450.0	0.9	22.8	29.2	6.1
	US82-S3-M1-1	132.8	220.0	0.7	22.7	34.1	5.4
	US82-S3-M2-1	143.5	280.0	0.6	17.1	35.8	5.6
	US82-S3-L1-1	69.1	100.0	0.7	13.8	26.8	4.6
	US82-S3-L2-1	29.0	215.0	1.4	25.2	26.4	5.4

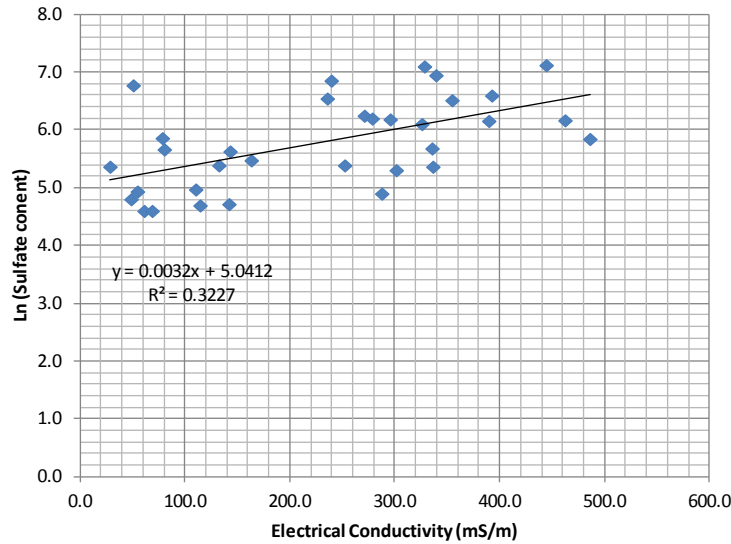


Figure 5-1. Natural Log of Sulfate Content versus Veris 3150 EC.

Table 5-2. Multivariate Regression Output for Predicting Veris EC.

```
. regress ecshallow02tt oc_avg mc_avg pi_avg lnscavg
```

Source	SS	df	MS			
Model	301162.453	4	75290.6134	Number of obs =	32	
Residual	228649.696	27	8468.50726	F(4, 27) =	8.89	
Total	529812.149	31	17090.7145	Prob > F =	0.0001	
				R-squared =	0.5684	
				Adj R-squared =	0.5045	
				Root MSE =	92.024	

ecshallow0~t	Coef.	Std. Err.	t	P> t	[95% Conf. Interval]	
oc_avg	.5014488	16.109	0.03	0.975	-32.5515	33.5544
mc_avg	8.346937	3.730845	2.24	0.034	.6918748	16.002
pi_avg	3.672605	2.938553	1.25	0.222	-2.356809	9.702018
lnscavg	87.3952	26.73399	3.27	0.003	32.54158	142.2488
_cons	-608.3848	141.6796	-4.29	0.000	-899.0874	-317.6822

Table 5-3. Robust Regression Output Using the Natural Log.

```
Robust regression
```

ecshallow0~t	Coef.	Std. Err.	t	P> t	[95% Conf. Interval]	
oc_avg	3.98675	17.387	0.23	0.820	-31.68842	39.66192
mc_avg	8.392413	4.026828	2.08	0.047	.1300436	16.65478
pi_avg	3.418039	3.17168	1.08	0.291	-3.089711	9.92579
lnscavg	86.63417	28.8549	3.00	0.006	27.4288	145.8395
_cons	-601.8856	152.9196	-3.94	0.001	-915.6507	-288.1204

The regression results presented in Tables 5-2 and 5-3 support the previous findings that the Veris EC is a function of the sulfate content (expressed as the natural log of the sulfate concentration) and the soil gravimetric water content (Harris et al., 2011). Although the regression models reduce the number of predictor variables down to two instead of four, the Veris EC is still influenced by multiple soil parameters. Therefore, zero and first order condition correlation analysis was conducted to investigate if the Veris EC and the soil sulfate content can be related each other without any other explanatory variables. Similar to Harris' results, the Veris EC is directly correlated with the sulfate content, which is expressed as the natural log of the actual sulfate content. Thus, the geospatial grouping approach was adopted to get a reasonable dataset for model development.

As shown in Figure 5-2, data obtained from the point sample locations in the field were divided into five geospatial zones ranging from 100 to 500 EC. The all-sulfate

contents within each geospatial population zone was averaged and transformed to the natural log of the SC. Finally, the relationship that Veris EC is a function of natural log of the sulfate content with a linear function (Eq. 5-1) was developed and presented in Figure 5-3. The correlation coefficient was 0.23 between the grouped EC and SC data.

$$\ln(\text{SC}) = 0.003(\text{EC}) + 5.25 \quad (\text{Eq. 4-1})$$

where SC = sulfate content and EC = electrical conductivity.

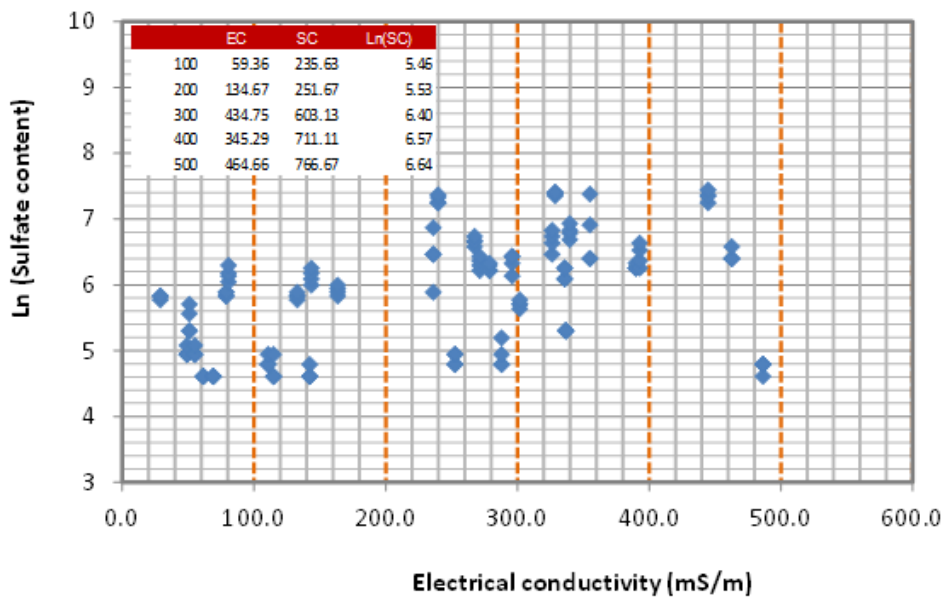


Figure 5-2. Geospatially Grouped Transformed Sulfate Content and EC Data.

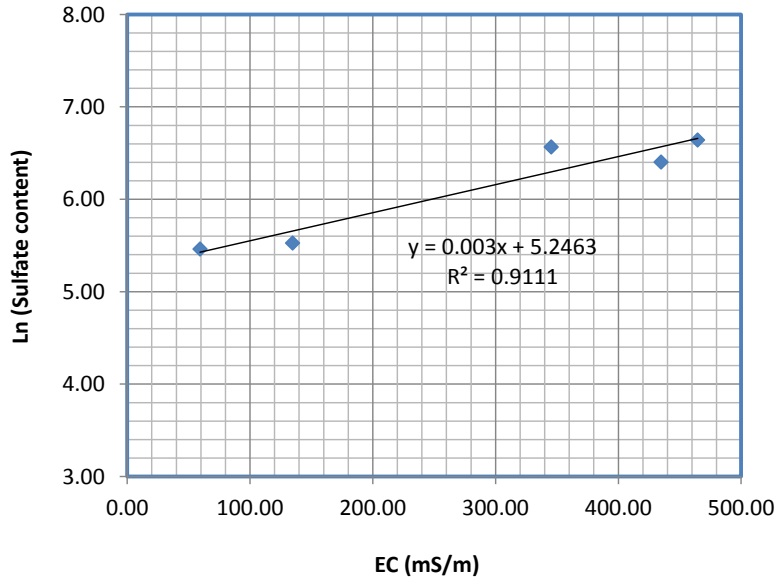
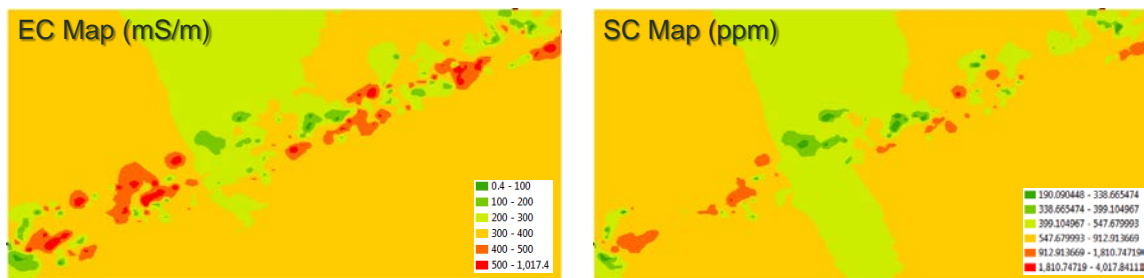


Figure 5-3. Relationship between Grouped EC and SC Data.

DEVELOPMENT OF SOIL SULFATE MAP

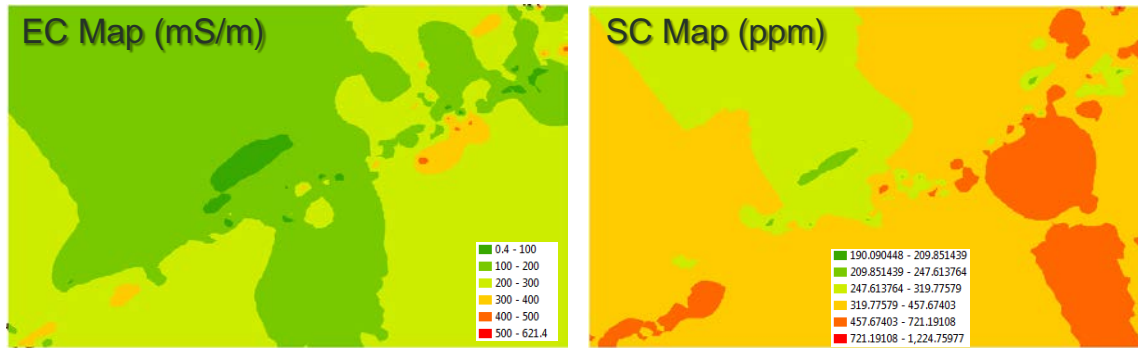
The regression equation (Eq. 5-1) obtained from geospatial data grouping analysis was used to develop a soil sulfate map for the individual projects studied in this implementation project. The sulfate contents for each project roadway were back-calculated from Eq. 5-4 and applied to corresponding GPS coordination. Figures 5-4, 5-5, and 5-6 present the comparison between the EC map and sulfate content prediction map for US67 East, US67 West, and US82, respectively. The EC map and SC map for all roadways seem to be well matched. The area with the greater EC shows the more sulfate content regardless of map color.



(a) Electrical Conductivity Map

(b) Sulfate Content Map

Figure 5-4. Electrical Conductivity and Sulfate Content Prediction Map (US67 East).



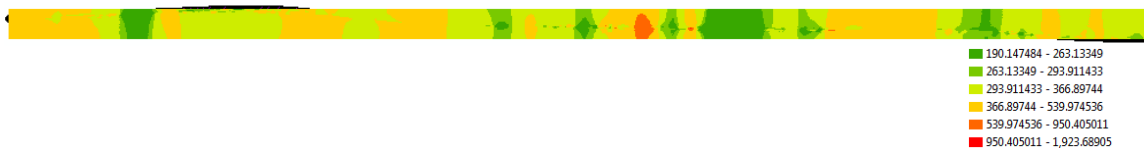
(a) Electrical Conductivity Map

(b) Sulfate Content Map

Figure 5-5. Electrical Conductivity and Sulfate Content Prediction Map (US67 West).



(a) Electrical Conductivity Map



(b) Sulfate Content Map

Figure 5-6. Electrical Conductivity and Sulfate Content Prediction Map (US82).

As presented in the prediction soil sulfate map, soil sulfate content increases as soil electrical conductivity increases. To verify this relationship, the multiple-ordered logit model was developed to investigate if the Veris EC can be a function of soil sulfate content. The multiple-ordered logit model called “ordered logistic regression” is a regression model for ordinal dependent variables. This model is generally applied to data that meet the proportional odds assumption, which has response categories to rate level.

The EC data listed in Table 5-1 were first grouped into 100 mS/m scales of EC. Each 100 mS/m EC is named from 1 through 5. For example, the EC that ranged from 0 to 100 mS/m is placed to 1 while the 401 to 500 mS/m EC is placed to 5. Table 5-4 shows the multiple-ordered logit modeling results. Except for organic content,

coefficients for SC, EC, and PI are significant at the 90 percent confident level. These results indicate that the Veris EC is a function of the sulfate content and higher EC of soil responds to higher sulfate content of soil.

Table 5-4. Multiple-Ordered Logit Regression Output.

ordered logistic regression

Number of obs = 32
 LR chi2 (4) = 84.76
 Prob > chi2 = 0.000
 Pseudo R2 = 0.2007

Log likelihood = -168.8336

shallow	Odds Ratio	Std. Err.	t	P> t	[95% Conf. Interval]	
lnscavg	4.22382	1.053311	5.78	0.000	2.590823	6.886095
oc_avg	1.135666	.1608911	0.90	0.369	.8603197	1.499137
mc_avg	1.22983	.0469654	5.42	0.000	1.14114	1.325413
pi_avg	1.087407	.0323141	2.82	0.005	1.025882	1.152622
/cut1	14.5867	1.970639			10.72432	18.44908
/cut2	16.03832	2.0701			11.981	20.09564
/cut3	17.61786	2.166034			13.37252	21.86321
/cut4	19.7747	2.250739			15.36334	24.18607

CHAPTER 6: DISCUSSION

SENSITIVITY OF SOIL PROPERTIES ON ELECTRICAL CONDUCTIVITY OF SOIL

The Veris 3150 unit continuously measures soil EC in the field. This device records simultaneous EC measurements for the top 2 ft and the top 4 ft of the soil from six coulter-mounted electrodes. As stated in previous chapters, soil is an electrical conductor. The electrical conductivity of soil presents a measure of how easily an electric current flows through the soil. Soil EC varies depending on the amount of moisture that the soil particles hold. For example, sand has a low EC, silt has a medium EC, and clay has a high EC (Sposito, 1989; Grisso et al., 2009). The EC of soils also responds to the amount of salt in the soil as well as organic matter content. Therefore, the characteristics of soils affect the EC data collected from the Veris 3150 unit.

As described in Chapters 3 to 5, the sensitivity analysis results of engineered soil properties on the EC of soils indicate that the Veris EC ranged from 29 to 445 is strongly related to soil sulfate content, although the EC of soil varies depending on moisture content, organic matter content, and plasticity index. However, Harris et al. (2011) have reported that conductivity values over 100 mS/m, as measured with the Veris 3150, can be used as a threshold value for detecting sulfate. They also reported that at least 10 percent volumetric moisture in the soil is needed to get acceptable conductivity readings with the Veris 3150. To verify the threshold of EC influencing the detection of sulfate content, the regression analyses using the multivariate regression model and robust model were performed for eight different combinations of data set (expressed in numbers embedded in black dots). Analysis variables include EC depth, EC above 100 mS/m, all-range EC, and all individual EC data as listed in Appendix C.

Table 6-1 summarizes all regression analysis results. Soil electrical conductivity is correlated with sulfate content, moisture content, and plasticity index, not organic matter content.

When average values of soil parameters and all-range of EC are used (No.1), EC is a function of SC (expressed by natural log of SC) and MC for 0–2 ft depth. When the average values of soil parameters and EC above 100 mS/m are used (No. 3), EC is only related to the SC for 0–2 ft depth. For 0–4 ft depth and average soil parameters (No.5 and No.7), none of the models are valid regardless of the EC data set.

When the spread-out engineered soil property data set and all-range of EC are used (No.2 and No.6), EC has correlation with SC, MC, and PI for both 0–2 ft and 0–4 ft depths. When the spread-out engineered soil property data set and EC above 100 mS/m are used, EC is a function of SC and MC (No.4), whereas EC is related to SC or SC, PI, and MC (No.8). Therefore, the ability to measure more than EC would help develop better models since EC is a function of multiple parameters.

Table 6-1. Summary of All Regression Analyses Results.

Road-Name	Depth	EC	Regression Model	Model-(Avg.)		Model-(All)	
US67+US82	0-2-ft	EC _{All-range}	Multivariate-Regression	Validity	Yes	Validity	Yes
				Order	LnSC->MC	Order	LnSC->MC->PI
			Robust	Validity	Yes	Validity	Yes
			Order	LnSC->MC	Order	LnSC->MC->PI	
		EC _{>100}	Multivariate-Regression	Validity	Yes	Validity	Yes
				Order	LnSC	Order	LnSC->MC
	Robust		Validity	Yes	Validity	Yes	
		Order	LnSC	Order	LnSC->MC		
	0-4-ft	EC _{All-range}	Multivariate-Regression	Validity	No	Validity	Yes
				Order	-	Order	LnSC->MC->PI
			Robust	Validity	No	Validity	Yes
			Order	-	Order	LnSC->MC->PI	
EC _{>100}		Multivariate-Regression	Validity	No	Validity	Yes	
			Order	-	Order	LnSC	
	Robust	Validity	No	Validity	Yes		
	Order	-	Order	LnSC->PI->MC			

*EC_{All-range}:As-obtained
 **EC_{>100}:Remove-EC-below-100
 ***(-):Negative-coefficient
 ****Model-(avg.):Average-value
 *****Model(All):All-data

EFFECT OF LIME TREATMENT ON SOIL PROPERTIES AND ELECTRICAL CONDUCTIVITY

Figures 6-1 through 6-4 present the soil property changes before and after lime treatment on the US82 roadway. As expected, moisture content, plasticity index, organic content, and sulfate content were generally reduced after lime treatment despite some stations that reflect opposite trends. The reduction rates for PI, SC, and MC are more

dominant than for OC after lime treatment. This may be attributed to the formation of calcium silicate hydrates (C-S-H), calcium aluminate hydrates (C-A-H), and ettringite. When water is added to lime, the considerable amount of C-S-H and/or C-A-H (the main inducer of strength development) are produced from the reaction of active SiO_2 and Al_2O_3 contained in the soil. $\text{Ca}(\text{OH})_2$ is generated from hydration of CaO while ettringite forms from the reaction of CaO , CaSO_4 , and Al_2O_3 . These hydration products are mainly responsible for the reduction of PI, SC, and MC.

However, the effect of lime treatment for OC is minimal. Organic matter has a high water holding capacity that limits the water available for the hydration process taking place, hence reducing the required cementation bonding. Therefore, the OC is less influenced by the lime treatment.

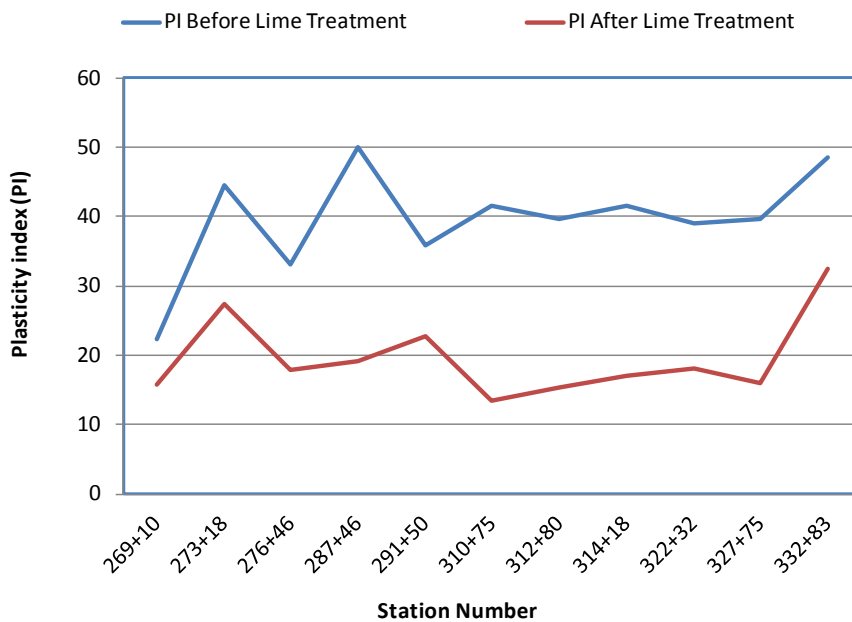


Figure 6-1. Plasticity Index Changes before and after Lime Treatment on US82.

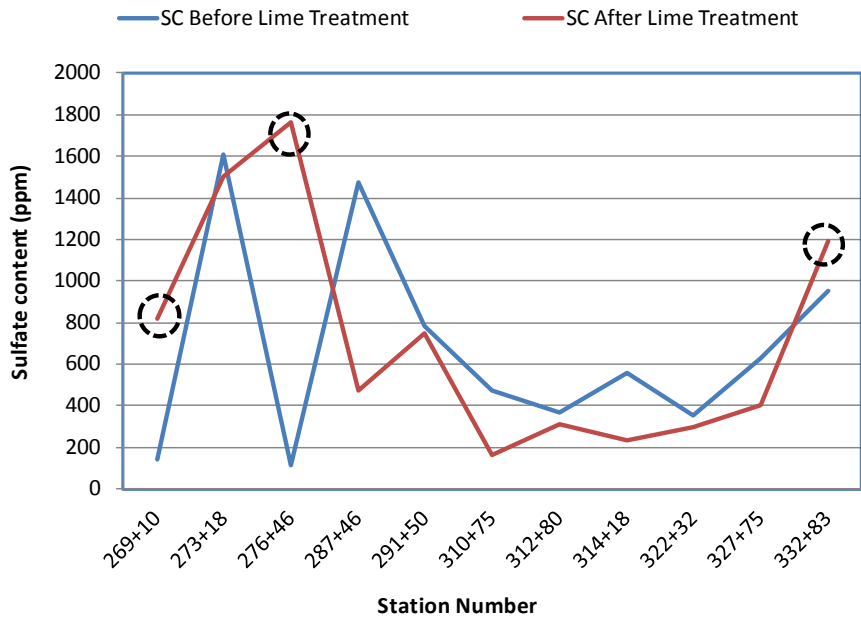


Figure 6-2. Sulfate Content before and after Lime Treatment on US82.

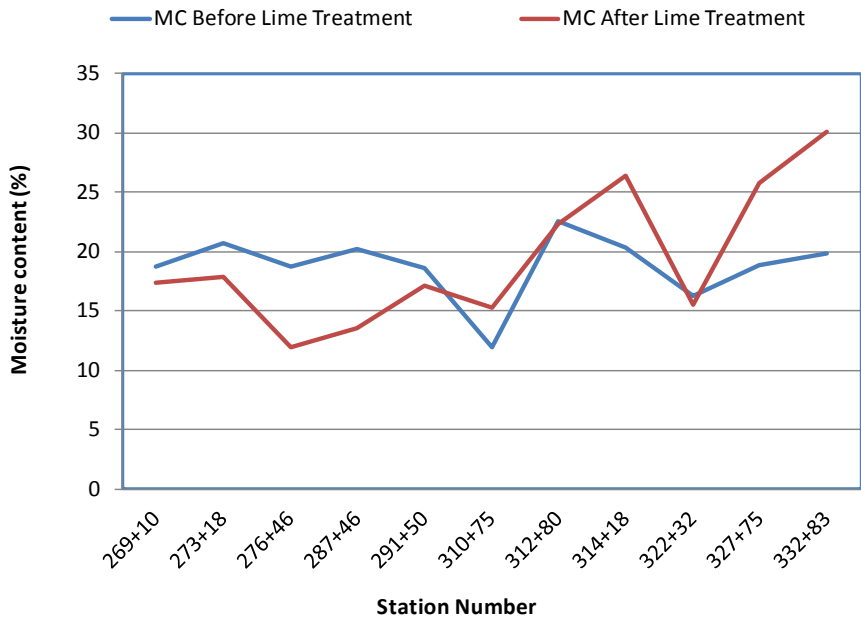


Figure 6-3. Moisture Content before and after Lime Treatment on US82.

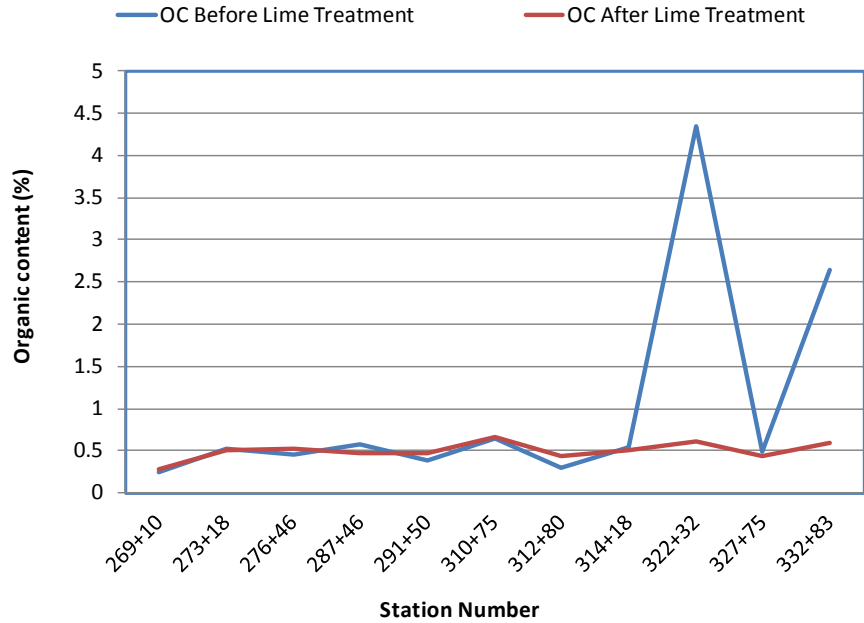


Figure 6-4. Organic Matter Content before and after Lime Treatment on US82.

Figure 6-5 presents the electrical conductivity color map changes before and after lime treatment on US82. The areas that show yellow and red colors indicate EC above 300 mS/m. All these areas have disappeared after lime treatment. While EC before lime treatment varies from 0.9 to 771.9 mS/m, the EC after lime treatment ranges from 30.8 to 290.2 mS/m. The highest EC values before and after lime treatment were 771.9 and 290.2 mS/m, respectively.



(a) Before lime treatment

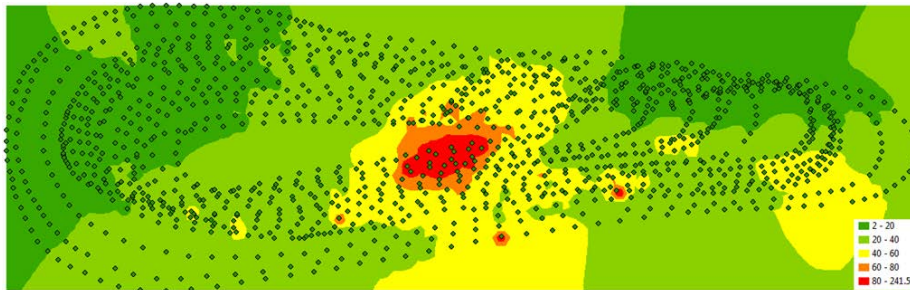


(b) After lime treatment

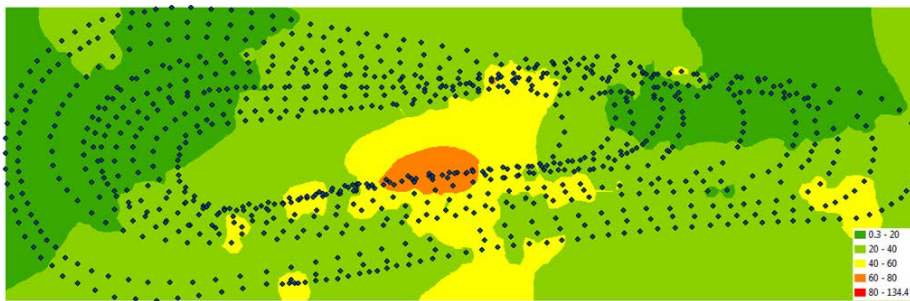
Figure 6-5. Electrical Conductivity before and after Lime Treatment on US82 (Station 334 to 358).

COMPARISON OF TXDOT VERIS 3150 TO TTI VERIS 3150 UNITS

As stated in Chapter 2, researchers from both TxDOT and TTI collected electrical conductivity data with their Veris 3150 units. Figures 6-6, 6-7, and 6-8 show the comparison of EC color maps generated with data collected by both TxDOT and TTI for the intersection of IH30-Spur 594, US67 East, and US82 roadways, respectively. The EC map for IH30-Spur 594 and US82 seems to be well-matched, while that of US67 is not exactly matched. Because the Veris 3150 unit uses a contact sensor measurement unit called coulter to measure the EC, it is critical how deeply and uniformly the coulter contacts with the soil to get the same data. EC must be ground-truth and trends among Veris 3150 devices are similar, although actual EC numbers may not be exactly matched. Therefore, the Veris 3150 unit may need to be calibrated by adjusting the penetration depth of a contact sensor before getting actual data.

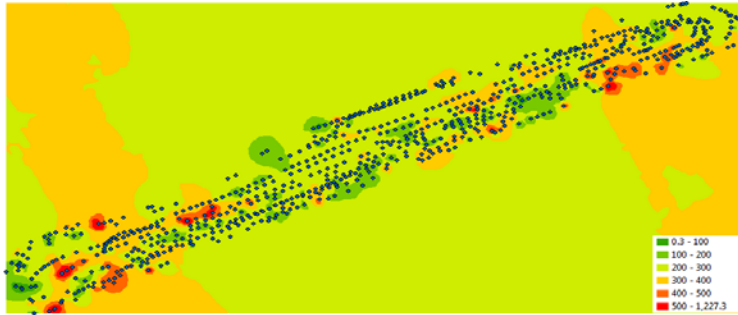


(a) TxDOT

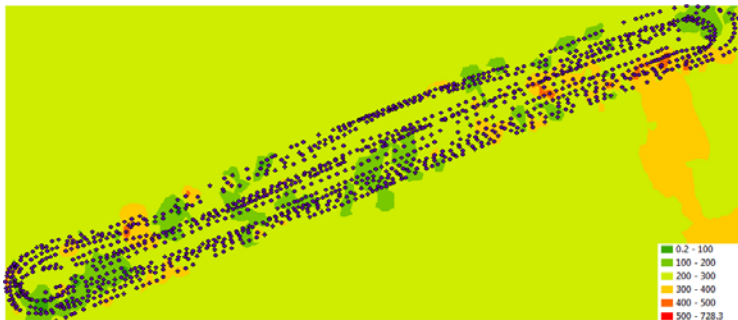


(b) TTI

Figure 6-6. Electrical Conductivity Map (IH30–Spur 594 NE; 1:500 Scales).



(a) TxDOT



(b) TTI

Figure 6-7. Electrical Conductivity Map (US67 East; 1:1500 Scales).



(a) TxDOT



(b) TTI

Figure 6-8. Electrical Conductivity Map (US82 Station 258 to 291; 1:5500 Scales).

CHAPTER 7: CONCLUSIONS AND RECOMMENDATIONS

The current TxDOT testing protocol in the field uses a spot test that measures sulfate content every 500-ft interval on a project (Tex-145-E). If a high sulfate zone lies between 500-ft intervals, the current testing protocol will miss this sulfate zone. The Veris 3150 unit was used as a continuous measurement of sulfate content as a function of electrical conductivity of soils. The protocol using the Veris 3150 to determine sulfate-rich soils has been implemented to two full-scale projects in Dallas and Paris Districts. Researchers at both the Texas Transportation Institute and Texas Department of Transportation collected electrical conductivity data with their Veris 3150 units, simultaneously. They collected soil samples for plasticity index, moisture content, sulfate content, and organic content tests on the basis of the EC color-coded map. Then, they analyzed data collected from these projects to identify potential relationships between conductivity measurements and sulfate contents for different types of soil. Key results from this project can be summarized as follows:

- Veris EC is a linear function of the natural log of the sulfate content and electrical conductivity, directly, if other soil parameters remain constant.
- The sensitivity analysis results of engineered soil properties for the EC of soils indicate that the Veris EC is strongly correlated with sulfate content, moisture content, and plasticity index, but not organic matter content.
- The multiple-ordered logit model verifies that the Veris EC is a function of the sulfate content. Higher EC of soil responds to higher sulfate content of soil. It is imperative that soil samples be collected based on the EC map generated from the Veris 3150 data. Therefore, it is recommended that the Veris EC be used as a viable screening tool to determine the sulfate content of soils.
- A soil sulfate prediction map using regression equation obtained from a geospatial data grouping analysis indicates that the area with the greater EC shows the higher sulfate content.

- After lime treatment, the MC, PI, OC, and SC of soils were reduced and the EC color-coded map shows changes of EC before and after lime treatment. Therefore, the Veris EC may be useful to check the uniformity of lime treatment.
- The comparison study of TxDOT and TTI Veris units shows that EC units must be ground-truth and trends between Veris 3150 devices are similar although the actual EC values may not be exactly matched. Therefore, it may be necessary to calibrate the Veris 3150 unit by adjusting the penetration depth of a contact sensor before collecting actual data.

REFERENCES

- Grisso, R.B., Alley, M., Holshouser, D., and Thomason, W. Precision Farming Tools: Soil Electrical Conductivity, Technical Report 442-508, Virginia Polytechnic Institute and State University, Petersburg, Virginia, November 2009.
- Harris, P.J., Sebesta, S., and Scullion, T. Hydrated Lime Stabilization of Sulfate-Bearing Vertisols in Texas. In *Transportation Research Record: Journal of the Transportation Research Board, No. 1868*, Transportation Research Board, National Research Council, Washington, D.C., 2004, pp. 31–39.
- Harris, P.J., Harvey, O., and Sebesta, S. Rapid Field Detection of Sulfate and Organic Content in Soils, Research Report 0-6362-1, Texas Transportation Institute, The Texas A&M University, College Station, Texas, October 2011.
- Puppala, A.J., Wattanasanticharoen, E., and Hoyos, L.R. Ranking of Four Chemical and Mechanical Stabilization Methods to Treat Low-Volume Road Subgrade in Texas. In *Transportation Research Record: Journal of the Transportation Research Board, No. 1819*, TRB, National Research Council, Washington, D.C., 2003, pp. 63–71.
- Saylak, D., Lytton, R.L., Mishra, S.K., and Sinn, D. Calcium Chloride-Fly Ash Stabilization in Roadway Construction. *Transactions Society of Mining, Metallurgy, and Exploration*, Vol. 318, 2005, pp. 109–118.
- Sposito, G. *The Chemistry of Soils*. Oxford University Press, New York, 1989, p. 277.
- Tastan, E.O., Edil, T.B., Benson, C.H., and Aydilek, A.H. Stabilization of Organic Soils with Fly Ash, *Journal of Geotechnical and Geoenvironmental Engineering*, American Society of Civil Engineering, Vol. 137, No. 9, 2011, pp.819–833.

**APPENDIX A:
CREATING ELECTRICAL CONDUCTIVITY MAP WITH
ARCGIS-ARCMAP 10 USING FIELD DATA OBTAINED FROM
VERIS 3150 DEVICE**

Summary

Creating an electrical conductivity map using data obtained from Veris 3150 consists of three steps:

- (a) Data preparation.
- (b) Data analysis.
- (c) EC mapping.

Data preparation can be done using Microsoft Excel[®] while data analysis and mapping can be conducted with any spatial interpolation software. The steps describe here are specific for the ArcGIS 10 software (ESRI).

Step 1. Data Preparation

Preparing data for data analysis, which is called pre-processing, is carried out in the following three sub-steps:

- (a) Retrieving/importing data.
- (b) Combining and labeling data.
- (c) Removal/exclusion of anomalous data

Step 1a: Retrieving/importing data

- 1) Insert SD card into the SD drive on the computer (Figure A-1) and navigate to the data files (if necessary).
- 2) Files names are of the form “VSEC0” plus three numbers (e.g., VSEC0082). The three numbers represent the file ID, which is created from the Veris data logger. Data is stored in the “.dat” file format and can be opened directly in Microsoft Excel.
- 3) One or more data files can be viewed by selecting the files, right click on the mouse, and selecting **Open** (Figure A-2).



Figure A-1. Insert SD Card into SD Drive on the Computer.

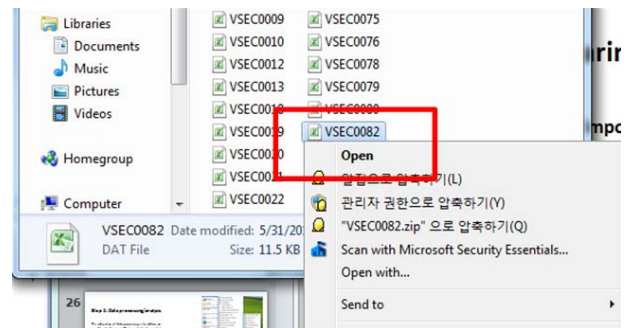


Figure A-2. Open Data File with Excel.

Step 1b: Combining and labeling data

If data are collected in a single file, ignore the procedure to combine data files. However, if data are collected with several different files over the same testing area, it is necessary to combine all data files into a single data file. In the road construction area, it is recommended that data be collected as single longitudinal transects (3–4 transects across a two-lane road) along the area of interest.

- 1) As shown in Figure A-3, during pre-processing, data from all transects should be combined into a single data file. To do this, **copy and paste data for all transects (end to end) into a single Excel sheet.**

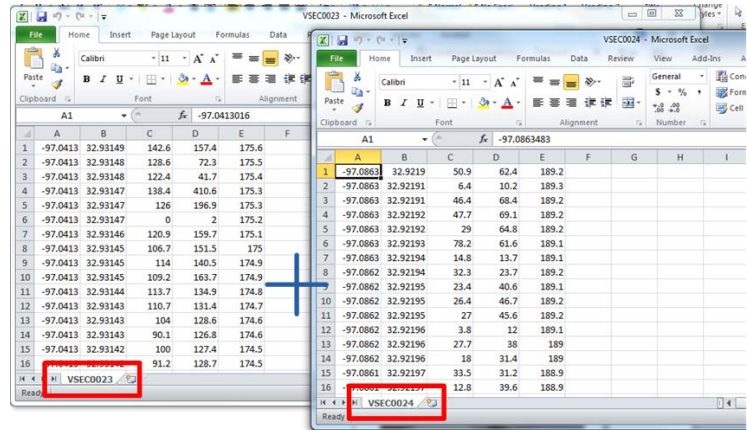


Figure A-3. Combining Two Date Files into a Single Excel Sheet.

- 2) When the Excel sheet, which has five columns data set, is ready, **label** the columns as: **X-location, Y-location, EC_SH, EC_DP, and ELEV_ft**, respectively (Figure A-4). X and Y locations are the GIS locations; EC_SH and EC_DP are electrical conductivity readings to a depth of 2 and 4 ft, respectively; ELEV_ft is the elevation in feet.

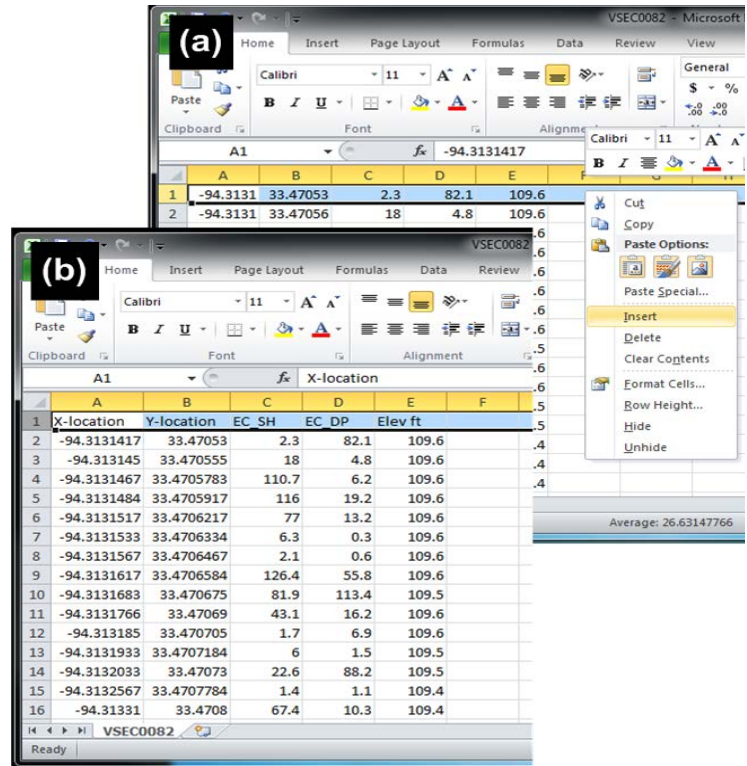


Figure A-4. Label Columns.

Step 1c: Removal/Exclusion of Anomalous Data

Anomalous data may be in the form of zero or negative values. It is recommended that these values be removed.

- 1) To remove these values (Figure A-5), **Select the row(s)** (hold down on Ctrl key for multiple selections), **right click** and choose **Delete**.
- 2) After removing anomalous data, **make sure to save** the data as an **Excel workbook** file or a **.csv** File (Figure A-6).
- 3) Copy or move data file to and/or to **c:\My Document>ArcGIS folder**. A new folder can be created under ArcGIS folder and data file can be saved into a New folder (e.g., c:\Documents\ArcGIS\I30_SH594).

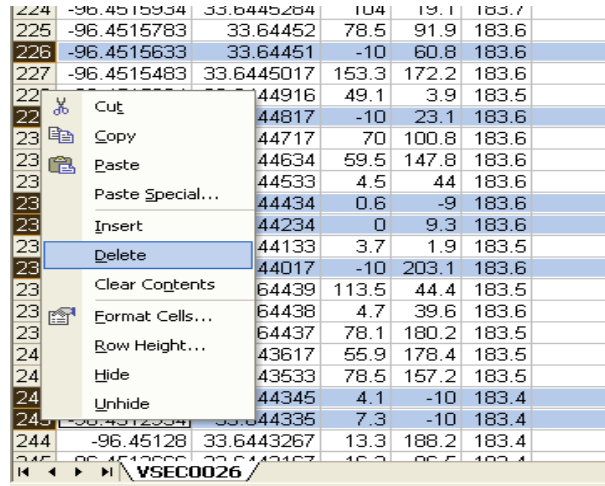


Figure A-5. Removal of Anomalous Data.

Congratulations!
You are ready to do data analysis
and mapping!

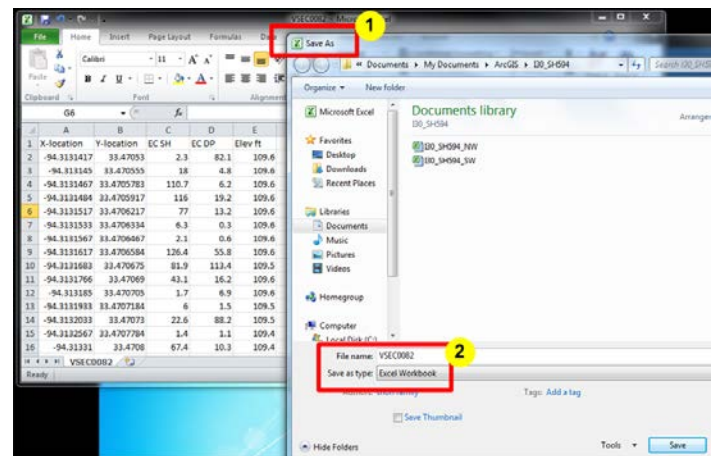


Figure A-6. Saving the Edited File as an MS Excel Workbook.

Step 2. Data Analysis

Data analysis shows how to incorporate data prepared from the pre-processing step into the spatial analysis software before obtaining an insight into how soil EC varies spatially. Any spatial analysis software can be used for data analysis. Here, data analysis using the ArcGIS 10 software is described. The data analysis step is conducted in the following sub-steps:

- (a) Opening ArcMap/Setting Geostatistical analysis extension tool.
- (b) Adding data to ArcMap.
- (c) Displaying data as Map.

Step 2a: Opening ArcMap/Setting Geostatistical Analyst Extension Tool

1) To **open ArcMap**, go to All Program>ArcGIS>ArcMA P1. Then, select **Blank Map** (Figure A-7).

2) Data analysis requires the **Geostatistical Analyst extension (GAE)**, which is used in creating an electrical conductivity map. Turning on the GAE is a two-step process (Figure A-8):

- a) On the menu bar, select **Customize> Toolbars> Geostatistical Analyst**.
- b) Select **Customize> Extensions**, then check **Geostatistical Analyst** and **Spatial Analyst**.

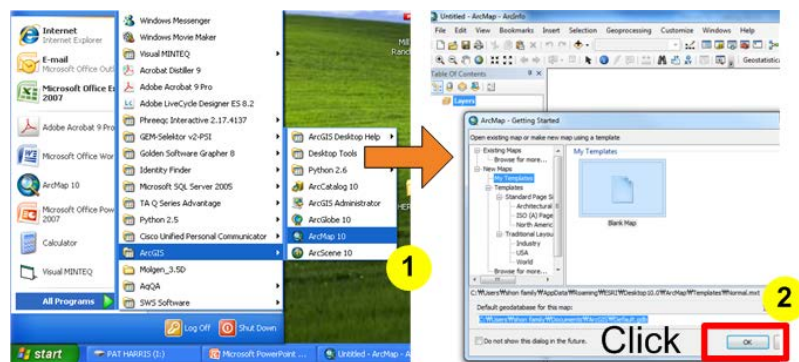


Figure A-7. Opening ArcMap.

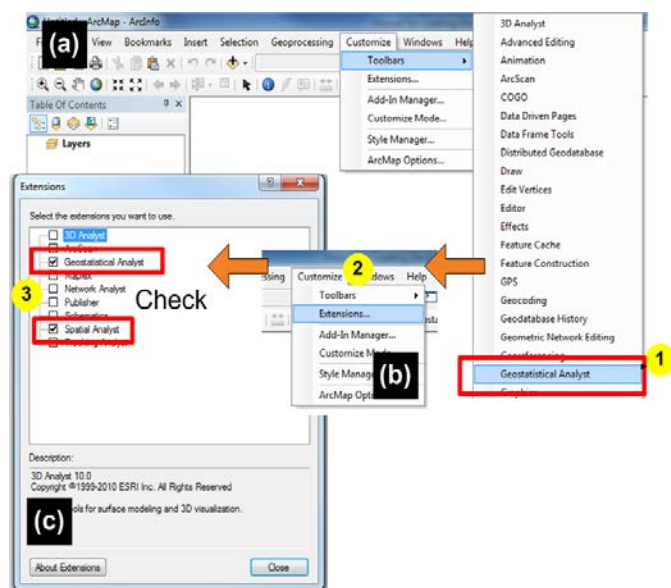
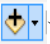


Figure A-8. Installation of Geostatistical Analyst.

Step 2b: Adding Data to ArcMap

Once the Geostatistical Analyst is displayed on the ArcMap menu bar, the next step is to bring the data prepared from Step 1 to ArcMap.

- 1) Click **Add Data** icon (), navigate to folder with data files. Then, select file and click **Add** (Figure A-9). A loaded data file is shown in layer windows as the 1st layer located on the left side.

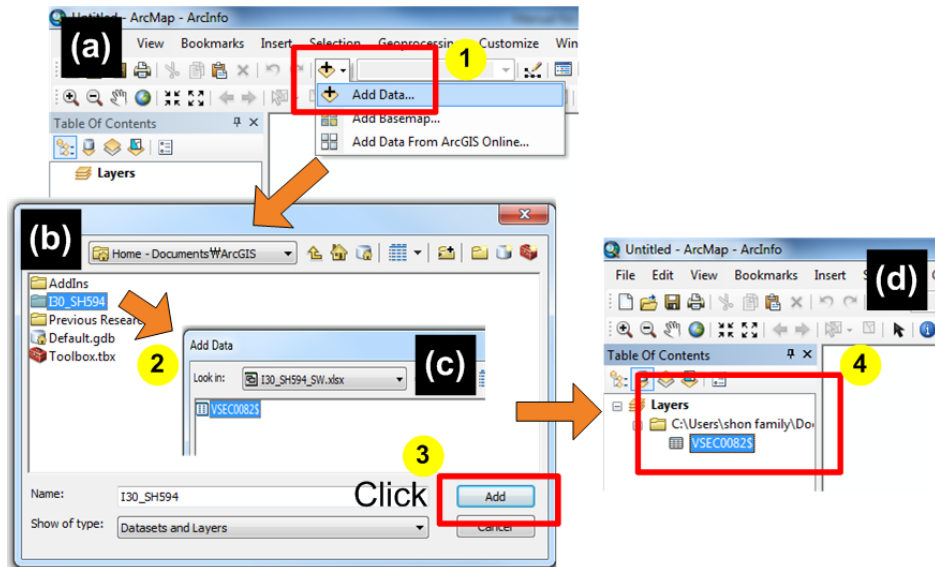


Figure A-9. Adding Data to ArcMap.

Step 2c: Display Data as Map

Once the data file is brought into layer windows, the next step is to **display data as map**.

In this step, it is necessary to **connect the loaded data to Geographic Coordinate Systems**, which is similar to the GPS coordinate system used in a Veris device.

- 1) Select the data file in layer windows, right-click on the mouse, click **Display XY Data**, and choose the appropriate field for X and Y (Figure A-10).
 - a) **X field**: X location/longitude.
 - b) **Y field**: Y location/latitude.
 - c) **Z field**: none.
- 2) The chosen X and Y field (field GPS data) should be matched with appropriate coordinate system. To get **Geographic Coordinate System (GCS)**, click **Edit** (Figure A-11).
- 3) As shown in Figure A-11, click **Select > Geographic Coordinate System > North America > NAD 1983.prj > Add > OK > OK** (message).
- 4) Now the data file is displayed as map.

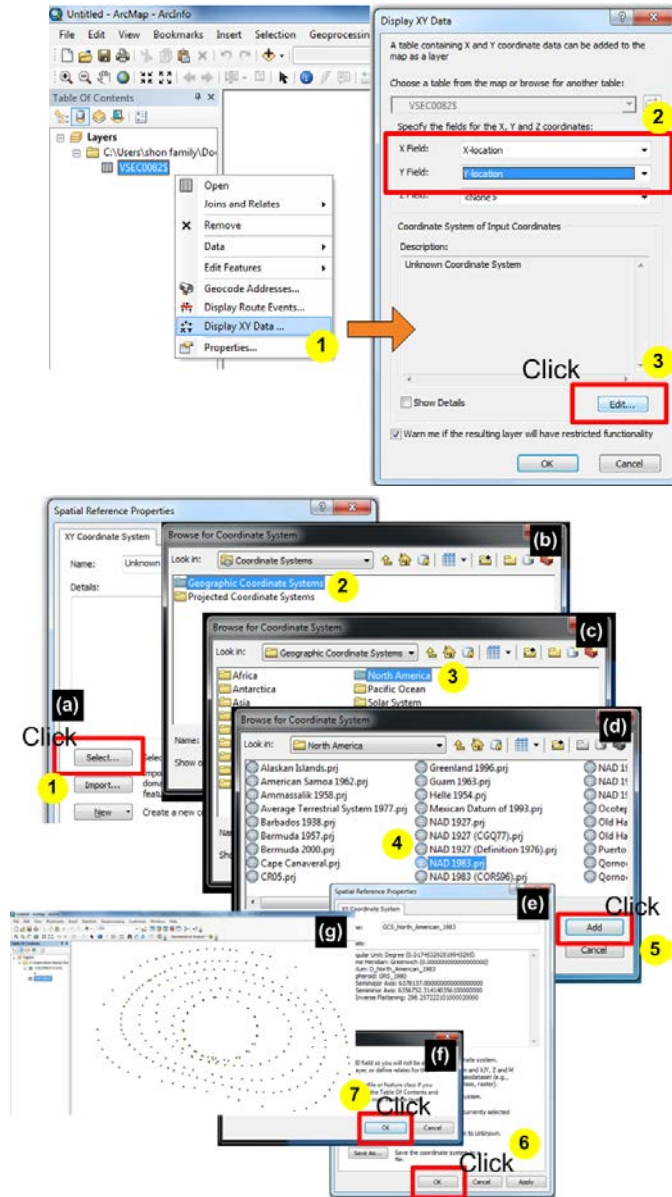


Figure A-11. Selection of Geographic Coordinate System.

Step 3. EC Mapping

The Electrical conductivity (EC) mapping step presents how to create an EC map using the Geostatistical Analyst Tool. This step is performed by the following three sub-steps:

- (a) Creating EC map.
- (b) Re-classification of EC categories.
- (c) Editing EC map.

Step 3a: Creating EC Map

- 1) When the data file is displayed as a map, an **events file** is created in the layers window. Select an **event file** and click **Geostatistical Analyst > Geostatistical Wizard** (Figure A-12).
- 2) As shown in Figure A-12, choose **Inverse Distance Weighting method** and click the drop-down arrow on the **Data Field**. Then, choose **EC_SH** or **EC_DP**, depending on the interested depth of 0–2 ft or 0–4 ft. Leave **Weight Field** blank, click **Next** button, choose **Use Mean**, and click **OK**.
- 3) When the **Inversion Distance Weight 2 of 3** window pops up, choose **Power 2, Max. Neighbor 150, and Min. Neighbor 100**. Then, click **Next > OK**. Map is displayed in the window (Figure A-13).

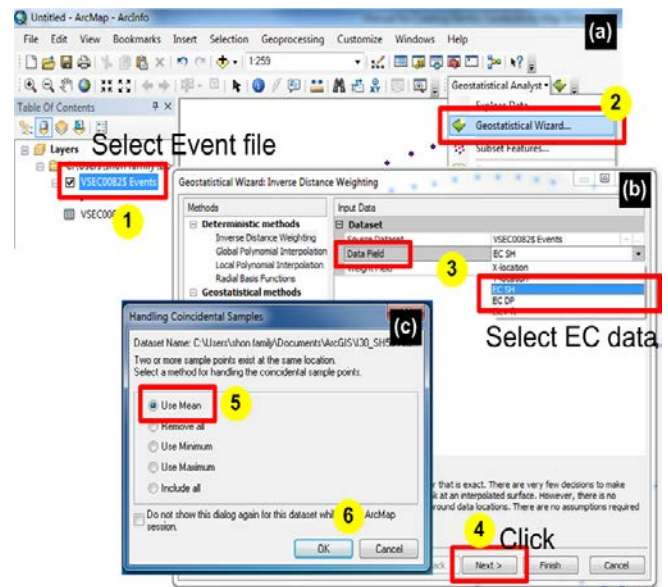


Figure A-12. Utilization of Geostatistical Wizard for EC Mapping.

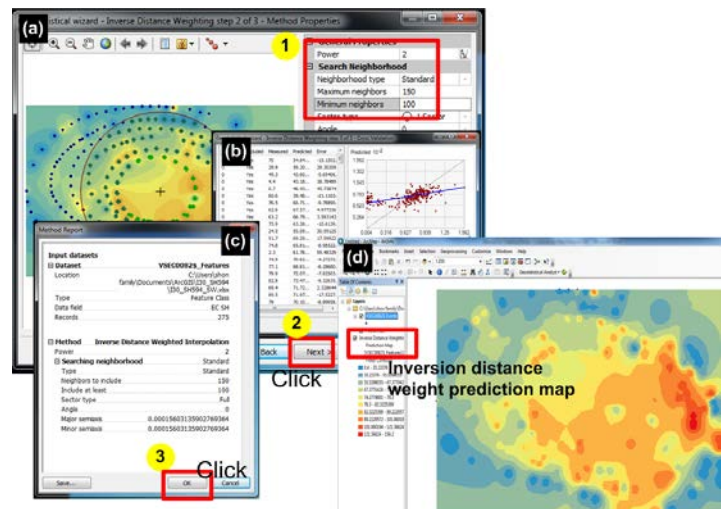


Figure A-13. Creating Inversion Distance Weight Prediction Map.

Step 3b: Reclassification of EC Categories

When the inversion distance weight prediction map is produced, the range of electrical conductivity is automatically created on the basis of data values. The range of EC can be reclassified.

- 1) Right-click **the layer** that you want to change the classification and click **Properties** (Figure A-14 [a]).
- 2) Click the **Symbology** tab and click **Classify** (Figure A-14 [b]).
- 3) Click the **Method** drop-down arrow and click on the classification method you want to use. Then, click the **Classes** drop-down arrow and click the number of classes you want to display (Figure A-14 [c]).
- 4) Click **OK** on the Classification dialog box and click **OK** on the Layer Properties dialog box. Now, the reclassification of EC range is shown in Figure A-14 (d).

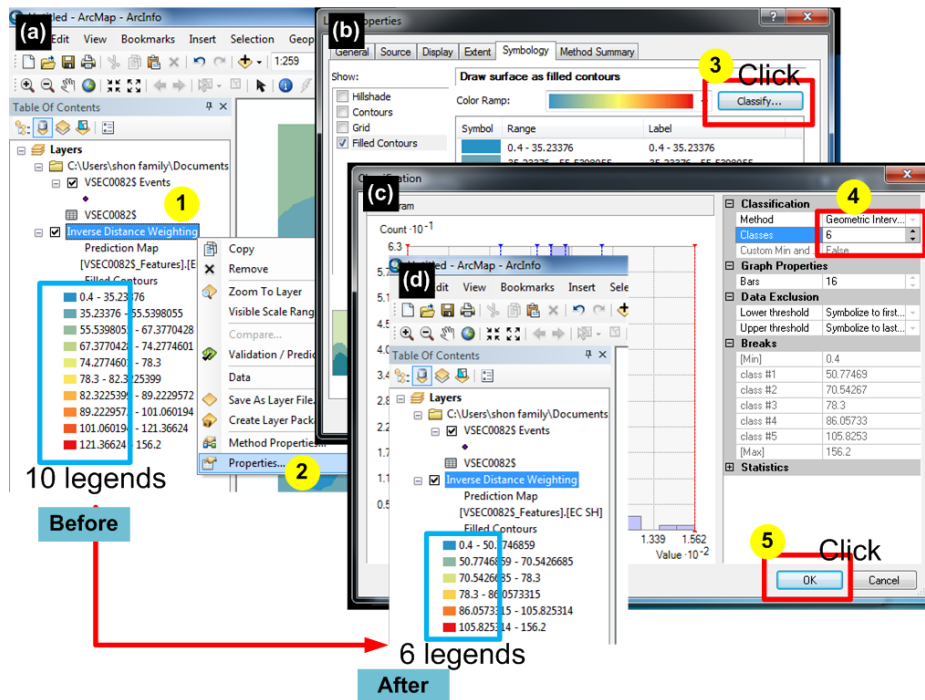


Figure A-14. Reclassification of EC Categories.

Step 3c: Editing EC Map

Although the predicted electrical conductivity map is shown in Figure A-15 (a), the original field data are not presented in this map. This step shows how to get the final map, which shows field collected data, filled contour areas of different shades, and a color scale.

- 1) To present the field collected data on the predicted map, **switch the List by source mode to List by drawing order mode** (Figures A-15 [b] and [c]). **Drag the event layer and place on the top** (Figure A-15 [d]). Now, the final map including field data is shown in Figure A-15 (e).

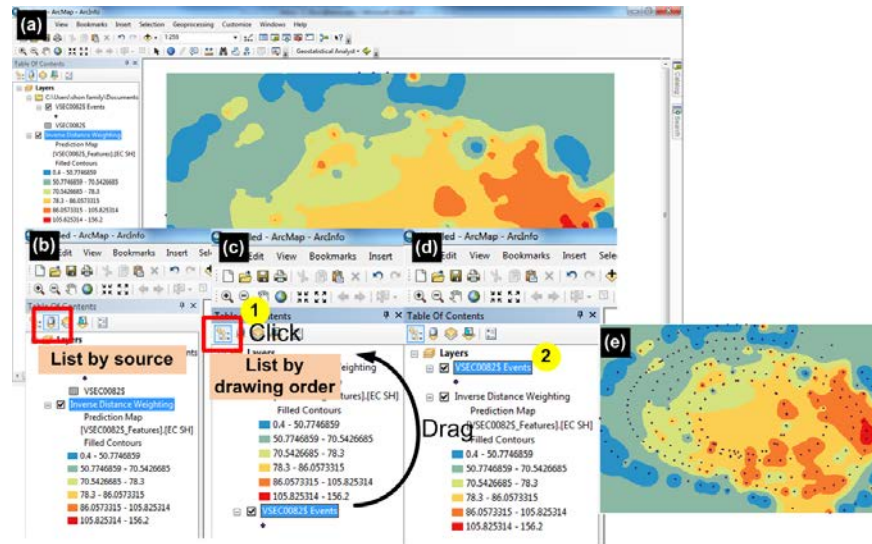


Figure A-15. Producing EC Map Containing Field Collected Data.

- 2) To add a legend, scale, etc., first select **View> Layout View** on the menu bar (Figure A-16 [a]). Main window in ArcMap program would then be changed to layout mode.
- 3) Next, click **Insert> Legend** or **Insert> Scale bar** to decorate the map (Figure A-16 [b]).

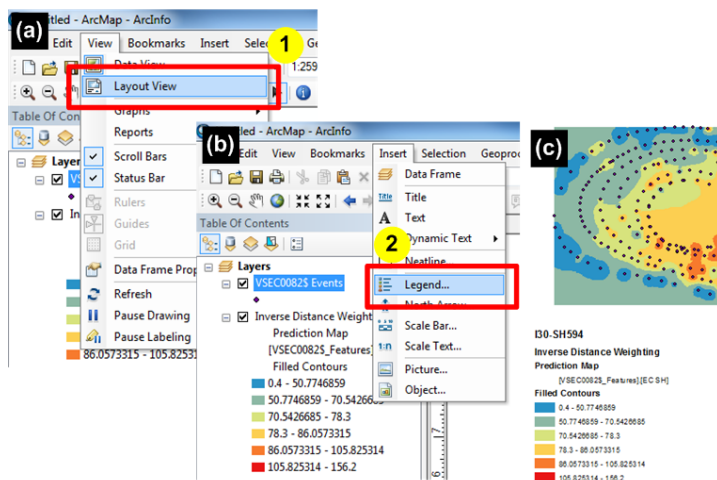


Figure A-16. Addition of Legend, Scale Bar, Etc.

**APPENDIX B:
DETERMINATION OF ORGANIC CARBON CONTENT USING
STELLARNET UV-VIS SPECTROMETER**

Summary

Determining organic carbon content in soil using Stellarnet UV-VIS[®] spectroscopy consists of three steps:

- (a) Sample preparation.
- (b) UV-Vis spectroscopy setup.
- (c) Measurement of organic content.

The following procedure describes preparing reagents, preparing soil samples, installing the UV-VIS spectrometer, and measuring soil organic carbon for estimating organic carbon content in the laboratory using an analytical method.

Step 1. Sample Preparation

Preparing test sample is carried out in the following three sub-steps:

- (a) Preparing reagents.
- (b) Preparing soil sample.
- (c) Extracting organic matter.

Step 1.1: Preparing Reagents

1.1.1. Preparation of sodium pyrophosphate (Figure B-1)

- (1) Place 500 ml of deionized water into 1L volumetric flask.
- (2) Add 10 g of NaOH and 44.6 g of $\text{Na}_4\text{P}_2\text{O}_7 \cdot 10\text{H}_2\text{O}$ to the flask.
- (3) Stir until dissolved.
- (4) Add additional deionized water to make 1L of solution.
- (5) Cap flask.

1.1.2. Preparation of 1N hydrochloric acid solution (Figure B-1)

- (1) Add 250 ml of deionized water to 500 ml volumetric flask.
- (2) Add 41.43 ml of 37 percent HCl to the deionized water and stir.
- (3) Add additional deionized water to make 500 ml of solution.
- (4) Cap flask.

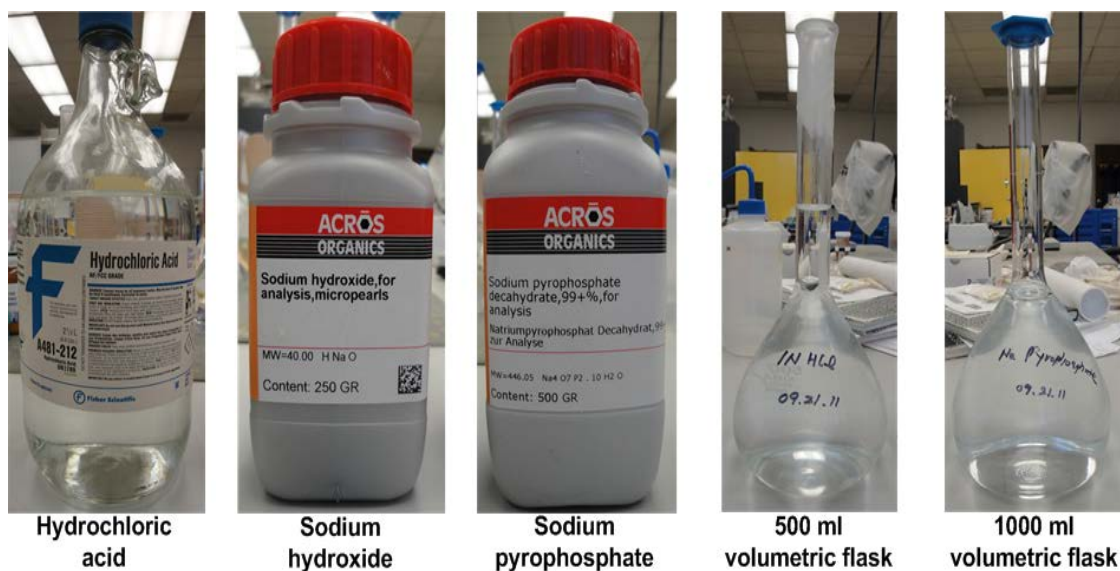


Figure B-1. Materials for Preparing Reagents.

Step 1.2: Preparing Soil Sample and Blank Tube

1.2.1. Preparation of standard sample

- (1) Obtain at least two standard soil samples of known soil organic carbon (SOC) content.
- (2) One soil with SOC < 1 percent and the other with SOC around 2 percent.
- (3) Obtain a 300 g standard sample.
- (4) Air-dry the standard to constant weight (Do not oven-dry sample).
- (5) Pulverize the 300 g to pass the No. 40 (425 μ m) sieve.
- (6) Weigh 0.1 g of each standard material.
- (7) Place the standard in a separate 50 ml (1.7 oz) polypropylene centrifuge tube.
- (8) The standard materials should have concentrations of: SH6 0.46 \pm 0.09 percent, Austin 1.2 \pm 0.24 percent, and Beaumont 1.5 \pm 0.30 percent (Figure B-2).

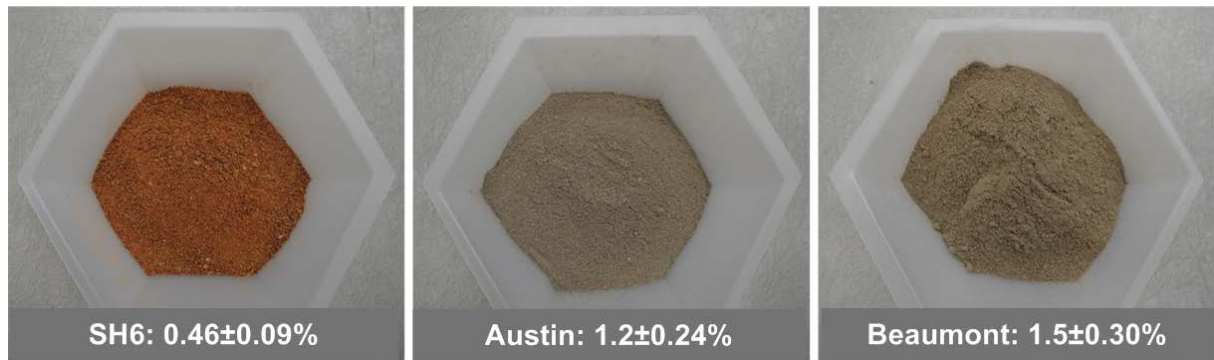


Figure B-2. Standard Materials and Their Organic Carbon Contents.

1.2.2. Preparation of soil sample

- (1) Collect soil samples where:
 - (a) There is an obvious change in soil type (plasticity) or color.
 - (b) There is an odor like sewage.
 - (c) The soil has a dark color. Creek beds, floodplains, and farm fields often have high concentrations of organic matter.
- (2) Obtain a 300 g representative sample.
- (3) Air-dry the standard to constant weight. Do not oven-dry sample (Figure B-3 [a]).
- (4) Pulverize the 300 g to pass the No. 40 (425 μ m) sieve (Figures B-3 [b] and [c]).
- (5) Split the sample and obtain ~15 g of three representative samples.
- (6) Obtain sample of 0.1 g \pm 0.01 g from each split sample (Figure B-3 [d]).
- (7) Place the weighed sample in a separate 50 ml (1.7 oz) polypropylene centrifuge tube (Figure B-3 [e]).

1.2.3. Preparation of blank centrifuge tube

- (1) Label a 50 ml (1.7 oz) polypropylene centrifuge tube as a blank (no soil in the Blank).

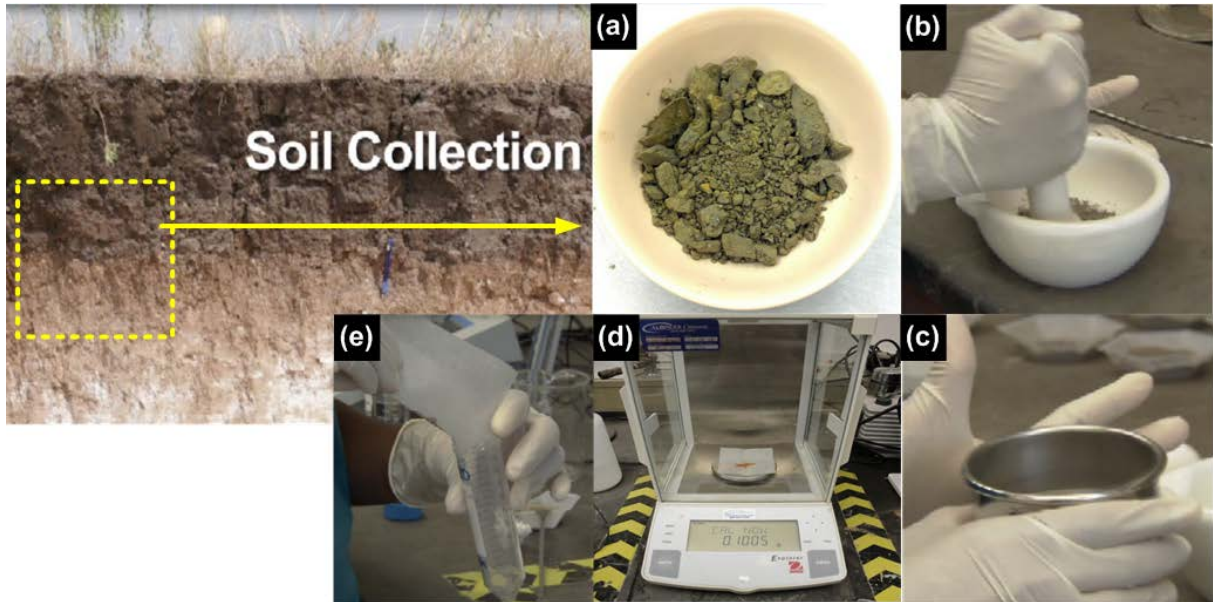


Figure B-3. Preparation of Soil Samples.

Step 1.3: Extracting Organic Matter

1.3.1. Chemical treatment

- (1) Add 5 ml of 1N HCl to each of the three replicates, the two standard samples, and the polypropylene centrifuge tube labeled as Blank (Figure B-4[a]).
- (2) Vigorously shake the centrifuge tubes of soil/HCl solution by hand or place on a mechanical shaker for 10 sec. at 1-min intervals for a total of 5 min (Figure B-4 [b]).
- (3) Add 20 ml of Na pyrophosphate solution to each of the three replicates, the two standard samples, and the polypropylene centrifuge tube labeled as Blank (Figure B-4 [c]).
- (4) Vigorously shake the centrifuge tubes of soil/HCl and Na pyrophosphate solution by hand or place on a mechanical shaker for 10 sec. at 1-min intervals for a total of 5 min (Figure B-4 [d]). There should be 25 ml of solution in each centrifuge tube.
- (5) Add approximately 10 ml of the liquid to a 10 ml syringe and attach a 0.45 μm polycarbonate syringe filter.

- (6) Gently depress the syringe plunger to dispose of ~1 ml of solution in a waste container. Use the rest of the solution in the syringe to fill the cuvette.
- (7) Place the filter opening above a clean 1 cm methacrylate cuvette and gently depress the syringe plunger to force the extract through the filter and into the cuvette (Figure B-4 [e]). (**Note.** Bubbles and particulates will result in measurement errors, so be careful to ensure that the extract in the cuvette is free of bubbles and particulates. Treat the Blank as the other samples [Figure B-4 (f)]. It should be filtered as well).
- (8) Wipe the outside of the cuvette clean with a Kimwipe® or equivalent delicate task wipe to remove dirt, fingerprints, or anything else that will obstruct a light beam from passing through the cuvette and filtrate (Figure B-4 [g]).
- (9) The sample is now ready to place in the UV-Vis instrument for determining the organic matter content of the soil (Figure B-4 [h]). (**Note.** The cuvettes are disposable. Use a new cuvette with each sample but make sure that these are clean before using; packing Styrofoam will adhere to the sides of the cuvette.)

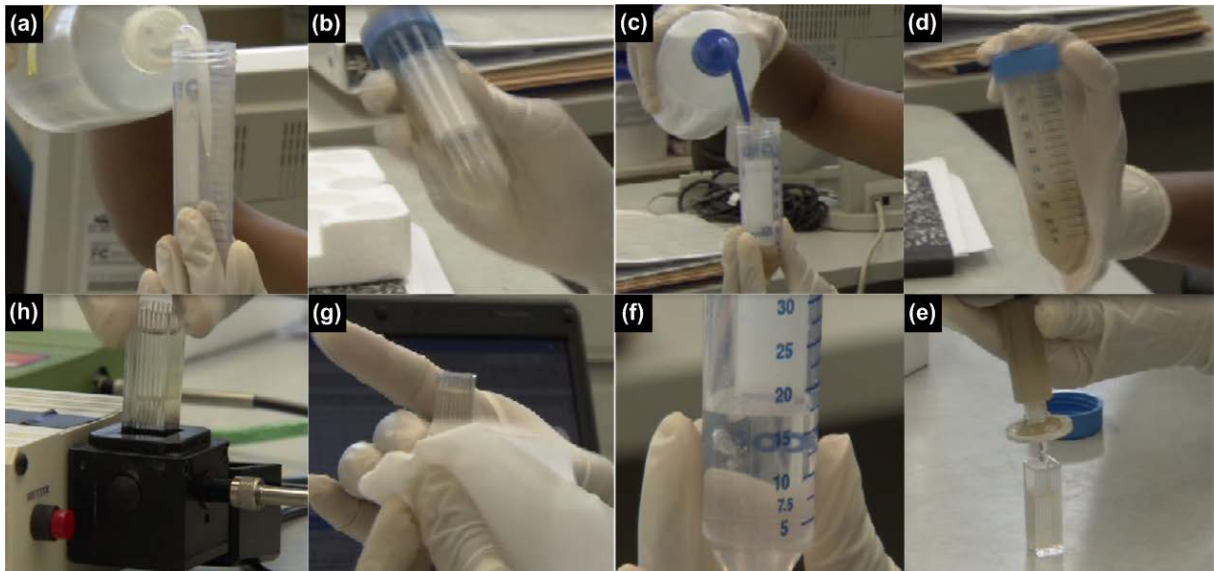


Figure B-4. Chemical Treatment to Extract Organic Matter.

Step 2. UV-VIS Spectroscopy Setup

Stellarnet UV-VIS is a spectrometer apparatus that consists mainly of a laptop with analytical software and spectrometer device (Figure B-5). The spectrometer contains a BP 2 battery pack, SL1 tungsten halogen light source, power regulator, AC power supply, green wave spectrometer (UVNb-50), fiber optic cable, green USB cable, 16v adapter cable, and cables (5v, 12v, and 16v). The following procedure describes how to connect each UV-VIS spectrometer component prior to determining organic matter content of soil sample.

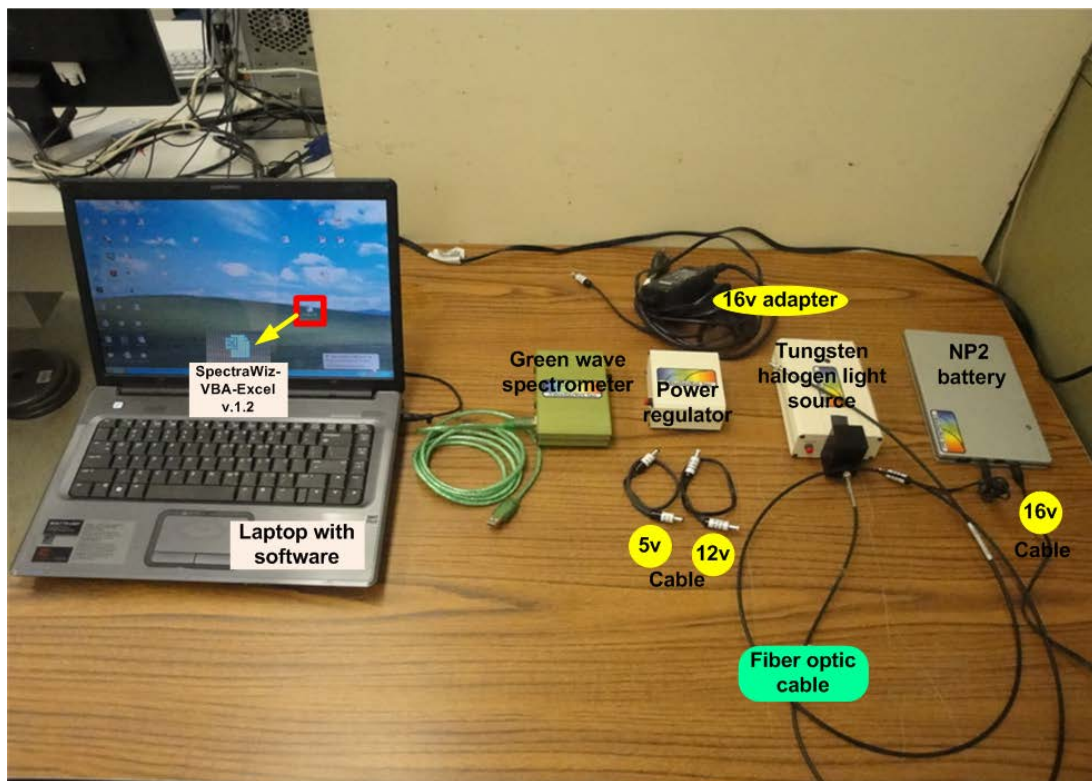


Figure B-5. Stellarnet UV-VIS Spectrometer Device.

- (1) Connect the BP2 battery to the power regulator by plugging the 16v cable in the left-hand female receptacle labeled OUT on the battery (Figure B-6 [a]).
- (2) Plug the 16v adapter cable in the right-hand female receptacle labeled OUT on the battery (Figure B-6 [b]).
- (3) Ensure that the switch on the battery pack is set to 16v.

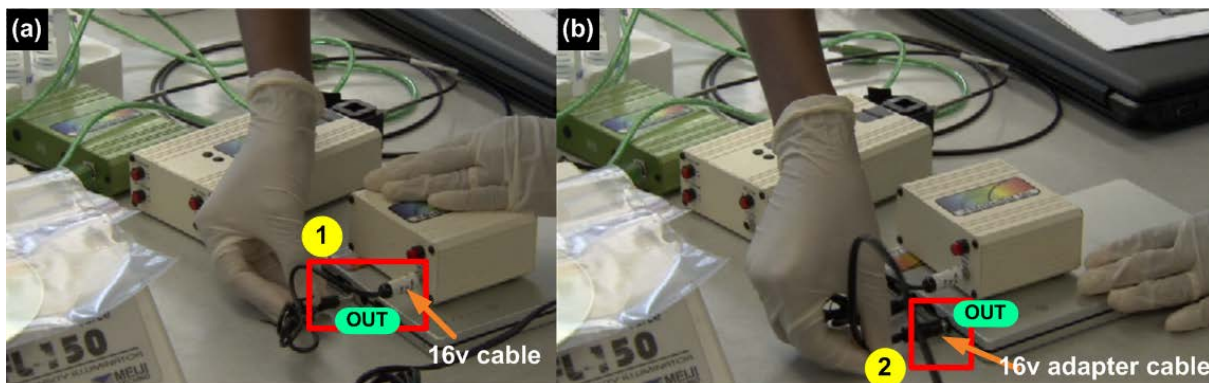


Figure B-6. Connection of the BP2 Battery to the Power Regulator.

- (4) Connect the UV-Vis tungsten halogen light source to the power regulator using the 12v cable. Make sure you use the cable labeled 12v when you connect it to the light source (Figure B-7).

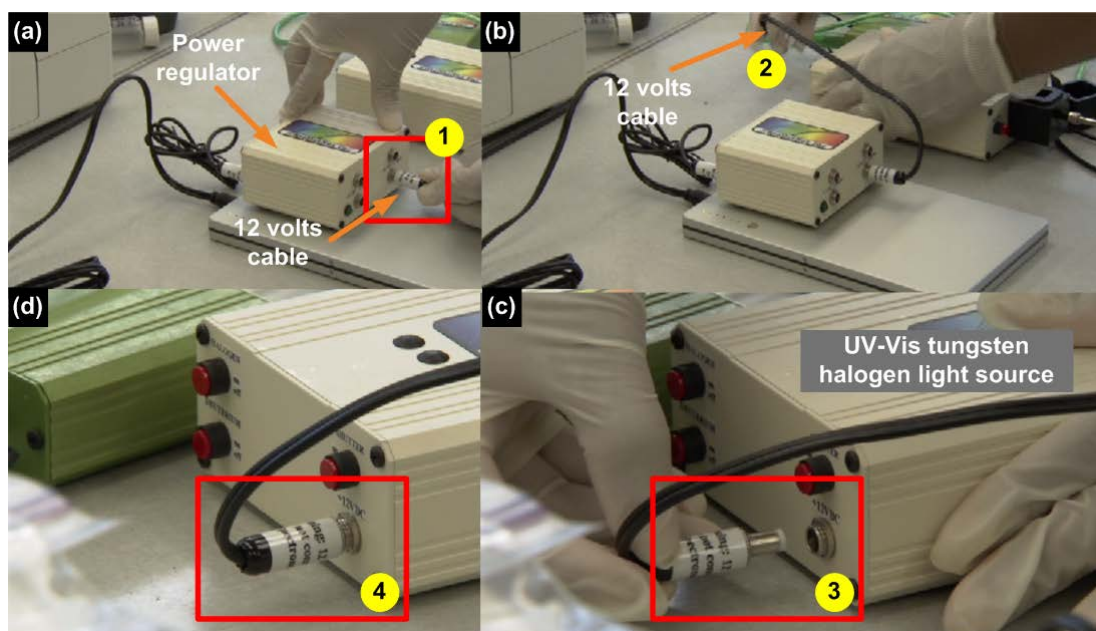


Figure B-7. Connection of UV-VIS Tungsten Halogen Light Source to the Power Regulator.

- (5) Connect the green wave spectrometer to the black cuvette holder attached to the front of the tungsten halogen light source via the fiber optic cable (Figure B-8) Make sure that the fiber optic cable is connected properly; there is an arrow on the cable that points to the green wave spectrometer when the cable is properly connected (Figure B-8 [b]).

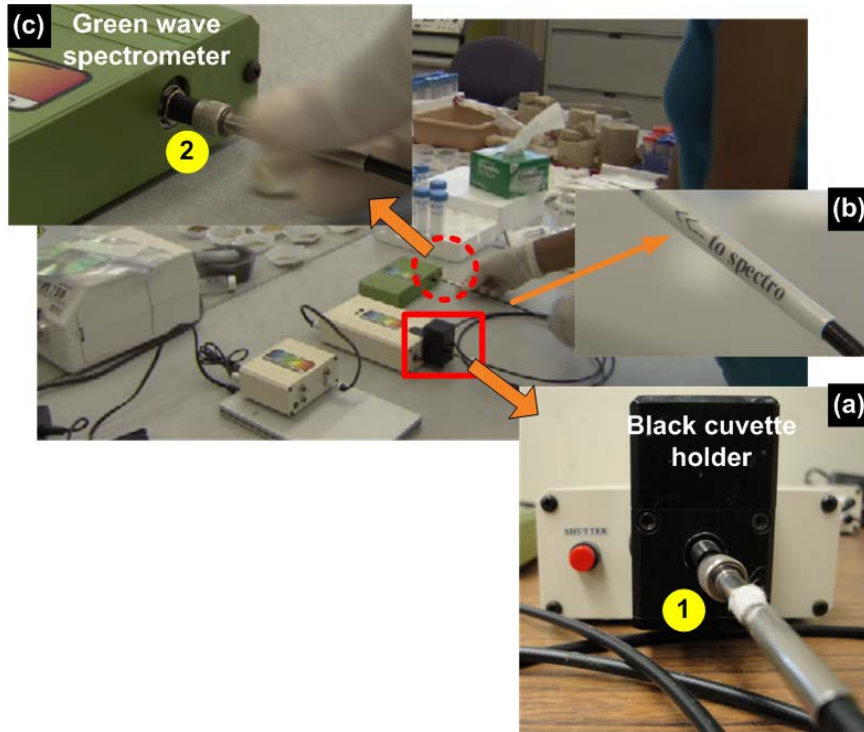


Figure B-8. Connection of Fiber Optic Cable to Green Wave Spectrometer and UV-VIS Tungsten Halogen Light Source.

- (6) Turn the computer on before connecting the USB cable to the computer (Figure B-9 [a]).
- (7) Connect the green wave spectrometer to the laptop computer with the green USB cable (Figures B-9 [b] and [c]).

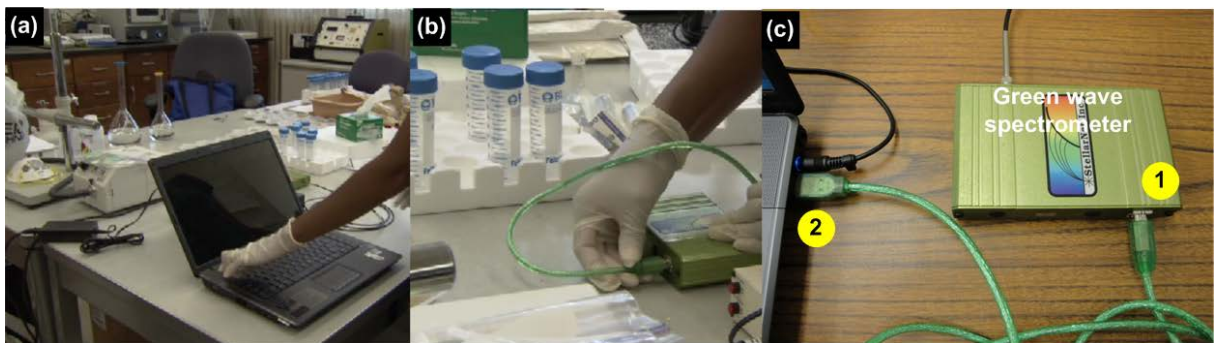


Figure B-9. Connection of the Green Wave Spectrometer to Laptop Computer.

Step 3. Measurement of Soil Organic Carbon Content

As previously stated, Stellarnet UV-VIS is a spectrometer apparatus that consists mainly of a laptop with analytical software and spectrometer device (Figure B-5). The following procedure describes how to determine organic matter content of soil sample using the SpectraWiz-VBA-Excel[®] v.1.2 software.

Step 3.1: Analysis Setup

- (1) Double-click the SpectraWiz Excel icon on the desktop to open the macro for measuring organic matter (Figure B-10 [a]).
- (2) Click on the organic carbon spreadsheet. At this point, you are ready to enter your sample labels or sample ID. (Note: Sample IDs should always start in row 2 of column A (Figure B-10 [b])).

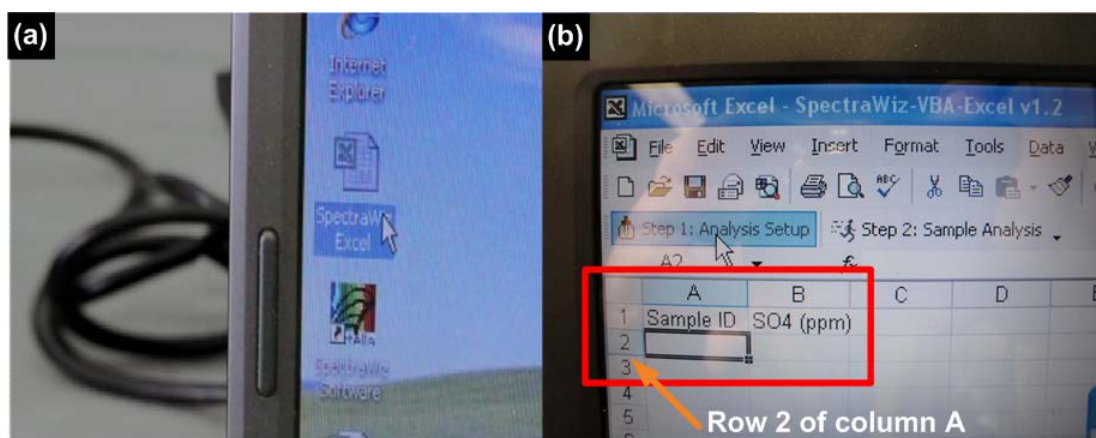


Figure B-10. SpectraWiz Excel Spreadsheet for Measuring Soil Organic Carbon.

- (3) Enter sample ID (Figure B-11 [a]).
- (4) The toolbar of the workbook should display two new control buttons: **Step 1: Analysis Setup** and **Step 2: Sample Analysis**. Click on the **Step 1: Analysis Setup** control button, and it will guide the user through important steps in a checklist that should be performed before sample analysis (Figures B-11 [b] and [c]).
- (5) After going over the checklist thoroughly, click **Continue**. At this point, the program will check the sample table. (**Note:** If there are no “Sample ID” values in row 2 of column A of the spreadsheet, a message will be displayed for the user to “Please enter sample ID” [Figure B-11 (d)]). If no messages are displayed after clicking **Continue**, you are ready to move on to sample analysis.

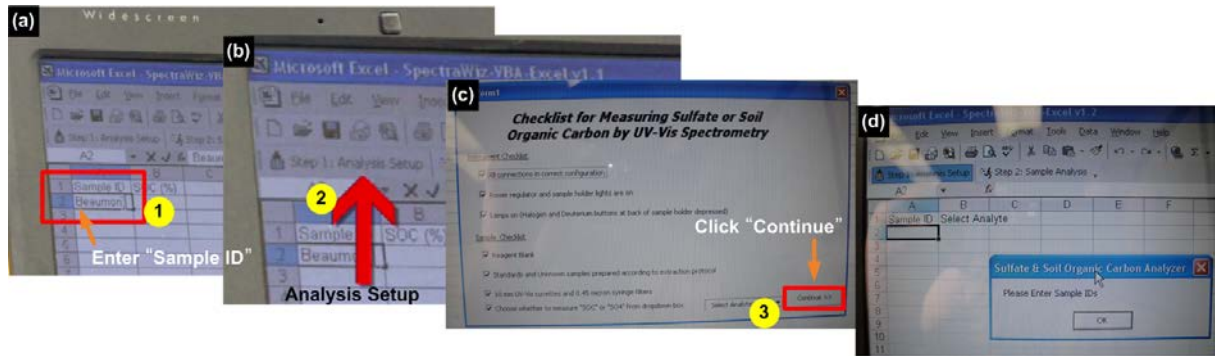


Figure B-11. Analysis Setup Procedure.

Step 3.2: Sample Analysis

3.2.1. Collection of dark spectrum.

- (1) Click on the **Step 2: Sample Analysis** button. The program will again check to make sure the instrument and sample table (input sample ID) are ready to go (Figure B-12 [a]).
- (2) A dialog box will appear with instructions for collecting the dark spectrum if everything is in place. The shutter button is at the back of the light source and is released when it is fully extended (Figure B-12 [b]).
- (3) Release the red shutter button on the back of the light source (fully extended), then click the **OK** button in the open spreadsheet, which will collect a dark spectrum (Figures B-12 [b] and [c]).

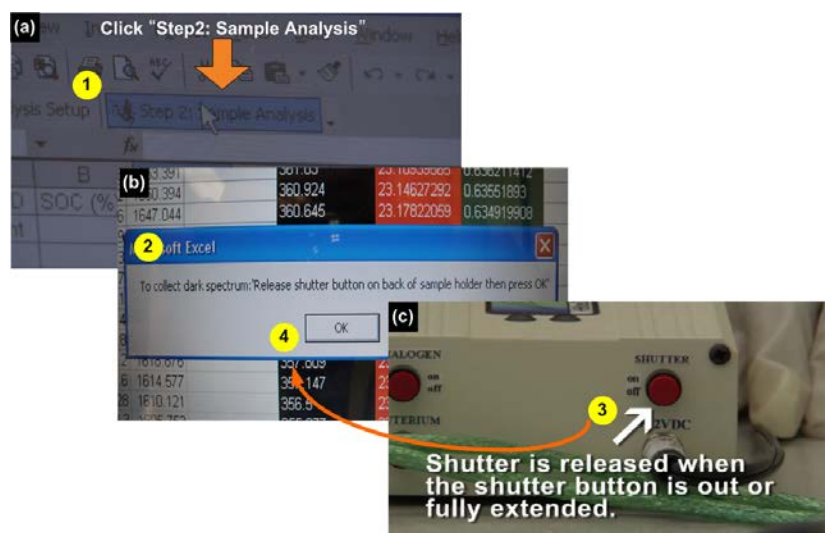


Figure B-12. Collection of Dark Spectrum.

3.2.2. Collection of reference spectrum.

- (1) After the dark spectrum is collected, instructions for collecting the “reference” spectrum will be displayed in a dialog box (Figure B-13 [a]).
- (2) Insert the reagent blank in the cuvette holder (Figure B-13 [b]). (**Note:** Prior to placing any cuvette into the cuvette holder, be sure to clean the cuvette with a Kimwipe or comparable lab wipe to remove any residue that may interfere with the beam.)
- (3) Depress the shutter button on the back of the sample holder (Figure B-13 [c]).
- (4) Click the **OK** button in the open spreadsheet to collect a reference spectrum.

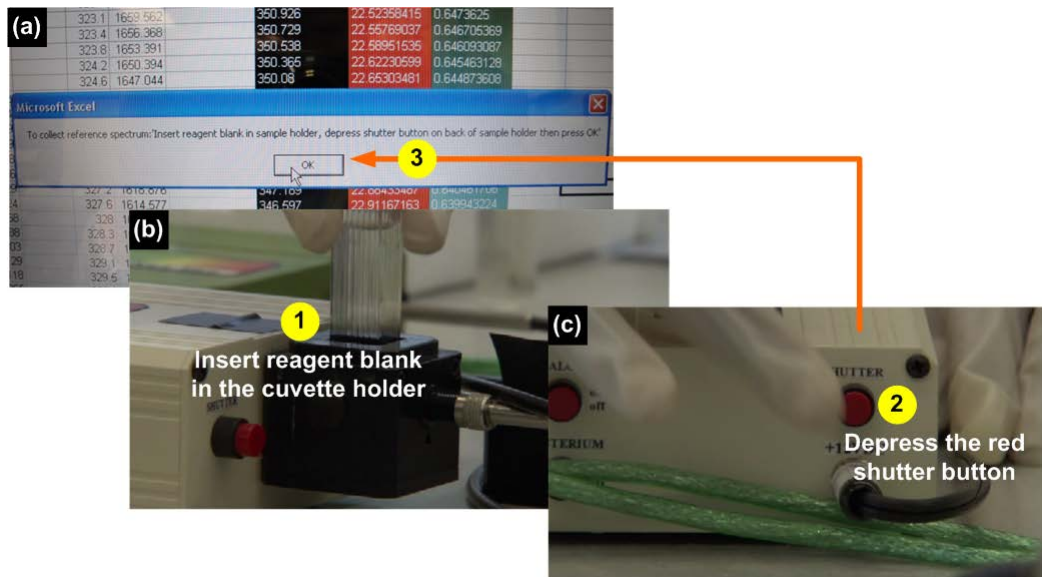


Figure B-13. Collection of Reference Spectrum.

3.2.3. Determination of the organic carbon content of soil sample.

- (1) After collecting the dark and reference spectra, samples are ready to be analyzed.
- (2) Insert soil sample and then press **OK** (Figures B-14 [a] and [b]). The soil organic carbon content will automatically be calculated and shown in the spreadsheet (Figures B-14 [c] and [d]).
- (3) After analyzing the sample in the sample table, the user can choose to save the data. If **Yes** is chosen, the data will be saved as a text file in the **SOCDATA** folder on the desktop, using the specified filename (Figure B-14 [e]). [**Note:** Do not save over the program].

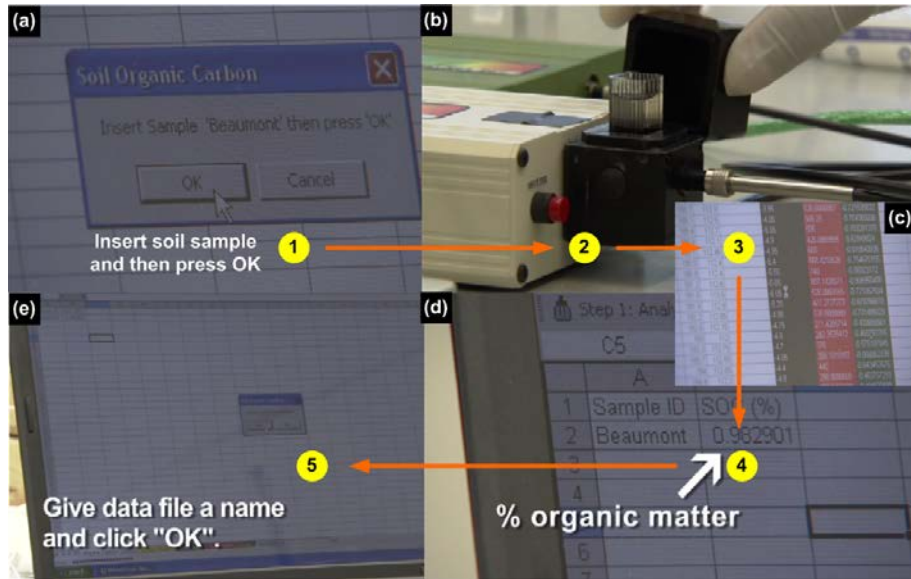


Figure B-14. Measurement of Soil Organic Carbon Content.

**APPENDIX C:
VERIS ELECTRICAL CONDUCTIVITY, SULFATE CONTENT,
ORGANIC CONTENT, WATER CONTENT, AND PLASTICITY
INDEX FOR COMBINED US67 AND US82 DATA**

Table C-1. Data for All-Range Shallow EC and Average OC, MC, PI, and ln(SC).

Roadway	Sample ID	EC Shallow (0-2 ft)	SC-avg.	OC_avg.	MC_avg.	PI_avg.	Ln (Sc-avg)
US67	US67 (MW)-H1-1	393.0	635.0	2.9	27.9	35.0	6.5
	US67 (MW)-H2-1	339.7	905.0	2.7	27.2	29.4	6.8
	US67 (MW)-M2-1	142.4	105.0	2.3	27.6	34.1	4.7
	US67 (ME)-H1-1	444.8	1555.0	3.2	29.7	38.5	7.3
	US67 (ME)-M1-1	336.8	200.0	2.9	30.4	37.4	5.3
	US67 (ME)-M2-1	288.1	140.0	2.1	29.3	36.1	4.9
	US67 (ME)-L1-1	51.2	240.0	3.3	25.7	32.1	5.5
	US67 (ME)-L2-1	110.7	125.0	3.5	20.5	37.2	4.8
US82	US82-H1-1	296.1	487.5	0.6	24.8	46.4	6.2
	US82-H2-1	328.8	1220.0	0.4	23.1	44.5	7.1
	US82-M1-1	239.9	955.0	0.6	21.6	50.1	6.9
	US82-M2-1	236.2	700.0	0.5	24.1	41.3	6.6
	US82-L1-1	49.1	122.5	0.5	17.2	22.2	4.8
	US82-L2-1	114.9	110.0	0.5	18.0	33.2	4.7
	US82-S1-H1-1	462.7	480.0	0.9	22.6	39.7	6.2
	US82-S1-H2-1	355.1	680.0	2.5	22.4	48.5	6.5
	US82-S1-M1-1	163.7	240.0	0.5	27.5	39.7	5.5
	US82-S1-M2-1	271.5	520.0	0.5	21.0	41.5	6.3
	US82-S1-L1-1	80.8	290.0	0.8	13.0	41.7	5.7
	US82-S1-L2-1	78.9	352.5	3.0	17.0	39.1	5.9
	US82-S2-H1-1	390.1	475.0	1.7	20.4	42.9	6.2
	US82-S2-H2-1	336.0	295.0	0.3	25.0	40.3	5.7
	US82-S2-M1-1	252.7	220.0	0.3	30.2	44.5	5.4
	US82-S2-M2-1	279.0	495.0	1.3	26.4	40.5	6.2
	US82-S2-L1-1	55.2	140.0	0.5	26.7	25.1	4.9
	US82-S2-L2-1	61.5	100.0	0.6	26.8	26.6	4.6
	US82-S3-H1-1	301.9	202.5	0.6	21.0	34.4	5.3
	US82-S3-H2-1	326.3	450.0	0.9	22.8	29.2	6.1
US82-S3-M1-1	132.8	220.0	0.7	22.7	34.1	5.4	
US82-S3-M2-1	143.5	280.0	0.6	17.1	35.8	5.6	
US82-S3-L1-1	69.1	100.0	0.7	13.8	26.8	4.6	
US82-S3-L2-1	29.0	215.0	1.4	25.2	26.4	5.4	

Table C-2. Data for All-Range Shallow EC and All-Range OC, MC, PI, and ln(SC).

Roadway	Sample ID	EC Shallow (0-2 ft)	SC1	OC1	MC1	PI1	Ln (SC1)	Roadway	Sample ID	EC Shallow (0-2 ft)	SC2	OC2	MC2	PI2	Ln (SC2)
US67	US67 (MW)-H1-1	393.0	740.0	3.1	28.6	35.0	6.6	US67	US67 (MW)-H1-1	393.0	680.0	3.1	28.6	35.0	6.5
	US67 (MW)-H2-1	339.7	1000.0	2.7	28.5	29.4	6.9		US67 (MW)-H2-1	339.7	1000.0	2.8	28.5	29.4	6.9
	US67 (MW)-M2-1	142.4	100.0	2.3	27.9	34.1	4.6		US67 (MW)-M2-1	142.4	110.0	2.4	27.9	34.1	4.7
	US67 (ME)-H1-1	444.8	1150.0	3.0	30.2	38.5	7.0		US67 (ME)-H1-1	444.8	1230.0	3.0	30.2	38.5	7.1
	US67 (ME)-M1-1	336.8	220.0	2.8	30.9	37.4	5.4		US67 (ME)-M1-1	336.8	200.0	2.7	30.9	37.4	5.3
	US67 (ME)-M2-1	288.1	120.0	2.0	30.7	36.1	4.8		US67 (ME)-M2-1	288.1	160.0	1.9	30.7	36.1	5.1
	US67 (ME)-L1-1	51.2	870.0	3.2	29.5	32.1	6.8		US67 (ME)-L1-1	51.2	810.0	3.2	29.5	32.1	6.7
	US67 (ME)-L2-1	110.7	150.0	3.1	20.5	37.2	5.0		US67 (ME)-L2-1	110.7	140.0	3.1	20.5	37.2	4.9
US82	US82-H1-1	296.1	420.0	0.6	24.8	46.4	6.0	US82	US82-H1-1	296.1	430.0	0.5	24.8	46.4	6.1
	US82-H2-1	328.8	1180.0	0.4	23.1	44.5	7.1		US82-H2-1	328.8	1200.0	0.4	23.1	44.5	7.1
	US82-M1-1	239.9	1000.0	0.6	21.6	50.1	6.9		US82-M1-1	239.9	960.0	0.7	21.6	50.1	6.9
	US82-M2-1	236.2	880.0	0.4	24.1	41.3	6.8		US82-M2-1	236.2	480.0	0.6	24.1	41.3	6.2
	US82-L1-1	49.1	130.0	0.5	17.2	22.2	4.9		US82-L1-1	49.1	120.0	0.5	17.2	22.2	4.8
	US82-L2-1	114.9	100.0	0.5	18.0	33.2	4.6		US82-L2-1	114.9	120.0	0.5	18.0	33.2	4.8
	US82-S1-H1-1	462.7	480.0	1.1	22.6	39.7	6.2		US82-S1-H1-1	462.7	460.0	0.7	22.6	39.7	6.1
	US82-S1-H2-1	355.1	980.0	2.1	22.4	48.5	6.9		US82-S1-H2-1	355.1	520.0	3.1	22.4	48.5	6.3
	US82-S1-M1-1	163.7	230.0	0.6	27.5	39.7	5.4		US82-S1-M1-1	163.7	230.0	0.6	27.5	39.7	5.4
	US82-S1-M2-1	271.5	510.0	0.5	21.0	41.5	6.2		US82-S1-M2-1	271.5	490.0	0.5	21.0	41.5	6.2
	US82-S1-L1-1	80.8	260.0	0.8	13.0	41.7	5.6		US82-S1-L1-1	80.8	300.0	0.8	13.0	41.7	5.7
	US82-S1-L2-1	78.9	350.0	2.8	17.0	39.1	5.9		US82-S1-L2-1	78.9	330.0	3.2	17.0	39.1	5.8
	US82-S2-H1-1	390.1	480.0	1.6	20.4	42.9	6.2		US82-S2-H1-1	390.1	460.0	1.7	20.4	42.9	6.1
	US82-S2-H2-1	336.0	280.0	0.3	25.0	40.3	5.6		US82-S2-H2-1	336.0	270.0	0.3	25.0	40.3	5.6
	US82-S2-M1-1	252.7	220.0	0.3	30.2	44.5	5.4		US82-S2-M1-1	252.7	200.0	0.3	30.2	44.5	5.3
	US82-S2-M2-1	279.0	470.0	1.2	26.4	40.5	6.2		US82-S2-M2-1	279.0	470.0	1.3	26.4	40.5	6.2
	US82-S2-L1-1	55.2	130.0	0.5	26.7	25.1	4.9		US82-S2-L1-1	55.2	140.0	0.5	26.7	25.1	4.9
	US82-S2-L2-1	61.5	100.0	0.6	26.8	26.6	4.6		US82-S2-L2-1	61.5	100.0	0.6	26.8	26.6	4.6
	US82-S3-H1-1	301.9	190.0	0.6	21.0	34.4	5.2		US82-S3-H1-1	301.9	200.0	0.6	21.0	34.4	5.3
	US82-S3-H2-1	326.3	380.0	0.9	22.8	29.2	5.9		US82-S3-H2-1	326.3	480.0	1.0	22.8	29.2	6.2
	US82-S3-M1-1	132.8	220.0	0.7	22.7	34.1	5.4		US82-S3-M1-1	132.8	210.0	0.7	22.7	34.1	5.3
	US82-S3-M2-1	143.5	290.0	0.6	17.1	35.8	5.7		US82-S3-M2-1	143.5	250.0	0.6	17.1	35.8	5.5
	US82-S3-L1-1	69.1	100.0	0.6	13.8	26.8	4.6		US82-S3-L1-1	69.1	100.0	0.7	13.8	26.8	4.6
	US82-S3-L2-1	29.0	210.0	1.4	25.2	26.4	5.3		US82-S3-L2-1	29.0	210.0	1.4	25.2	26.4	5.3
US67	US67 (MW)-H1-1	393.0	790.0	3.0	28.6	35.0	6.7	US67	US67 (MW)-H1-1	393.0	740.0	3.0	28.6	35.0	6.6
	US67 (MW)-H2-1	339.7	1100.0	2.7	28.5	29.4	7.0		US67 (MW)-H2-1	339.7	1090.0	2.7	28.5	29.4	7.0
	US67 (MW)-M2-1	142.4	110.0	2.3	27.9	34.1	4.7		US67 (MW)-M2-1	142.4	130.0	2.3	27.9	34.1	4.9
	US67 (ME)-H1-1	444.8	1270.0	3.0	30.2	38.5	7.1		US67 (ME)-H1-1	444.8	1340.0	3.0	30.2	38.5	7.2
	US67 (ME)-M1-1	336.8	220.0	2.8	30.9	37.4	5.4		US67 (ME)-M1-1	336.8	220.0	2.8	30.9	37.4	5.4
	US67 (ME)-M2-1	288.1	130.0	2.1	30.7	36.1	4.9		US67 (ME)-M2-1	288.1	130.0	2.1	30.7	36.1	4.9
	US67 (ME)-L1-1	51.2	970.0	3.3	29.5	32.1	6.9		US67 (ME)-L1-1	51.2	870.0	3.3	29.5	32.1	6.8
	US67 (ME)-L2-1	110.7	140.0	3.1	20.5	37.2	4.9		US67 (ME)-L2-1	110.7	150.0	3.1	20.5	37.2	5.0
US82	US82-H1-1	296.1	550.0	0.6	24.8	46.4	6.3	US82	US82-H1-1	296.1	550.0	0.6	24.8	46.4	6.3
	US82-H2-1	328.8	1250.0	0.4	23.1	44.5	7.1		US82-H2-1	328.8	1250.0	0.5	23.1	44.5	7.1
	US82-M1-1	239.9	930.0	0.6	21.6	50.1	6.8		US82-M1-1	239.9	930.0	0.6	21.6	50.1	6.8
	US82-M2-1	236.2	720.0	0.4	24.1	41.3	6.6		US82-M2-1	236.2	720.0	0.4	24.1	41.3	6.6
	US82-L1-1	49.1	120.0	0.6	17.2	22.2	4.8		US82-L1-1	49.1	120.0	0.5	17.2	22.2	4.8
	US82-L2-1	114.9	110.0	0.5	18.0	33.2	4.7		US82-L2-1	114.9	110.0	0.5	18.0	33.2	4.7
	US82-S1-H1-1	462.7	480.0	1.2	22.6	39.7	6.2		US82-S1-H1-1	462.7	500.0	0.7	22.6	39.7	6.2
	US82-S1-H2-1	355.1	700.0	2.1	22.4	48.5	6.6		US82-S1-H2-1	355.1	520.0	2.9	22.4	48.5	6.3
	US82-S1-M1-1	163.7	250.0	0.5	27.5	39.7	5.5		US82-S1-M1-1	163.7	250.0	0.5	27.5	39.7	5.5
	US82-S1-M2-1	271.5	550.0	0.5	21.0	41.5	6.3		US82-S1-M2-1	271.5	530.0	0.5	21.0	41.5	6.3
	US82-S1-L1-1	80.8	280.0	0.7	13.0	41.7	5.6		US82-S1-L1-1	80.8	320.0	0.8	13.0	41.7	5.8
	US82-S1-L2-1	78.9	380.0	2.8	17.0	39.1	5.9		US82-S1-L2-1	78.9	350.0	3.3	17.0	39.1	5.9
	US82-S2-H1-1	390.1	500.0	1.6	20.4	42.9	6.2		US82-S2-H1-1	390.1	460.0	1.7	20.4	42.9	6.1
	US82-S2-H2-1	336.0	320.0	0.4	25.0	40.3	5.8		US82-S2-H2-1	336.0	310.0	0.3	25.0	40.3	5.7
	US82-S2-M1-1	252.7	240.0	0.3	30.2	44.5	5.5		US82-S2-M1-1	252.7	220.0	0.3	30.2	44.5	5.4
	US82-S2-M2-1	279.0	510.0	1.2	26.4	40.5	6.2		US82-S2-M2-1	279.0	530.0	1.3	26.4	40.5	6.3
	US82-S2-L1-1	55.2	150.0	0.5	26.7	25.1	5.0		US82-S2-L1-1	55.2	140.0	0.4	26.7	25.1	4.9
	US82-S2-L2-1	61.5	100.0	0.6	26.8	26.6	4.6		US82-S2-L2-1	61.5	100.0	0.6	26.8	26.6	4.6
	US82-S3-H1-1	301.9	210.0	0.6	21.0	34.4	5.3		US82-S3-H1-1	301.9	210.0	0.7	21.0	34.4	5.3
	US82-S3-H2-1	326.3	430.0	0.9	22.8	29.2	6.1		US82-S3-H2-1	326.3	510.0	0.9	22.8	29.2	6.2
	US82-S3-M1-1	132.8	230.0	0.7	22.7	34.1	5.4		US82-S3-M1-1	132.8	220.0	0.7	22.7	34.1	5.4
	US82-S3-M2-1	143.5	310.0	0.5	17.1	35.8	5.7		US82-S3-M2-1	143.5	270.0	0.6	17.1	35.8	5.6
	US82-S3-L1-1	69.1	100.0	0.7	13.8	26.8	4.6		US82-S3-L1-1	69.1	100.0	0.7	13.8	26.8	4.6
	US82-S3-L2-1	29.0	220.0	1.4	25.2	26.4	5.4		US82-S3-L2-1	29.0	220.0	1.4	25.2	26.4	5.4

Table C-3. Data for Shallow EC_{>100} and Average OC, MC, PI, and ln(SC).

Roadway	Sample ID	EC Shallow (0-2 ft)	SC-avg.	OC_avg.	MC_avg.	PI_avg.	Ln (Sc-avg)
US67	US67 (MW)-H1-1	393.0	737.5	3.0	28.6	35.0	6.6
	US67 (MW)-H2-1	339.7	1047.5	2.7	28.5	29.4	7.0
	US67 (MW)-M2-1	142.4	112.5	2.3	27.9	34.1	4.7
	US67 (ME)-H1-1	444.8	1247.5	3.0	30.2	38.5	7.1
	US67 (ME)-M1-1	336.8	215.0	2.8	30.9	37.4	5.4
	US67 (ME)-M2-1	288.1	135.0	2.0	30.7	36.1	4.9
	US67 (ME)-L2-1	110.7	145.0	3.1	20.5	37.2	5.0
US82	US82-H1-1	296.1	487.5	0.6	24.8	46.4	6.2
	US82-H2-1	328.8	1220.0	0.4	23.1	44.5	7.1
	US82-M1-1	239.9	955.0	0.6	21.6	50.1	6.9
	US82-M2-1	236.2	700.0	0.5	24.1	41.3	6.6
	US82-L2-1	114.9	110.0	0.5	18.0	33.2	4.7
	US82-S1-H1-1	462.7	480.0	0.9	22.6	39.7	6.2
	US82-S1-H2-1	355.1	680.0	2.5	22.4	48.5	6.5
	US82-S1-M1-1	163.7	240.0	0.5	27.5	39.7	5.5
	US82-S1-M2-1	271.5	520.0	0.5	21.0	41.5	6.3
	US82-S2-H1-1	390.1	475.0	1.7	20.4	42.9	6.2
	US82-S2-H2-1	336.0	295.0	0.3	25.0	40.3	5.7
	US82-S2-M1-1	252.7	220.0	0.3	30.2	44.5	5.4
	US82-S2-M2-1	279.0	495.0	1.3	26.4	40.5	6.2
	US82-S3-H1-1	301.9	202.5	0.6	21.0	34.4	5.3
	US82-S3-H2-1	326.3	450.0	0.9	22.8	29.2	6.1
	US82-S3-M1-1	132.8	220.0	0.7	22.7	34.1	5.4
US82-S3-M2-1	143.5	280.0	0.6	17.1	35.8	5.6	

Table C-4. Data for Shallow EC_{>100} and All-Range OC, MC, PI, and Ln(SC).

Roadway	Sample ID	EC Shallow (0-2 ft)	SC1	OC1	MC1	PI1	Ln (SC1)	Roadway	Sample ID	EC Shallow (0-2 ft)	SC2	OC2	MC2	PI2	Ln (SC2)
US67	US67 (MW)-H1-1	393.0	740.0	3.1	28.6	35.0	6.6	US67	US67 (MW)-H1-1	393.0	680.0	3.1	28.6	35.0	6.5
	US67 (MW)-H2-1	339.7	1000.0	2.7	28.5	29.4	6.9		US67 (MW)-H2-1	339.7	1000.0	2.8	28.5	29.4	6.9
	US67 (MW)-M2-1	142.4	100.0	2.3	27.9	34.1	4.6		US67 (MW)-M2-1	142.4	110.0	2.4	27.9	34.1	4.7
	US67 (ME)-H1-1	444.8	1150.0	3.0	30.2	38.5	7.0		US67 (ME)-H1-1	444.8	1230.0	3.0	30.2	38.5	7.1
	US67 (ME)-M1-1	336.8	220.0	2.8	30.9	37.4	5.4		US67 (ME)-M1-1	336.8	200.0	2.7	30.9	37.4	5.3
	US67 (ME)-M2-1	288.1	120.0	2.0	30.7	36.1	4.8		US67 (ME)-M2-1	288.1	160.0	1.9	30.7	36.1	5.1
	US67 (ME)-L2-1	110.7	150.0	3.1	20.5	37.2	5.0		US67 (ME)-L2-1	110.7	140.0	3.1	20.5	37.2	4.9
US82	US82-H1-1	296.1	420.0	0.6	24.8	46.4	6.0	US82	US82-H1-1	296.1	430.0	0.5	24.8	46.4	6.1
	US82-H2-1	328.8	1180.0	0.4	23.1	44.5	7.1		US82-H2-1	328.8	1200.0	0.4	23.1	44.5	7.1
	US82-M1-1	239.9	1000.0	0.6	21.6	50.1	6.9		US82-M1-1	239.9	960.0	0.7	21.6	50.1	6.9
	US82-M2-1	236.2	880.0	0.4	24.1	41.3	6.8		US82-M2-1	236.2	480.0	0.6	24.1	41.3	6.2
	US82-L2-1	114.9	100.0	0.5	18.0	33.2	4.6		US82-L2-1	114.9	120.0	0.5	18.0	33.2	4.8
	US82-S1-H1-1	462.7	480.0	1.1	22.6	39.7	6.2		US82-S1-H1-1	462.7	460.0	0.7	22.6	39.7	6.1
	US82-S1-H2-1	355.1	980.0	2.1	22.4	48.5	6.9		US82-S1-H2-1	355.1	520.0	3.1	22.4	48.5	6.3
	US82-S1-M1-1	163.7	230.0	0.6	27.5	39.7	5.4		US82-S1-M1-1	163.7	230.0	0.6	27.5	39.7	5.4
	US82-S1-M2-1	271.5	510.0	0.5	21.0	41.5	6.2		US82-S1-M2-1	271.5	490.0	0.5	21.0	41.5	6.2
	US82-S2-H1-1	390.1	480.0	1.6	20.4	42.9	6.2		US82-S2-H1-1	390.1	460.0	1.7	20.4	42.9	6.1
	US82-S2-H2-1	336.0	280.0	0.3	25.0	40.3	5.6		US82-S2-H2-1	336.0	270.0	0.3	25.0	40.3	5.6
	US82-S2-M1-1	252.7	220.0	0.3	30.2	44.5	5.4		US82-S2-M1-1	252.7	200.0	0.3	30.2	44.5	5.3
	US82-S2-M2-1	279.0	470.0	1.2	26.4	40.5	6.2		US82-S2-M2-1	279.0	470.0	1.3	26.4	40.5	6.2
	US82-S3-H1-1	301.9	190.0	0.6	21.0	34.4	5.2		US82-S3-H1-1	301.9	200.0	0.6	21.0	34.4	5.3
	US82-S3-H2-1	326.3	380.0	0.9	22.8	29.2	5.9		US82-S3-H2-1	326.3	480.0	1.0	22.8	29.2	6.2
	US82-S3-M1-1	132.8	220.0	0.7	22.7	34.1	5.4		US82-S3-M1-1	132.8	210.0	0.7	22.7	34.1	5.3
US82-S3-M2-1	143.5	290.0	0.6	17.1	35.8	5.7	US82-S3-M2-1	143.5	250.0	0.6	17.1	35.8	5.5		
Roadway	Sample ID	EC Shallow (0-2 ft)	SC3	OC3	MC3	PI3	Ln (SC3)	Roadway	Sample ID	EC Shallow (0-2 ft)	SC4	OC4	MC4	PI4	Ln (SC4)
US67	US67 (MW)-H1-1	393.0	790.0	3.0	28.6	35.0	6.7	US67	US67 (MW)-H1-1	393.0	740.0	3.0	28.6	35.0	6.6
	US67 (MW)-H2-1	339.7	1100.0	2.7	28.5	29.4	7.0		US67 (MW)-H2-1	339.7	1090.0	2.7	28.5	29.4	7.0
	US67 (MW)-M2-1	142.4	110.0	2.3	27.9	34.1	4.7		US67 (MW)-M2-1	142.4	130.0	2.3	27.9	34.1	4.9
	US67 (ME)-H1-1	444.8	1270.0	3.0	30.2	38.5	7.1		US67 (ME)-H1-1	444.8	1340.0	3.0	30.2	38.5	7.2
	US67 (ME)-M1-1	336.8	220.0	2.8	30.9	37.4	5.4		US67 (ME)-M1-1	336.8	220.0	2.8	30.9	37.4	5.4
	US67 (ME)-M2-1	288.1	130.0	2.1	30.7	36.1	4.9		US67 (ME)-M2-1	288.1	130.0	2.1	30.7	36.1	4.9
	US67 (ME)-L2-1	110.7	140.0	3.1	20.5	37.2	4.9		US67 (ME)-L2-1	110.7	150.0	3.1	20.5	37.2	5.0
US82	US82-H1-1	296.1	550.0	0.6	24.8	46.4	6.3	US82	US82-H1-1	296.1	550.0	0.6	24.8	46.4	6.3
	US82-H2-1	328.8	1250.0	0.4	23.1	44.5	7.1		US82-H2-1	328.8	1250.0	0.5	23.1	44.5	7.1
	US82-M1-1	239.9	930.0	0.6	21.6	50.1	6.8		US82-M1-1	239.9	930.0	0.6	21.6	50.1	6.8
	US82-M2-1	236.2	720.0	0.4	24.1	41.3	6.6		US82-M2-1	236.2	720.0	0.4	24.1	41.3	6.6
	US82-L2-1	114.9	110.0	0.5	18.0	33.2	4.7		US82-L2-1	114.9	110.0	0.5	18.0	33.2	4.7
	US82-S1-H1-1	462.7	480.0	1.2	22.6	39.7	6.2		US82-S1-H1-1	462.7	500.0	0.7	22.6	39.7	6.2
	US82-S1-H2-1	355.1	700.0	2.1	22.4	48.5	6.6		US82-S1-H2-1	355.1	520.0	2.9	22.4	48.5	6.3
	US82-S1-M1-1	163.7	250.0	0.5	27.5	39.7	5.5		US82-S1-M1-1	163.7	250.0	0.5	27.5	39.7	5.5
	US82-S1-M2-1	271.5	550.0	0.5	21.0	41.5	6.3		US82-S1-M2-1	271.5	530.0	0.5	21.0	41.5	6.3
	US82-S2-H1-1	390.1	500.0	1.6	20.4	42.9	6.2		US82-S2-H1-1	390.1	460.0	1.7	20.4	42.9	6.1
	US82-S2-H2-1	336.0	320.0	0.4	25.0	40.3	5.8		US82-S2-H2-1	336.0	310.0	0.3	25.0	40.3	5.7
	US82-S2-M1-1	252.7	240.0	0.3	30.2	44.5	5.5		US82-S2-M1-1	252.7	220.0	0.3	30.2	44.5	5.4
	US82-S2-M2-1	279.0	510.0	1.2	26.4	40.5	6.2		US82-S2-M2-1	279.0	530.0	1.3	26.4	40.5	6.3
	US82-S3-H1-1	301.9	210.0	0.6	21.0	34.4	5.3		US82-S3-H1-1	301.9	210.0	0.7	21.0	34.4	5.3
	US82-S3-H2-1	326.3	430.0	0.9	22.8	29.2	6.1		US82-S3-H2-1	326.3	510.0	0.9	22.8	29.2	6.2
	US82-S3-M1-1	132.8	230.0	0.7	22.7	34.1	5.4		US82-S3-M1-1	132.8	220.0	0.7	22.7	34.1	5.4
US82-S3-M2-1	143.5	310.0	0.5	17.1	35.8	5.7	US82-S3-M2-1	143.5	270.0	0.6	17.1	35.8	5.6		

Table C-5. Data for All-Range Deep EC and Average OC, MC, PI, and ln(SC).

Roadway	Sample ID	EC Deep (0-4 ft)	SC-avg.	OC_avg.	MC_avg.	PI_avg.	Ln (Sc-avg)
US67	US67 (MW)-H1-1	135.4	1032.5	2.9	30.0	36.1	6.9
	US67 (MW)-H2-1	139.5	1222.5	2.5	30.0	32.5	7.1
	US67 (MW)-M2-1	98.0	288.8	2.3	29.1	33.3	5.7
	US67 (ME)-H1-1	397.5	8587.5	2.4	29.6	38.2	9.1
	US67 (ME)-M1-1	231.1	8997.5	2.1	29.2	34.8	9.1
	US67 (ME)-M2-1	317.7	561.3	1.7	30.9	38.4	6.3
	US67 (ME)-L1-1	36.8	4182.5	2.9	31.7	35.1	8.3
	US67 (ME)-L2-1	145.2	8103.8	2.4	24.7	37.2	9.0
US82	US82-H1-1	117.3	306.3	0.5	25.1	39.5	5.7
	US82-H2-1	137.2	673.8	0.4	22.9	33.8	6.5
	US82-M1-1	148.7	598.8	0.6	24.8	42.9	6.4
	US82-M2-1	131.1	520.0	0.5	25.3	34.6	6.3
	US82-L1-1	51.5	111.3	0.5	18.5	24.8	4.7
	US82-L2-1	96.2	105.0	0.4	15.0	20.7	4.7
	US82-S1-H1-1	205.3	318.8	0.7	21.7	30.6	5.8
	US82-S1-H2-1	187.2	402.5	2.9	22.8	33.7	6.0
	US82-S1-M1-1	98.2	233.8	0.6	22.7	36.1	5.5
	US82-S1-M2-1	153.8	343.8	0.4	23.3	37.4	5.8
	US82-S1-L1-1	61.0	262.5	0.7	14.2	36.5	5.6
	US82-S1-L2-1	63.8	330.0	1.8	23.4	42.7	5.8
	US82-S2-H1-1	240.7	296.3	1.4	23.3	33.3	5.7
	US82-S2-H2-1	178.8	406.3	0.4	24.2	36.1	6.0
	US82-S2-M1-1	134.6	413.8	0.2	28.3	46.8	6.0
	US82-S2-M2-1	151.5	312.5	1.0	26.1	39.9	5.7
	US82-S2-L1-1	35.6	131.3	0.3	25.7	26.1	4.9
	US82-S2-L2-1	48.0	426.3	0.8	27.8	39.4	6.1
	US82-S3-H1-1	166.0	186.3	0.7	22.8	33.9	5.2
	US82-S3-H2-1	59.7	468.8	0.8	22.0	27.3	6.2
	US82-S3-M1-1	89.4	160.0	0.6	23.9	31.7	5.1
	US82-S3-M2-1	93.1	325.0	1.1	21.2	39.6	5.8
	US82-S3-L1-1	73.4	100.0	0.6	15.5	18.3	4.6
	US82-S3-L2-1	40.1	157.5	1.0	23.1	23.8	5.1

Table C-6. Data for All-Range Deep EC and All-Range OC, MC, PI, and ln(SC).

Roadway	Sample ID	EC Deep (0-4 ft)	SC1	OC1	MC1	PI1	Ln (SC1)	Roadway	Sample ID	EC Deep (0-4 ft)	SC2	OC2	MC2	PI2	Ln (SC2)
	US67 (MW)-H1-1	135.4	1075.0	2.9	30.0	36.1	7.0		US67 (MW)-H1-1	135.4	905.0	2.9	30.0	36.1	6.8
	US67 (MW)-H2-1	139.5	1175.0	2.5	30.0	32.5	7.1		US67 (MW)-H2-1	139.5	1165.0	2.6	30.0	32.5	7.1
	US67 (MW)-M2-1	98.0	280.0	2.3	29.1	33.3	5.6		US67 (MW)-M2-1	98.0	265.0	2.3	29.1	33.3	5.6
US67	US67 (ME)-H1-1	397.5	8445.0	2.4	29.6	38.2	9.0	US67	US67 (ME)-H1-1	397.5	8620.0	2.4	29.6	38.2	9.1
	US67 (ME)-M1-1	231.1	8670.0	2.1	29.2	34.8	9.1		US67 (ME)-M1-1	231.1	9020.0	2.1	29.2	34.8	9.1
	US67 (ME)-M2-1	317.7	580.0	1.7	30.9	38.4	6.4		US67 (ME)-M2-1	317.7	505.0	1.6	30.9	38.4	6.2
	US67 (ME)-L1-1	36.8	3815.0	2.9	31.7	35.1	8.2		US67 (ME)-L1-1	36.8	4145.0	2.9	31.7	35.1	8.3
	US67 (ME)-L2-1	145.2	7910.0	2.4	24.7	37.2	9.0		US67 (ME)-L2-1	145.2	8195.0	2.4	24.7	37.2	9.0
	US82-H1-1	117.3	280.0	0.5	25.1	39.5	5.6		US82-H1-1	117.3	265.0	0.5	25.1	39.5	5.6
	US82-H2-1	137.2	650.0	0.4	22.9	33.8	6.5		US82-H2-1	137.2	655.0	0.5	22.9	33.8	6.5
	US82-M1-1	148.7	625.0	0.5	24.8	42.9	6.4		US82-M1-1	148.7	580.0	0.6	24.8	42.9	6.4
	US82-M2-1	131.1	605.0	0.5	25.3	34.6	6.4		US82-M2-1	131.1	385.0	0.5	25.3	34.6	6.0
	US82-L1-1	51.5	115.0	0.5	18.5	24.8	4.7		US82-L1-1	51.5	110.0	0.5	18.5	24.8	4.7
	US82-L2-1	96.2	100.0	0.4	15.0	20.7	4.6		US82-L2-1	96.2	110.0	0.4	15.0	20.7	4.7
	US82-S1-H1-1	205.3	315.0	0.8	21.7	30.6	5.8		US82-S1-H1-1	205.3	300.0	0.6	21.7	30.6	5.7
	US82-S1-H2-1	187.2	550.0	2.9	22.8	33.7	6.3		US82-S1-H2-1	187.2	325.0	3.1	22.8	33.7	5.8
	US82-S1-M1-1	98.2	225.0	0.6	22.7	36.1	5.4		US82-S1-M1-1	98.2	220.0	0.6	22.7	36.1	5.4
US82	US82-S1-M2-1	153.8	340.0	0.4	23.3	37.4	5.8	US82	US82-S1-M2-1	153.8	325.0	0.4	23.3	37.4	5.8
	US82-S1-L1-1	61.0	245.0	0.7	14.2	36.5	5.5		US82-S1-L1-1	61.0	265.0	0.7	14.2	36.5	5.6
	US82-S1-L2-1	63.8	320.0	1.6	23.4	42.7	5.8		US82-S1-L2-1	63.8	315.0	1.9	23.4	42.7	5.8
	US82-S2-H1-1	240.7	295.0	1.3	23.3	33.3	5.7		US82-S2-H1-1	240.7	295.0	1.5	23.3	33.3	5.7
	US82-S2-H2-1	178.8	405.0	0.4	24.2	36.1	6.0		US82-S2-H2-1	178.8	370.0	0.4	24.2	36.1	5.9
	US82-S2-M1-1	134.6	395.0	0.3	28.3	46.8	6.0		US82-S2-M1-1	134.6	395.0	0.2	28.3	46.8	6.0
	US82-S2-M2-1	151.5	300.0	0.9	26.1	39.9	5.7		US82-S2-M2-1	151.5	295.0	1.0	26.1	39.9	5.7
	US82-S2-L1-1	35.6	125.0	0.3	25.7	26.1	4.8		US82-S2-L1-1	35.6	130.0	0.3	25.7	26.1	4.9
	US82-S2-L2-1	48.0	410.0	0.9	27.8	39.4	6.0		US82-S2-L2-1	48.0	410.0	0.6	27.8	39.4	6.0
	US82-S3-H1-1	166.0	145.0	0.7	22.8	33.9	5.0		US82-S3-H1-1	166.0	220.0	0.7	22.8	33.9	5.4
	US82-S3-H2-1	59.7	435.0	0.7	22.0	27.3	6.1		US82-S3-H2-1	59.7	470.0	0.8	22.0	27.3	6.2
	US82-S3-M1-1	89.4	160.0	0.6	23.9	31.7	5.1		US82-S3-M1-1	89.4	155.0	0.6	23.9	31.7	5.0
	US82-S3-M2-1	93.1	330.0	1.1	21.2	39.6	5.8		US82-S3-M2-1	93.1	295.0	1.1	21.2	39.6	5.7
	US82-S3-L1-1	73.4	100.0	0.6	15.5	18.3	4.6		US82-S3-L1-1	73.4	100.0	0.6	15.5	18.3	4.6
	US82-S3-L2-1	40.1	155.0	1.0	23.1	23.8	5.0		US82-S3-L2-1	40.1	155.0	1.0	23.1	23.8	5.0
Roadway	Sample ID	EC Deep (0-4 ft)	SC3	OC3	MC3	PI3	Ln (SC3)	Roadway	Sample ID	EC Deep (0-4 ft)	SC4	OC4	MC4	PI4	Ln (SC4)
	US67 (MW)-H1-1	135.4	1165.0	2.9	30.0	36.1	7.1		US67 (MW)-H1-1	135.4	985.0	2.9	30.0	36.1	6.9
	US67 (MW)-H2-1	139.5	1285.0	2.5	30.0	32.5	7.2		US67 (MW)-H2-1	139.5	1265.0	2.5	30.0	32.5	7.1
	US67 (MW)-M2-1	98.0	310.0	2.3	29.1	33.3	5.7		US67 (MW)-M2-1	98.0	300.0	2.3	29.1	33.3	5.7
US67	US67 (ME)-H1-1	397.5	8535.0	2.3	29.6	38.2	9.1	US67	US67 (ME)-H1-1	397.5	8750.0	2.4	29.6	38.2	9.1
	US67 (ME)-M1-1	231.1	9090.0	2.1	29.2	34.8	9.1		US67 (ME)-M1-1	231.1	9210.0	2.2	29.2	34.8	9.1
	US67 (ME)-M2-1	317.7	635.0	1.8	30.9	38.4	6.5		US67 (ME)-M2-1	317.7	525.0	1.8	30.9	38.4	6.3
	US67 (ME)-L1-1	36.8	4205.0	2.9	31.7	35.1	8.3		US67 (ME)-L1-1	36.8	4565.0	2.9	31.7	35.1	8.4
	US67 (ME)-L2-1	145.2	8250.0	2.4	24.7	37.2	9.0		US67 (ME)-L2-1	145.2	8060.0	2.4	24.7	37.2	9.0
	US82-H1-1	117.3	340.0	0.5	25.1	39.5	5.8		US82-H1-1	117.3	340.0	0.5	25.1	39.5	5.8
	US82-H2-1	137.2	695.0	0.4	22.9	33.8	6.5		US82-H2-1	137.2	695.0	0.5	22.9	33.8	6.5
	US82-M1-1	148.7	595.0	0.6	24.8	42.9	6.4		US82-M1-1	148.7	595.0	0.6	24.8	42.9	6.4
	US82-M2-1	131.1	545.0	0.5	25.3	34.6	6.3		US82-M2-1	131.1	545.0	0.5	25.3	34.6	6.3
	US82-L1-1	51.5	110.0	0.5	18.5	24.8	4.7		US82-L1-1	51.5	110.0	0.5	18.5	24.8	4.7
	US82-L2-1	96.2	105.0	0.4	15.0	20.7	4.7		US82-L2-1	96.2	105.0	0.4	15.0	20.7	4.7
	US82-S1-H1-1	205.3	325.0	0.8	21.7	30.6	5.8		US82-S1-H1-1	205.3	335.0	0.6	21.7	30.6	5.8
	US82-S1-H2-1	187.2	410.0	2.8	22.8	33.7	6.0		US82-S1-H2-1	187.2	325.0	2.9	22.8	33.7	5.8
	US82-S1-M1-1	98.2	245.0	0.5	22.7	36.1	5.5		US82-S1-M1-1	98.2	245.0	0.5	22.7	36.1	5.5
US82	US82-S1-M2-1	153.8	355.0	0.4	23.3	37.4	5.9	US82	US82-S1-M2-1	153.8	355.0	0.4	23.3	37.4	5.9
	US82-S1-L1-1	61.0	265.0	0.6	14.2	36.5	5.6		US82-S1-L1-1	61.0	275.0	0.7	14.2	36.5	5.6
	US82-S1-L2-1	63.8	350.0	1.7	23.4	42.7	5.9		US82-S1-L2-1	63.8	335.0	1.9	23.4	42.7	5.8
	US82-S2-H1-1	240.7	300.0	1.4	23.3	33.3	5.7		US82-S2-H1-1	240.7	295.0	1.5	23.3	33.3	5.7
	US82-S2-H2-1	178.8	450.0	0.5	24.2	36.1	6.1		US82-S2-H2-1	178.8	400.0	0.4	24.2	36.1	6.0
	US82-S2-M1-1	134.6	430.0	0.2	28.3	46.8	6.1		US82-S2-M1-1	134.6	435.0	0.2	28.3	46.8	6.1
	US82-S2-M2-1	151.5	325.0	0.9	26.1	39.9	5.8		US82-S2-M2-1	151.5	330.0	1.0	26.1	39.9	5.8
	US82-S2-L1-1	35.6	135.0	0.3	25.7	26.1	4.9		US82-S2-L1-1	35.6	135.0	0.3	25.7	26.1	4.9
	US82-S2-L2-1	48.0	440.0	0.9	27.8	39.4	6.1		US82-S2-L2-1	48.0	445.0	0.6	27.8	39.4	6.1
	US82-S3-H1-1	166.0	155.0	0.7	22.8	33.9	5.0		US82-S3-H1-1	166.0	225.0	0.7	22.8	33.9	5.4
	US82-S3-H2-1	59.7	495.0	0.8	22.0	27.3	6.2		US82-S3-H2-1	59.7	475.0	0.8	22.0	27.3	6.2
	US82-S3-M1-1	89.4	165.0	0.6	23.9	31.7	5.1		US82-S3-M1-1	89.4	160.0	0.6	23.9	31.7	5.1
	US82-S3-M2-1	93.1	355.0	1.1	21.2	39.6	5.9		US82-S3-M2-1	93.1	320.0	1.1	21.2	39.6	5.8
	US82-S3-L1-1	73.4	100.0	0.7	15.5	18.3	4.6		US82-S3-L1-1	73.4	100.0	0.6	15.5	18.3	4.6
	US82-S3-L2-1	40.1	160.0	0.9	23.1	23.8	5.1		US82-S3-L2-1	40.1	160.0	1.0	23.1	23.8	5.1

Table C-7. Data for Deep EC_{>100} and Average OC, MC, PI, and ln(SC).

Roadway	Sample ID	EC Deep (0-4 ft)	SC-avg.	OC_avg.	MC_avg.	PI_avg.	Ln (Sc-avg)
	US67 (MW)-H1-4	135.4	1032.5	2.9	30.0	36.1	6.9
	US67 (MW)-H2-4	139.5	1222.5	2.5	30.0	32.5	7.1
	US67 (ME)-H1-4	397.5	8587.5	2.4	29.6	38.2	9.1
US67	US67 (ME)-M1-4	231.1	8997.5	2.1	29.2	34.8	9.1
	US67 (ME)-M2-4	317.7	561.3	1.7	30.9	38.4	6.3
	US67 (ME)-L2-4	145.2	8103.8	2.4	24.7	37.2	9.0
	US82-H1-4	117.3	306.3	0.5	25.1	39.5	5.7
	US82-H2-4	137.2	673.8	0.4	22.9	33.8	6.5
	US82-M1-4	148.7	598.8	0.6	24.8	42.9	6.4
	US82-M2-4	131.1	520.0	0.5	25.3	34.6	6.3
	US82-S1-H1-4	205.3	318.8	0.7	21.7	30.6	5.8
	US82-S1-H2-4	187.2	402.5	2.9	22.8	33.7	6.0
	US82-S1-M2-4	153.8	343.8	0.4	23.3	37.4	5.8
	US82-S2-H1-4	240.7	296.3	1.4	23.3	33.3	5.7
	US82-S2-H2-4	178.8	406.3	0.4	24.2	36.1	6.0
	US82-S2-M1-4	134.6	413.8	0.2	28.3	46.8	6.0
US82	US82-S2-M2-4	151.5	312.5	1.0	26.1	39.9	5.7
	US82-S3-H1-4	166.0	186.3	0.7	22.8	33.9	5.2

Table C-8. Data for Deep EC_{>100} and All-Range OC, MC, PI, and ln(SC).

Roadway	Sample ID	EC Deep (0-4 ft)	SC1	OC1	MC1	PI1	Ln (SC1)	Roadway	Sample ID	EC Deep (0-4 ft)	SC2	OC2	MC2	PI2	Ln (SC2)		
US67	US67 (MW)-H1-4	135.4	135.4	1075.0	2.9	30.0	36.1	US67	US67 (MW)-H1-4	135.4	135.4	905.0	2.9	30.0	36.1		
	US67 (MW)-H2-4	139.5	139.5	1175.0	2.5	30.0	32.5		US67 (MW)-H2-4	139.5	139.5	1165.0	2.6	30.0	32.5		
	US67 (ME)-H1-4	397.5	397.5	8445.0	2.4	29.6	38.2		US67 (ME)-H1-4	397.5	397.5	8620.0	2.4	29.6	38.2		
	US67 (ME)-M1-4	231.1	231.1	8670.0	2.1	29.2	34.8		US67 (ME)-M1-4	231.1	231.1	9020.0	2.1	29.2	34.8		
	US67 (ME)-M2-4	317.7	317.7	580.0	1.7	30.9	38.4		US67 (ME)-M2-4	317.7	317.7	505.0	1.6	30.9	38.4		
	US67 (ME)-L2-4	145.2	145.2	7910.0	2.4	24.7	37.2		US67 (ME)-L2-4	145.2	145.2	8195.0	2.4	24.7	37.2		
US82	US82-H1-4	117.3	117.3	280.0	0.5	25.1	39.5	US82	US82-H1-4	117.3	117.3	265.0	0.5	25.1	39.5		
	US82-H2-4	137.2	137.2	650.0	0.4	22.9	33.8		US82-H2-4	137.2	137.2	655.0	0.5	22.9	33.8		
	US82-M1-4	148.7	148.7	625.0	0.5	24.8	42.9		US82-M1-4	148.7	148.7	580.0	0.6	24.8	42.9		
	US82-M2-4	131.1	131.1	605.0	0.5	25.3	34.6		US82-M2-4	131.1	131.1	385.0	0.5	25.3	34.6		
	US82-S1-H1-4	205.3	205.3	315.0	0.8	21.7	30.6		US82-S1-H1-4	205.3	205.3	300.0	0.6	21.7	30.6		
	US82-S1-H2-4	187.2	187.2	550.0	2.9	22.8	33.7		US82-S1-H2-4	187.2	187.2	325.0	3.1	22.8	33.7		
	US82-S1-M2-4	153.8	153.8	340.0	0.4	23.3	37.4		US82-S1-M2-4	153.8	153.8	325.0	0.4	23.3	37.4		
	US82-S2-H1-4	240.7	240.7	295.0	1.3	23.3	33.3		US82-S2-H1-4	240.7	240.7	295.0	1.5	23.3	33.3		
	US82-S2-H2-4	178.8	178.8	405.0	0.4	24.2	36.1		US82-S2-H2-4	178.8	178.8	370.0	0.4	24.2	36.1		
	US82-S2-M1-4	134.6	134.6	395.0	0.3	28.3	46.8		US82-S2-M1-4	134.6	134.6	395.0	0.2	28.3	46.8		
	US82-S2-M2-4	151.5	151.5	300.0	0.9	26.1	39.9		US82-S2-M2-4	151.5	151.5	295.0	1.0	26.1	39.9		
	US82-S3-H1-4	166.0	166.0	145.0	0.7	22.8	33.9		US82-S3-H1-4	166.0	166.0	220.0	0.7	22.8	33.9		
	Roadway	Sample ID	EC Deep (0-4 ft)	SC3	OC3	MC3	PI3		Ln (SC3)	Roadway	Sample ID	EC Deep (0-4 ft)	SC4	OC4	MC4	PI4	Ln (SC4)
	US67	US67 (MW)-H1-4	135.4	135.4	1165.0	2.9	30.0		36.1	US67	US67 (MW)-H1-4	135.4	985.0	2.9	30.0	36.1	6.9
US67 (MW)-H2-4		139.5	139.5	1285.0	2.5	30.0	32.5	US67 (MW)-H2-4	139.5		1265.0	2.5	30.0	32.5	7.1		
US67 (ME)-H1-4		397.5	397.5	8535.0	2.3	29.6	38.2	US67 (ME)-H1-4	397.5		8750.0	2.4	29.6	38.2	9.1		
US67 (ME)-M1-4		231.1	231.1	9090.0	2.1	29.2	34.8	US67 (ME)-M1-4	231.1		9210.0	2.2	29.2	34.8	9.1		
US67 (ME)-M2-4		317.7	317.7	635.0	1.8	30.9	38.4	US67 (ME)-M2-4	317.7		525.0	1.8	30.9	38.4	6.3		
US67 (ME)-L2-4		145.2	145.2	8250.0	2.4	24.7	37.2	US67 (ME)-L2-4	145.2		8060.0	2.4	24.7	37.2	9.0		
US82	US82-H1-4	117.3	117.3	340.0	0.5	25.1	39.5	US82	US82-H1-4	117.3	340.0	0.5	25.1	39.5	5.8		
	US82-H2-4	137.2	137.2	695.0	0.4	22.9	33.8		US82-H2-4	137.2	695.0	0.5	22.9	33.8	6.5		
	US82-M1-4	148.7	148.7	595.0	0.6	24.8	42.9		US82-M1-4	148.7	595.0	0.6	24.8	42.9	6.4		
	US82-M2-4	131.1	131.1	545.0	0.5	25.3	34.6		US82-M2-4	131.1	545.0	0.5	25.3	34.6	6.3		
	US82-S1-H1-4	205.3	205.3	325.0	0.8	21.7	30.6		US82-S1-H1-4	205.3	335.0	0.6	21.7	30.6	5.8		
	US82-S1-H2-4	187.2	187.2	410.0	2.8	22.8	33.7		US82-S1-H2-4	187.2	325.0	2.9	22.8	33.7	5.8		
	US82-S1-M2-4	153.8	153.8	355.0	0.4	23.3	37.4		US82-S1-M2-4	153.8	355.0	0.4	23.3	37.4	5.9		
	US82-S2-H1-4	240.7	240.7	300.0	1.4	23.3	33.3		US82-S2-H1-4	240.7	295.0	1.5	23.3	33.3	5.7		
	US82-S2-H2-4	178.8	178.8	450.0	0.5	24.2	36.1		US82-S2-H2-4	178.8	400.0	0.4	24.2	36.1	6.0		
	US82-S2-M1-4	134.6	134.6	430.0	0.2	28.3	46.8		US82-S2-M1-4	134.6	435.0	0.2	28.3	46.8	6.1		
	US82-S2-M2-4	151.5	151.5	325.0	0.9	26.1	39.9		US82-S2-M2-4	151.5	330.0	1.0	26.1	39.9	5.8		
	US82-S3-H1-4	166.0	166.0	155.0	0.7	22.8	33.9		US82-S3-H1-4	166.0	225.0	0.7	22.8	33.9	5.4		

